

# **5**

**Retention and elimination of  
cyanobacterial toxins  
(microcystins) through artificial  
recharge and bank filtration.**

**“algae” group: Federal Environmental Agency of Germany (UBA)**

**Responsible project leader: Dr. Ingrid Chorus, Dr. Hartmut Bartel**

# Content

<b>1 Analytical Methods for Microcystin Analysis .....</b>	<b>11</b>
1.1 Introduction .....	11
1.2 Analytical Methods for MCYST Analysis .....	11
1.2.1 Sample preparation.....	12
1.2.2 ELISA (Enzyme-Linked-ImmunoSorbent Assay) .....	12
1.2.2.1 MCYST-ELISA .....	12
1.2.2.2 Adda-ELISA.....	13
1.2.3 HPLC.....	13
1.2.4 MALDI-TOF (Matrix Assisted Laser Desorption Ionization Time-of-Flight Mass Spectrometry).....	13
1.3 Analytical Problems / Open Questions .....	13
1.3.1 Values below detection limit and limit of quantification (ELISA).....	13
1.3.2 Comparability of ELISA and HPLC Results .....	14
1.3.3 Appearance of new peaks in the HPLC Chromatogram .....	16
1.4 References .....	17
<b>2 Field Investigations on Transect Lake Tegel .....</b>	<b>19</b>
2.1 Introduction .....	19
2.2 Results and Interpretation.....	19
2.3 Conclusions .....	22
2.4 References .....	22
<b>3 Field Investigations on the Transects at Lake Wannsee .....</b>	<b>23</b>
3.1 Introduction .....	23
3.2 Results and Interpretation.....	23
3.2.1 Surface water.....	23
3.2.1.1 Groundwater.....	26
3.2.3 Conclusions .....	32
<b>4 Artificial Recharge Pond .....</b>	<b>33</b>
4.1 Introduction .....	33
4.2 Methods and Materials .....	33
4.3 Results .....	33
4.4 References .....	35
<b>5 Laboratory Experiments: Batch Experiments on MCYST-Degradation.....</b>	<b>36</b>
5.1 Introduction .....	36
5.2 Materials and Methods .....	36
5.2.1 Experimental setup.....	36
5.2.1.1 Preliminary experiment.....	36
5.2.1.2 Main series of batch experiments.....	37
5.2.2 Analytical Methods .....	38
5.3 Results .....	38
5.3.1 Preliminary experiment .....	38
5.3.2 Main series of batch experiments.....	39
5.3.3 Summary of the Results .....	43
5.4 Interpretation and Discussion.....	43
5.5 References .....	44

<b>6 Column Experiments to assess Effects of Temperature on MCYST-Degradation .....</b>	<b>46</b>
6.1    Introduction .....	46
6.2    Materials and Methods .....	46
6.2.1    Microcystin extract.....	46
6.2.2    Soil column experiments.....	46
6.2.2.1    General characteristics .....	46
6.2.2.2    Experiment 1 .....	48
6.2.2.3    Experiment 2 .....	48
6.2.2.4    Analytical methods.....	49
6.2.2.5    ELISA.....	49
6.2.2.6    HPLC.....	49
6.2.2.7    Numerical methods .....	49
6.3    Results .....	51
6.3.1    Experiment 1 .....	51
6.3.1.1    Soil column results .....	51
6.3.1.2    Modelling Results .....	53
6.3.2    Experiment 2 .....	55
6.3.2.1    Soil column results .....	55
6.3.2.2    Modelling results.....	57
6.4    Interpretation and Discussion.....	59
6.4.1    Elimination.....	59
6.4.2    Degradation rates.....	60
6.4.3    Retardation factor.....	61
6.5    Conclusions .....	61
6.6    References .....	62
<b>7 Clogging Column Experiments .....</b>	<b>64</b>
7.1    Introduction .....	64
7.2    Materials and Methods .....	64
7.2.1    Sediment chemistry .....	64
7.2.2    Water chemistry .....	64
7.2.3    Experimental Methods .....	64
7.2.3.1    Column setup.....	64
7.2.3.2    Experiment with dissolved MCYST (CC1) .....	65
7.2.3.3    Experiment with cyanobacterial cells (CC2) .....	65
7.3    Results .....	66
7.3.1    Experiment with dissolved MCYST (CC1) .....	66
7.3.2    Experiment with cell-bound MCYST (CC2) .....	68
7.4    Interpretation and Discussion.....	70
7.5    References .....	71
<b>8 Slow sand filter experiments .....</b>	<b>73</b>
8.1    Introduction .....	73
8.2    Materials and Methods .....	74
8.2.1    Technical scale slow sand filter on the UBA's experimental field .....	74
8.2.2    Characterization of the virgin filter material .....	76
8.2.3    Hydrochemistry under normal operating conditions.....	77
8.2.4    Experimental Methods .....	77
8.3    Results .....	78
8.3.1.1    Organic substance determined by loss on ignition (LOI) .....	79
8.3.1.2    Geochemistry of the clogging layer .....	81

8.3.1.3	Hydraulic properties determined by tracer experiments .....	81
8.3.1.4	Assessing the clogging situation of the slow sand filter during the experiments .....	84
8.3.2	Changes in general hydrochemistry during the experiments .....	85
8.3.3	Elimination of trace substances during the experiments.....	87
8.3.3.1	Cyanobacterial Toxins.....	87
8.4	Interpretation and Discussion.....	91
8.5	References .....	92
<b>9</b>	<b>Enclosure experiments on UBA's experimental field.....</b>	<b>93</b>
9.1	Introduction .....	93
9.2	Materials and Methods .....	95
9.2.1	Semi technical scale enclosures on the UBA's experimental field.....	95
9.2.1.1	Experimental design .....	95
9.2.1.2	Hydro- and geochemical conditions.....	96
9.2.2	Experimental Methods .....	98
9.2.2.1	Experiments with pulsed application (E1 to E7).....	98
9.2.2.2	Experiments under anaerobic conditions (E8, E9, E11) .....	99
9.2.2.3	Experiments with continuous application (E10, E12, E13) .....	99
9.2.2.4	Experiment with continuous application of cell-bound MCYST (E12) ....	100
9.2.3	Analytical Methods .....	100
9.2.4	Modelling .....	101
9.3	Results .....	103
9.3.1	Tracer experiments .....	103
9.3.1.1	Differences between the enclosures .....	103
9.3.1.2	Differences within the enclosures .....	105
9.3.2	Experiments with pulsed application of trace substances .....	107
9.3.2.1	Changes in hydrochemistry .....	107
9.3.2.2	Cyanobacterial Toxins (Microcystins) .....	107
9.3.3	Experiments under anaerobic conditions .....	122
9.3.3.1	Changes in hydrochemistry .....	122
9.3.4	Experiments with continuous application (E10, E12 and E13) .....	126
9.3.4.1	Changes in hydraulics and hydrochemistry during the experiment .....	126
9.3.4.2	Experiment with cyanobacterial cells (E12) .....	131
9.4	Interpretation and Discussion.....	135
9.4.1	Clogging of the enclosures .....	135
9.4.2	Cyanobacterial Toxins (Microcystins) .....	137
9.5	References .....	142

# List of Figures

FIGURE 1: STRUCTURE OF MCYST-LR .....	11
FIGURE 2: ELISA AND HPLC ANALYSIS IN RELATION .....	15
FIGURE 3: PEAKS IN THE HPLC CHROMATOGRAM WITH UV SPECTRA CHARACTERISTIC FOR MCYST IN SAMPLES FROM EXPERIMENT E2 (SAMPLING PORT IN 20 CM DEPTH). THE INPUT SOLUTION SHOWED ONLY ONE PEAK AT 13.6 MINUTES RETENTION TIME (CORRESPONDING TO DEM. [ASP <sup>3</sup> ] MCYST-RR) WHICH WAS NO LONGER DETECTED IN THE EFFLUENT.....	16
FIGURE 4 : TOTAL AND EXTRACELLULAR MICROCYSTIN (MCYST) CONCENTRATIONS DETERMINED WITH DIFFERENT ELISAS (SPECIFICALLY FOR ADDA AND FOR THE MCYST MOLECULE) IN LAKE TEGEL'S SURFACE WATER 2002 - 2004.....	19
FIGURE 5 : CELL-BOUND MCYST FOR SAMPLES TAKEN FROM THE SHORE, ANALYSED WITH ADDA-ELISA, AND THE LAKE CENTRE, ANALYSED WITH HPLC.....	20
FIGURE 6 TOTAL PHYTOPLANKTON BIOVOLUME, TOTAL MCYST DETERMINED BY ADDA-ELISA (LEFT AXIS) AND BIOVOLUME OF TOXIC CYANOBACTERIA MICROCYSTIS SP. (RIGHT AXIS) IN LAKE TEGEL.....	21
FIGURE 7: RESULTS OF THE SURFACE WATER MONITORING AT LAKE WANNSEE: BIOVOLUME OF CYANOBACTERIA AND MCYST ANALYSED BY HPLC AND ELISA. (MEAN VALUES OF UP TO 4 SAMPLES FROM DIFFERENT PLACES ON ONE OCCASION. SHADED AREAS: NO DATA.) .....	25
FIGURE 8: RESULTS OF TOTAL MCYST AT TRANSECT 1 AND 2, ANALYSED BY MCYST-ELISA (MAY 2002 TO AUGUST 2004).....	28
FIGURE 9: RESULTS OF TOTAL MCYST AT TRANSECT 1 AND 2, ANALYSED BY ADDA-ELISA (MAY 2002 TO AUGUST 2004).....	29
FIGURE 10: RESULTS OF EXTRACELLULAR MCYST AT TRANSECT 1 AND 2, ANALYSED BY ADDA-ELISA (MAY 2002 TO AUGUST 2004).....	30
FIGURE 11: MCYST CONCENTRATIONS IN SURFACE- AND GROUNDWATER ANALYSED DURING THE INTENSIVE SAMPLING CAMPAIGN IN AUTUMN 2003 (EXTRACELLULAR MCYST WAS NOT DETECTED IN THE GROUNDWATER SAMPLES).....	31
FIGURE 12: SCREW CAP TUBES FILLED WITH SULFIDE REDUCED ANOXIC MEDIUM SUPPLEMENTED WITH KNO <sub>3</sub> . THE PINK BOTTLE SHOWS AN EXAMPLE OF OXIDIZED MEDIUM. 38	
FIGURE 13: DEGRADATION OF DEM. MCYST-RR UNDER AEROBIC AND ANOXIC CONDITIONS DURING FIRST BATCH SERIES.....	39
FIGURE 14: MCYST (SUM OF ALL VARIANTS) DURING THE FIRST MAIN SERIES OF DEGRADATION EXPERIMENTS UNDER ANOXIC CONDITIONS WITH ADDITION OF KNO <sub>3</sub> , GLUCOSE AND CASAMINOACIDS (AVERAGE VALUES AND STANDARD DEVIATION OF THREE PARALLELS EACH) .....	40
FIGURE 15: CONCENTRATIONS OF DEM. MCYST-RR (FULL SQUARES) AND AN UNIDENTIFIED MCYST VARIANT (RETENTION TIME: 10.5 MIN, SMALL DIAMONDS) DURING THE THREE PARALLEL EXPERIMENTS WITH CASAMINOACIDS IN THE FIRST MAIN SERIES. 40	
FIGURE 16: MCYST (SUM OF ALL VARIANTS) DURING THE SECOND MAIN SERIES OF DEGRADATION EXPERIMENTS UNDER ANOXIC CONDITIONS WITH ADDITION OF KNO <sub>3</sub> , GLUCOSE AND WITHOUT INOCULUM (AVERAGE VALUES AND STANDARD DEVIATION OF THREE PARALLELS EACH) .....	41
FIGURE 17: CONCENTRATIONS OF DEM. MCYST-RR AND UNIDENTIFIED MCYST VARIANTS DURING ONE SERIES WITH GLUCOSE IN THE SECOND MAIN SERIES (RT = RETENTION TIME). 42	
FIGURE 18 SIMPLIFIED DIAGRAM OF THE INSTALLATION.....	47
FIGURE 19 PHOTOGRAPH OF ONE OF THE COLUMNS.....	48
FIGURE 20 EVOLUTION OF LOSS RATE ( $\Lambda$ ) WITH THE TIME FOR C FROM -1 TO 1. PARAMETERS FOR THE GIVEN SITUATION ARE: $\Lambda_1 = 1E-10$ , $\Lambda_2 = 1$ AND $T = 31$ .....	50
FIGURE 21 MICROCYSTIN CONCENTRATION IN THE WATER RESERVOIR.....	51
FIGURE 22 MICROCYSTIN CONCENTRATIONS AT COLUMN OUTLETS INVESTIGATED AT THREE EXPERIMENTAL TEMPERATURES, T <sub>1</sub> = 5°C, T <sub>2</sub> = 15°C AND T <sub>3</sub> = 25°C FOR AN INPUT CONCENTRATION AROUND 19.2 µG/L.....	52
FIGURE 23 MICROCYSTIN ELIMINATION DURING EXPERIMENT 1 (INPUT CONCENTRATION 19.2 µG/L FOR DAYS 0 TO 31 AND 7.6 µG/L FOR DAYS 32 TO 47). ....	53

FIGURE 24 MEASURED AND MODELLED MICROCYSTIN OUTLET CONCENTRATION FOR EXPERIMENT 1.....	54
FIGURE 25 MICROCYSTIN DEGRADATION RATES OVER TIME AT 3 DIFFERENT TEMPERATURES.....	55
FIGURE 26 MICROCYSTIN CONCENTRATION AT T <sub>1</sub> = 5°C, T <sub>2</sub> = 15°C AND T <sub>3</sub> = 25°C FOR AN INPUT CONCENTRATION OF ABOUT 63.5 µG/L.....	56
FIGURE 27 MICROCYSTIN ELIMINATION DURING THE TIME OF THE EXPERIMENT FOR EACH COLUMN (INPUT CONCENTRATION ABOUT 63.5 µG/L).....	57
FIGURE 28 MEASURED AND MODELLED MICROCYSTIN OUTLET CONCENTRATION FOR EXPERIMENT 2 WITH THE PARAMETERS ESTIMATED FOR THE EXPERIMENT 1.....	58
FIGURE 29 MEASURED AND MODELLED MICROCYSTIN OUTLET CONCENTRATION FOR EXPERIMENT 2 (COLUMN 2 AT 15°C) WITH A LAG PHASE FOR THE DEGRADATION T <sub>0</sub> = 5 D.....	59
FIGURE 30: CONCENTRATIONS OF MCYST IN THE WATER RESERVOIR DURING THE EXPERIMENT WITH DISSOLVED MCYST. LINES INDICATE SAMPLES TAKEN FROM THE SAMPE FLASK, NOT CONCENTRATION DEVELOPMENTS (CIRCLE MARKS MCYST CONCENTRATION CALCULATED FROM EXTRACT CONCENTRATION AND DILUTION FACTOR). 67	
FIGURE 31: MCYST CONCENTRATIONS IN THE WATER RESERVOIR (DEPTH = 0) AND IN THE SAMPLING PORTS DURING EXPERIMENT CC1 (TWO VALUES AT DEPTH = 0 CORRESPOND TO TWO SAMPLES TAKEN BEFORE AND AFTER EXCHANGE OF RESERVOIR; OPEN SQUARES: VALUES BELOW DETECTION LIMIT).....	68
FIGURE 32: TOTAL AND EXTRACELLULAR MCYST AS WELL CYANOBACTERIAL BIOVOLUME IN THE WATER RESERVOIR DURING EXPERIMENT CC2.....	69
FIGURE 33: CELL-BOUND AND EXTRA-CELLULAR MCYST IN THE SAMPLING PORTS ON DAY 4 AFTER APPLICATION.....	70
FIGURE 34: OVERVIEW OF THE INVESTIGATIONS AND EXPERIMENTS CARRIED OUT ON THE SSF. 73	
FIGURE 35: SCHEMATICAL CROSS SECTION OF THE SLOW SAND FILTER .....	74
FIGURE 36: DRAINAGE PIPES ON THE BASIS OF THE SLOW SAND FILTER DURING SAND EXCHANGE.....	75
FIGURE 37: PREPARATION OF THE FILTER SAND DURING SAND EXCHANGE.....	75
FIGURE 38: GRAIN SIZE DISTRIBUTION OF THE FILTER MATERIAL IN THE SSF (DATA BY FU BERLIN). 76	
FIGURE 39: FLOW RATE AND HYDRAULIC CONDUCTIVITY IN THE SLOW SAND FILTER USED FOR THE SSF EXPERIMENTS DURING 2003 (TIME SCALE CORRESPONDING TO FIGURE 41).78	
FIGURE 40: PHOTOGRAPH TAKEN DURING RAKING OF THE SSF IN ORDER TO DESTROY THE SUPERFICIAL CLOGGING LAYER.....	79
FIGURE 41: LOSS ON IGNITION (LOI) AS MEASURE FOR ORGANIC SUBSTANCE IN THE FILTER BED OF THE SSF.....	80
FIGURE 42: VARIATION OF LOI DURING ONE SAMPLING EVENT (ERROR BARS INDICATE THE 95 % CONFIDENCE INTERVAL, N = 6).....	80
FIGURE 43: MEASURED ELECTRICAL CONDUCTIVITY AND MODELED OUTPUT FUNCTION FOR SSF TRACER EXPERIMENTS. SYMBOLS: HAND MEASUREMENTS, GREY LINES: ONLINE MEASUREMENTS, BLACK LINES: MODELED CURVES. A: SSF1 (THICK LINES) AND SSF3 (THIN LINES); B: SSF 5; C: SSF6 (NOTE DIFFERENT TIME SCALES ON X-AXIS FOR A, B AND C). 83	
FIGURE 44: DOC VALUES DURING SSF5 (DATA BY TUB). POLYSACCHARIDES WERE REDUCED SUBSTANTIALLY THROUGH THE FILTRATION PROCESS, AS INDICATED BY THE PRONOUNCED REDUCTION OF THE PEAK AT 39 MIN. IN LC-OCD CHROMATOGRAMS (FIG. 12). 86	
FIGURE 45: LC-OCD CHROMATOGRAM OF SAMPLES TAKEN BEFORE AND DURING EXPERIMENT SSF 5 (DATA BY TUB).....	86
FIGURE 46: CONCENTRATION OF DEMETHYLATED MCYST-RR (MAIN MCYST VARIANT OF MASS CULTURE) IN THE WATER RESERVOIR DURING THE SLOW SAND FILTER EXPERIMENT SSF2).....	88
FIGURE 47: EFFLUENT CONCENTRATIONS OF MCYST IN EXPERIMENT SSF2 (TRACER RESULTS REFER TO SEPARATE TRACER EXPERIMENTS, BEFORE AND AFTER SSF2).....	88
FIGURE 48: EFFLUENT CONCENTRATIONS OF MCYST IN EXPERIMENT SSF5. ....	89
FIGURE 49: EFFLUENT CONCENTRATIONS OF MCYST IN EXPERIMENT SSF6 (AFTER 50 H MCYST CONCENTRATIONS WERE NO LONGER DETECTABLE). ....	89

FIGURE 50: HPLC CHROMATOGRAM PEAKS IDENTIFIED AS MICROCYSTINS IN THE SSF2 EFFLUENT SAMPLES (RT: RETENTION TIME). COLUMNS REFER TO LEFT Y-AXIS AND REPRESENT THE RELATIVE SHARES OF THE DIFFERENT PEAKS IN RELATION TO THE SUM OF MCYST (DOTS, RIGHT Y-AXIS).....	90
FIGURE 51: OVERVIEW OF THE INVESTIGATIONS AND EXPERIMENTS CARRIED OUT ON THE ENCLOSURES IN 2002 AND 2003. LEGEND: YELLOW FIELDS: ENCLOSURES DRY; LIGHT-BLUE: FLOODED WITH LITTLE OR NO CLOGGING; DARKER BLUE: FLOODED WITH PRONOUNCED CLOGGING; HATCHED FIELDS: FLOODED, BUT NO EXPERIMENT. ....	93
FIGURE 52: OVERVIEW OF THE INVESTIGATIONS AND EXPERIMENTS CARRIED OUT ON THE ENCLOSURES IN 2004. LEGEND: YELLOW FIELDS: ENCLOSURES DRY; LIGHT-BLUE: FLOODED WITH LITTLE OR NO CLOGGING; DARKER BLUE: FLOODED WITH PRONOUNCED CLOGGING; HATCHED FIELDS: FLOODED, BUT NO EXPERIMENT. ....	94
FIGURE 53: POSITION OF THE ENCLOSURES INSIDE THE INFILTRATION PONDS (CROSS SECTION; DOTTED BOXES SHOW BIRD'S-EYE VIEW AND MAGNIFICATION), WITHOUT TUBING, PUMPS AND SAMPLING PORTS.....	95
FIGURE 54: CROSS SECTION OF ENCLOSURE III WITH SAMPLING PORTS. ....	96
FIGURE 55: AVERAGE NITRATE CONCENTRATIONS DURING EXPERIMENT E3 (ERROR BARS INDICATING STANDARD DEVIATIONS OF 3 SAMPLES).....	97
FIGURE 56: EFFECTIVE PORE VOLUMES IN ENCLOSURE III CALCULATED FROM TRACER BREAKTHROUGH CURVES ("CLOGGING" REFERS TO THE EXISTENCE OF A VISIBLE, SUPERFICIAL "SCHMUTZDECKE" ON THE FILTER).....	105
FIGURE 57: EFFECTIVE PORE VOLUMES IN ENCLOSURE II CALCULATED FROM TRACER BREAKTHROUGH CURVES ("CLOGGING" REFERS TO THE EXISTENCE OF A VISIBLE, SUPERFICIAL "SCHMUTZDECKE" ON THE FILTER).....	106
FIGURE 58: GAS BUBBLE FORMATION DURING REMOVAL OF CLOGGING LAYER ON ENCLOSURE III IN DECEMBER 2004. ....	107
FIGURE 59: MEASURED MCYST CONCENTRATION IN THE WATER RESERVOIR AND FITTED TRACER CURVE DURING EXPERIMENT E 5 AT MODERATE TEMPERATURES (< 23.5°C)....	109
FIGURE 60: MEASURED MCYST CONCENTRATION IN THE WATER RESERVOIR, FITTED DECAY FUNCTION AND FITTED TRACER CURVE DURING EXPERIMENT E 2 AT TEMPERATURES OF 24 TO 32°C. ....	109
FIGURE 61: MCYST CONCENTRATIONS AND MODELED TRACER BREAKTHROUGH CURVES AT SAMPLING PORTS IN 20 CM, 40 CM, 60 CM AND 80 CM DEPTH AS WELL AS IN THE EFFLUENT (FROM TOP TO BOTTOM) DURING E2 ( $C_0 = 6.1 \mu\text{G/L}$ ). DOTTED CURVE: MCYST IN WATER RESERVOIR (MODELED); SOLID CURVES: TRACER MODELED AT THE RESPECTIVE PORT; SOLID SQUARES; MCYST MEASURED AT THE RESPECTIVE PORT; OPEN SQUARES: MCYST BELOW DETECTION LIMIT, I.E. < $0.01 \mu\text{G/L}$ .....	110
FIGURE 62: MCYST CONCENTRATIONS AND MODELED TRACER BREAKTHROUGH CURVES IN SAMPLING PORTS IN 20 CM, 40 CM, 60 CM AND 80 CM DEPTH AS WELL AS IN THE EFFLUENT (FROM TOP TO BOTTOM) DURING E3 ( $C_0 = 6.15 \mu\text{G/L}$ ). DOTTED CURVE: MCYST IN WATER RESERVOIR (MODELED); SOLID CURVES: TRACER MODELED AT THE RESPECTIVE PORT; SOLID SQUARES; MCYST MEASURED AT THE RESPECTIVE PORT; OPEN SQUARES: MCYST BELOW DETECTION LIMIT, I.E. < $0.01 \mu\text{G/L}$ .....	111
FIGURE 63: MCYST CONCENTRATIONS AND MEASURED TRACER BREAKTHROUGH CURVES IN SAMPLING PORTS IN 40 CM AND 80 CM DEPTH AS WELL AS IN THE EFFLUENT DURING E4 ( $C_0 = 9.0 \mu\text{G/L}$ ). DOTTED CURVE: MCYST IN WATER RESERVOIR (MEASURED); SOLID CURVES: TRACER MEASURED AT THE RESPECTIVE PORT; SOLID SQUARES; MCYST MEASURED AT THE RESPECTIVE PORT; OPEN SQUARES: MCYST BELOW DETECTION LIMIT, I.E. < $0.01 \mu\text{G/L}$ .....	112
FIGURE 64: MCYST CONCENTRATIONS AND MEASURED TRACER BREAKTHROUGH CURVES IN SAMPLING PORTS IN 40 CM AND 80 CM DEPTH AS WELL AS IN THE EFFLUENT DURING E5 ( $C_0 = 7.6 \mu\text{G/L}$ ). DOTTED CURVE: MCYST IN WATER RESERVOIR (MEASURED); SOLID CURVES: TRACER MEASURED AT THE RESPECTIVE PORT; SOLID SQUARES; MCYST MEASURED AT THE RESPECTIVE PORT; OPEN SQUARES: MCYST BELOW DETECTION LIMIT, I.E. < $0.01 \mu\text{G/L}$ .....	113
FIGURE 65: INVERSE MODELLING RESULT FOR EXPERIMENT E2, INLET TO 20 CM (SOLID CURVE, LEFT SCALE); MEASURED INLET VALUES: DIAMONDS, RIGHT SCALE; MEASURED VALUES IN 20 CM DEPTH: CROSSES, LEFT SCALE.....	115
FIGURE 66: INVERSE MODELLING RESULT FOR EXPERIMENT E2, 20 CM TO 40 CM (SOLID CURVE, LEFT SCALE); MEASURED VALUES IN 20 CM DEPTH: DIAMONDS, RIGHT SCALE; MEASURED VALUES IN 40 CM DEPTH: CROSSES, LEFT SCALE.....	116

FIGURE 67: INVERSE MODELLING RESULT FOR EXPERIMENT E2, 40 CM TO 60 CM (SOLID CURVE, LEFT SCALE); MEASURED VALUES IN 40 CM DEPTH: DIAMONDS, RIGHT SCALE; MEASURED VALUES IN 60 CM DEPTH: CROSSES, LEFT SCALE.....	116
FIGURE 68: INVERSE MODELLING RESULT FOR EXPERIMENT E2, 60 CM TO 80 CM (SOLID CURVE, LEFT SCALE); MEASURED VALUES IN 60 CM DEPTH: DIAMONDS, RIGHT SCALE; MEASURED VALUES IN 80 CM DEPTH: CROSSES, LEFT SCALE.....	117
FIGURE 69: INVERSE MODELLING RESULT FOR EXPERIMENT E2, 60 CM TO 80 CM WITHOUT OUTLIER (SOLID CURVE, LEFT SCALE); MEASURED VALUES IN 60 CM DEPTH: DIAMONDS, RIGHT SCALE; MEASURED VALUES IN 80 CM DEPTH: CROSSES, LEFT SCALE.....	117
FIGURE 70: INVERSE MODELLING RESULT FOR EXPERIMENT E2, 80 CM TO EFFLUENT (SOLID CURVE, LEFT SCALE); MEASURED VALUES IN 80 CM DEPTH: DIAMONDS, RIGHT SCALE; MEASURED VALUES IN EFFLUENT: CROSSES, LEFT SCALE.....	118
FIGURE 71: INVERSE MODELLING RESULT FOR EXPERIMENT E3, INLET TO 20 CM DEPTH (SOLID CURVE, LEFT SCALE); MEASURED VALUES IN INLET: DIAMONDS, RIGHT SCALE; MEASURED VALUES IN 20 CM DEPTH: CROSSES, LEFT SCALE.....	118
FIGURE 72: INVERSE MODELLING RESULT FOR EXPERIMENT E3, 20 CM TO 40 CM DEPTH (SOLID CURVE, LEFT SCALE); MEASURED VALUES IN 20 CM DEPTH: DIAMONDS, RIGHT SCALE; MEASURED VALUES IN 40 CM DEPTH: CROSSES, LEFT SCALE.....	119
FIGURE 73: INVERSE MODELLING RESULT FOR EXPERIMENT E3, 20 CM TO 40 CM DEPTH WITHOUT OUTLIER (SOLID CURVE, LEFT SCALE); MEASURED VALUES IN 20 CM DEPTH: DIAMONDS, RIGHT SCALE; MEASURED VALUES IN 40 CM DEPTH: CROSSES, LEFT SCALE.....	119
FIGURE 74: INVERSE MODELLING RESULT FOR EXPERIMENT E3, 40 CM TO 60 CM DEPTH (SOLID CURVE, LEFT SCALE); MEASURED VALUES IN 40 CM DEPTH: DIAMONDS, RIGHT SCALE; MEASURED VALUES IN 60 CM DEPTH: CROSSES, LEFT SCALE.....	120
FIGURE 75: INVERSE MODELLING RESULT FOR EXPERIMENT E3, 40 CM TO 60 CM DEPTH WITHOUT OUTLIER (SOLID CURVE, LEFT SCALE); MEASURED VALUES IN 40 CM DEPTH: DIAMONDS, RIGHT SCALE; MEASURED VALUES IN 60 CM DEPTH: CROSSES, LEFT SCALE.....	120
FIGURE 76: INVERSE MODELLING RESULT FOR EXPERIMENT E3, 60 CM TO 80 CM DEPTH (SOLID CURVE, LEFT SCALE); MEASURED VALUES IN 60 CM DEPTH: DIAMONDS, RIGHT SCALE; MEASURED VALUES IN 80 CM DEPTH: CROSSES, LEFT SCALE.....	121
FIGURE 77: INVERSE MODELLING RESULT FOR EXPERIMENT E3, 80 CM DEPTH TO EFFLUENT (SOLID CURVE, LEFT SCALE); MEASURED VALUES IN 80 CM DEPTH: DIAMONDS, RIGHT SCALE; MEASURED VALUES IN EFFLUENT: CROSSES, LEFT SCALE... ..	121
FIGURE 78: DEVELOPMENT OF OXYGEN CONCENTRATIONS AND REDOXPOTENTIAL DURING ADDITIONAL DOC DOSING (EXPERIMENT E8).....	123
FIGURE 79: MCYST AND TRACER CONCENTRATIONS IN THE WATER RESERVOIR DURING EXPERIMENT E9. DUE TO THE MISSING SAMPLES BETWEEN 12 AND 22 H MAXIMUM MCYST CONCENTRATIONS WERE PROBABLY ALSO MISSED IN THE EFFLUENT. TWO UNUSUALLY HIGH MCYST VALUES OBTAINED BY HPLC AT 23 AND 24 H COULD NOT BE CONFIRMED BY ELISA, SO THEY MAY BIAS THE RESULTS TOWARDS HIGHER RECOVERY RATES.	124
FIGURE 80: MCYST CONCENTRATIONS AND TRACER BREAKTHROUGH CURVES IN 40 CM AND 80 CM DEPTH AS WELL AS IN THE EFFLUENT (FROM TOP TO BOTTOM) DURING E9 (C0 = 6.031 µG/L). DOTTED CURVE: MCYST IN WATER RESERVOIR (MEASURED); SOLID CURVES: TRACER MEASURED AT THE RESPECTIVE PORT; SOLID SQUARES: MCYST MEASURED AT THE RESPECTIVE PORT; OPEN SQUARES: MCYST BELOW DETECTION LIMIT, I.E. < 0.01 µG/L.....	125
FIGURE 81: HYDRAULIC PARAMETERS DURING EXPERIMENT E10 (12TH OCT. 04 TO 1ST NOV. 04).	127
FIGURE 82: MCYST CONCENTRATIONS IN STOCK SOLUTION AND WATER RESERVOIR DURING EXPERIMENT E10, MEASURED BY ELISA (ERROR BARS INDICATE MINIMUM AND MAXIMUM VALUES) (A): STARTING PHASE WITH LOWER CONCENTRATIONS DUE TO DILUTION AND ADSORPTION, B): LOW CONCENTRATIONS DUE TO TECHNICAL PROBLEMS, C): END PHASE WITH DECLINING CONCENTRATIONS).....	128
FIGURE 83: MCYST CONCENTRATION IN EFFLUENT AND WATER RESERVOIR AS WELL AS ELIMINATION RATE DURING EXPERIMENT E10 (SHADE AREAS, SEE FIGURE 32, ENCIRCLED VALUES: EFFLUENT CONCENTRATIONS BELOW LIMIT OF DETERMINATION).	130
FIGURE 84: CORRELATION BETWEEN MCYST CONCENTRATIONS MEASURED BY HPLC AND BY ELISA IN THE WATER RESERVOIR DURING E10 (MASKED VALUES IN LIGHT BLUE)... ..	130

FIGURE 85: DEVELOPMENT OF FLOW RATE AND HYDRAULIC CONDUCTIVITY DURING EXPERIMENT E12.....	131
FIGURE 86: CONCENTRATIONS OF DISSOLVED ORGANIC CARBON (DOC) IN WATER RESERVOIR AND EFFLUENT DURING EXPERIMENT E12.....	132
FIGURE 87: MCYST (BY HPLC AND ELISA) AND PLANKTOTHRIX BIOVOLUME IN THE WATER RESERVOIR DURING EXPERIMENT E12 (CIRCLE: VALUES INFLUENCED BY FLOW INTERRUPTION, ARROW: TIME SPAN OF DOSING; OPEN DIAMONDS INDICATE VALUES BELOW DETECTION LIMIT).....	133
FIGURE 88: TOTAL MCYST (IN PERCENT OF MAXIMUM CONCENTRATION - 1023 µG/L - AT THE END OF THE DOSING PHASE) IN THE PORE WATER OF SEDIMENT CORES DURING EXPERIMENT E12.....	134
FIGURE 89: RECOVERED PORTIONS OF MCYST DURING AEROBIC ENCLOSURE EXPERIMENTS E2 THROUGH E5.....	139
FIGURE 90: RECOVERED PORTIONS OF MCYST DURING ANAEROBIC (E9) AND AEROBIC ENCLOSURE EXPERIMENTS (E4 AND E5).....	140

## List of Tables

TABLE 1 MEDIAN VALUES AND 90TH PERCENTILE FOR SUMMER AND WINTER CONCENTRATIONS OF MCYST IN LAKE WANNSEE'S SURFACE WATER DETERMINED BY HPLC, MCYST-ELISA AND ADDA-ELISA.....	26
TABLE 2: RESULTS OF MICROSCOPIC AND HPLC-ANALYSIS OF SURFACE WATER AT THE ARTIFICIAL RECHARGE POND IN TEGEL (GWA TEGEL).....	34
TABLE 3 AVERAGE TEMPERATURE OF EACH COLUMN DURING EXPERIMENT 1 (A) AND EXPERIMENT 2 (B). THE NUMBER OF MEASUREMENTS WAS 23 AND 7 FOR A) AND B), RESPECTIVELY.....	47
TABLE 4 FITTING PARAMETERS FOR EXPERIMENT 1 ( $V = 0.2 \text{ M/D}$ , $AL = 0.05 \text{ M}$ , $T = 31 \text{ D}$ ).....	53
TABLE 5 MICROCYSTIN VARIANTS IN THE INPUT SOLUTION WITH THEIR CONCENTRATION IN THE SOLUTION AND THE CALCULATED CONCENTRATION INJECTED INTO THE COLUMN (DILUTION OF 1/50).....	55
TABLE 6 MEAN VALUE OF THE ELIMINATION FOR EACH TEMPERATURE AND EXPERIMENT. EXPERIMENT 1: MCYST ADDED TO THE WATER RESERVOIR FEEDING THE COLUMNS, EXPERIMENT 2: MCYST INJECTED DIRECTLY ON COLUMN.....	59
TABLE 7: GEOCHEMICAL PROPERTIES OF THE VIRGIN SSF SAND IN COMPARISON TO SAND FROM LAKE WANNSEE'S SHORE (DATA BY FU BERLIN).....	76
TABLE 8: GEOCHEMICAL PROPERTIES OF THE CLOGGING LAYER IN COMPARISON TO VIRGIN SSF SAND. (MASSMANN ET AL. 2004).....	81
TABLE 9: PORE VELOCITIES, DISPERSION LENGTHS, EFFECTIVE PORE VOLUMES AND HYDRAULIC CONDUCTIVITIES DURING THE TRACER EXPERIMENTS ON SLOW SAND FILTER.....	81
TABLE 10: MAIN ANIONS AND CATIONS DURING TV 6 (DATA BY FU BERLIN).....	85
TABLE 11: INITIAL PARAMETERS OF THE SSF EXPERIMENTS WITH MCYST.....	87
TABLE 12: RECOVERED AMOUNTS OF MCYST THE EXPERIMENTS SSF2, SSF5 AND SSF6.....	90
TABLE 13: RETARDATION COEFFICIENTS ( $R$ ) AND DEGRADATION RATES ( $\Lambda$ ) OBTAINED BY MODELLING SSF EXPERIMENTS WITH MCYST.....	91
TABLE 14: DISTRIBUTION OF SAMPLING TUBES INSIDE THE ENCLOSURES.....	96
TABLE 15: OVERVIEW OF THE ANALYTICAL METHODS USED FOR ON-SITE WATER ANALYSIS.....	101
TABLE 16: HYDRAULIC PROPERTIES OF THE ENCLOSURES DETERMINED BY TRACER EXPERIMENTS (EFFLUENT DATA ONLY).....	104
TABLE 17: INITIAL PARAMETERS OF THE ENCLOSURE EXPERIMENTS E2 TO E5.....	108
TABLE 18: RECOVERED AMOUNTS OF MCYST IN EXPERIMENTS E2 THROUGH E5.....	114
TABLE 19: INITIAL PARAMETERS OF THE ANAEROBIC ENCLOSURE EXPERIMENT E9 IN COMPARISON TO MINIMUM AND MAXIMUM VALUES OF SIMILAR AEROBIC EXPERIMENTS E2 TO E5 (SEE TABLE 17).....	124
TABLE 20: RECOVERED AMOUNTS OF MCYST DURING EXPERIMENTS E9 (ANAEROBIC) AND E2 THROUGH E5 (AEROBIC).....	126
TABLE 21: AVERAGE VALUES OF HYDROCHEMICAL PARAMETERS DURING EXPERIMENT E10.....	127
TABLE 22: AVERAGE VALUES OF HYDROCHEMICAL PARAMETERS DURING EXPERIMENT E12. 132	132
TABLE 23: HYDRAULIC DATA OF ALL ENCLOSURE EXPERIMENTS WITH RESULTING ASSESSMENT OF THE CLOGGING SITUATION.....	136
TABLE 24: SUMMARY OF RETARDATION COEFFICIENTS AND DEGRADATION RATES OBTAINED BY MODELLING.....	137

# 1 Analytical Methods for Microcystin Analysis

## 1.1 Introduction

Among the known cyanotoxins (cyanobacterial toxins or toxins produced by blue-green-algae), the hepatotoxic cyclic peptides called microcystins are considered to occur most commonly (Sivonen & Jones 1999). Their general structure reads as follows: Cyclo-(D-anlanine<sup>1</sup>-X<sup>2</sup>-C-MeAsp<sup>3</sup>-Z<sup>4</sup>-Adda<sup>5</sup>-D-glutamate<sup>6</sup>-Mdha<sup>7</sup>) with X and Z being variable L-amino-acids (Figure 1). So far 70 structural variants have been identified from natural samples (Sivonen & Jones 1999) with microcystin-LR and microcystin-YR being the most toxic so far (LD<sub>50</sub> i.p. mouse (μg/kg) = 50, Botes et al. 1985).

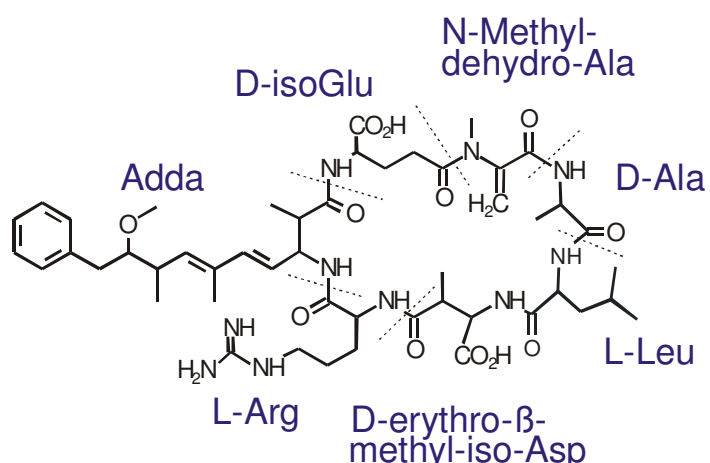


Figure 1: Structure of MCYST-LR.

In the NASRI project, different methods of analysis were used to determine microcystin (MCYST) concentrations in water from the field sites and from the experiments (see final report working group algae, part I to VII). These will be described below (chapter 1.2). Some results were, however, surprising and not always unambiguous. This and possible reasons will be discussed in chapter 1.3.

## 1.2 Analytical Methods for MCYST Analysis

In most cases microcystin analyses were carried out by ELISA (Enzyme-Linked ImmunoSorbent Assay) and HPLC (High Performance Liquid Chromatography) with a photodiode array (PDA) detector. In the field experiments samples were first tested for their microcystin content using the ELISA and selected ones subsequently analyzed by HPLC to verify the results and distinguish the different MCYST variants. Structural identification of MCYST variants was carried out by MALDI-TOF MS (Matrix Assisted Laser Desorption Ionization Time-of-Flight Mass Spectrometry).

### **1.2.1        *Sample preparation***

The water samples for analysis of **total microcystins** (i.e. extra-cellular plus cell-bound) were deep frozen and thawed in order to release cell-bound microcystins, filtered by membrane filters (RC 55, pore size 0.45 µm) and either analyzed directly (ELISA) or enriched by solid phase extraction (SPE) over C<sub>18</sub>-cartridges according to Harada et al. (1999). If analysis or SPE was not possible within 24 h the samples were stored deep frozen (-18 °C).

For analyzing the **extra-cellular microcystins** samples were filtered (RC 55, pore size 0.45 µm) directly after sampling and then stored deep frozen for subsequent analysis by ELISA or HPLC. In most cases (all samples with exception of those obtained in the microbiological degradation experiments - see part VII) samples for HPLC analysis were filtered again after thawing (RC 55, 0.45 µm pore size) and then enriched via C<sub>18</sub>-SPE (see above).

Samples for determination of **cell-bound microcystins** were filtered (membrane filter, RC 55, pore size 0.45 µm) immediately after sampling and the filter stored deep frozen until further treatment. The extraction procedure of the filters is described in Fastner et al. (1998).

### **1.2.2        *ELISA (Enzyme-Linked-ImmunoSorbent Assay)***

Two different ELISAs were used in the course of the project:

1. MCYST-ELISA, responding to a structural element typical only for MCYST as a cyclic peptide.
2. Adda-ELISA, responding to the adda-group typical for MCYST, but possibly also present in degradation products.

Usually the samples were first analyzed by Adda-ELISA and those with positive results subsequently analyzed by MCYST-ELISA. As the MCYST-ELISA and the HPLC analysis showed comparable results for the sum of different MCYST variants (with exception of some false negative ELISA results due to technical problems, see chapter 1.3.2) and an HPLC analysis gives further information on the different MCYST variants present, the MCYST ELISA was omitted from the analytical program after the first series of experiments.

#### **1.2.2.1      *MCYST-ELISA***

The method applied was developed by the Technical University of Munich and is described in Zeck et al. (2001). It is based on an immunological reaction with a [4-arginine]MCYST-specific antibody. This antibody has a strong binding (cross reactivity, see Zeck et al. 2001) only with intact microcystin molecules containing an arginine at the 4<sup>th</sup> position in the cyclic peptide. It therefore does not react with degradation products.

Standard solutions with known concentrations of MCYST-LR as well as solutions without MCYST (blanks, deionized water) were applied to each plate and each calibration point of the calibration curve as well as each sample value was determined by calculation of the

arithmetic mean of the data ( $n = 2$  to  $4$ ). Standard curves were obtained by fitting the calculated averages to a four parameter function according to Zeck et al. (2001).

The range of determination lies between about  $0.1 \mu\text{g/L}$  and  $1.0 \mu\text{g/L}$  (for details see chapter 3) and was determined for each plate separately. In case of concentrations exceeding  $1.0 \mu\text{g/L}$  the sample was diluted with deionized water for repeated analysis.

### **1.2.2.2 Adda-ELISA**

The Adda-ELISA used was a generic microcystin immunoassay based on monoclonal antibodies against the unusual adda group characteristic for microcystins, nodularins and certain peptide fragments (Zeck et al. 2002). The concentrations measured therefore comprise MCYST as well as possible degradation products. Calibration and determination of blind values was done following the method described for the MCYST-ELISA.

The range of determination also lies between about  $0.1 \mu\text{g/L}$  and  $1.0 \mu\text{g/L}$  (for details see chapter 3). As for the MCYST ELISA each value was determined as the average of two or three parallels taken from the same sample.

### **1.2.3 HPLC**

After  $\text{C}_{18}$ -SPE (see above) the microcystin variants were analyzed by HPLC - photodiode array detection (PDA) and identified by means of their characteristic UV-spectra (Lawton et al. 1994). A Waters 616 solvent delivery system with 717 WISP autosampler and a 991 photo diode array detector by Waters (Eschborn) was used. The separation was carried out on a LiCrospher® 100, ODS,  $5 \mu\text{m}$ , LiChroCART® 250 – 4 column system at a flow rate of  $1 \text{ mL/min}$ . The detection limit amounted to  $0.1 \mu\text{g/L}$ .

### **1.2.4 MALDI-TOF (Matrix Assisted Laser Desorption Ionization Time-of-Flight Mass Spectrometry)**

For structural identification a MALDI-TOF MS analysis was carried out in selected samples subsequently to the separation by HPLC according to am method by Fastner et al. (1999).

## **1.3 Analytical Problems / Open Questions**

### **1.3.1 Values below detection limit and limit of quantification (ELISA)**

The detection limits for the ELISA were calculated for each plate separately according to the  $3s$  definition using the mean value of the blanks measured in parallel ( $n = 11$ ) and setting the detection limit as the 3-fold standard deviation. Depending on various factors like water matrix, temperature or age of reagents, the detection limits varied between  $0.04 \mu\text{g/L}$  and  $3.59 \mu\text{g/L}$  for the Adda-ELISA and  $0.02 \mu\text{g/L}$  and  $0.42 \mu\text{g/L}$  for the MCYST-ELISA. The

median values were 0.2 µg/L and 0.09 µg/L, respectively. The limits of quantification were calculated as the 3-fold detection limit, thus ranging from 0.12 µg/L to 10.77 µg/L (Adda-ELISA) and from 0.06 µg/L to 1.26 µg/L (MCYST-ELISA). In cases of unusually high detection limits (> 1 µg/L) analyses were repeated.

In the field samples from the transects at Lake Tegel and Lake Wannsee, the majority of the values measured were below the limit of quantification. In agreement with the other NASRI working groups, the results for these samples were set to half the limit of quantification and those below detection limit were set zero for the statistical calculations. For the diagrams showing median values and 90th percentile (see final NASRI Report "algae", part I) values below detection limit were labeled "n.d." (not detected) and values below quantification limit were labeled "T" (for traces). In cases of only one value below quantification limit (and the others not detectable), the exact quantification limit was given (e.g. < 0.22 µg/L).

### **1.3.2        *Comparability of ELISA and HPLC Results***

The MCYST-ELISA was performed in parallel to HPLC analysis only during the first field scale experiments (SSF 2, SSF 5, SSF 6 and E 1). Figure 2 shows the results of both methods in relation to each other. Two groups of data points can be distinguished: one group showing a good correlation between ELISA and HPLC-results and a second one with only very little MCYST detected by ELISA and values of up to nearly 2 µg/L by HPLC.

For the first group the regression coefficient amounts to 0.939. The gradient of the linear regression curve is, however, only 0.18, showing that ELISA results exceed those measured by HPLC by a factor of about five. This is only secondarily due to losses during C<sub>18</sub> solid phase extraction, as this account for losses only between 10 and 20 %. The main reason for the distinctively higher values by ELISA is probably the varying response of the ELISA to the different MCYST variants and the fact that the ELISA responds to the sum of all MCYST variants present, while the HPLC gives only results for variants present in concentrations above 0.1 µg/L.

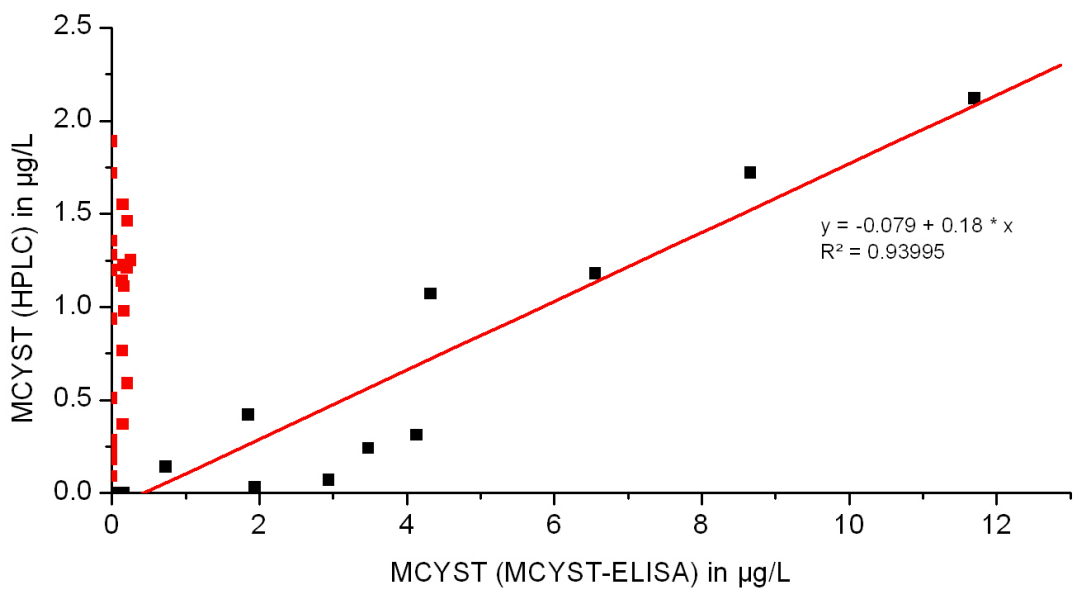


**Figure 2: ELISA and HPLC analysis in relation**

The second group of data points in Figure 2 was due to analytical problems with the ELISA in summer 2003, during which the temperature in the laboratory exceeded the optimal range of 20° to 25°. This problem was solved in the following summer by using a laboratory with air conditioning. The regression coefficient between results obtained by Adda-ELISA and those acquired by HPLC amounted to 0.24 - showing only very little agreement of both methods. This is due to the fact that the Adda-ELISA responds to all substances with the Adda-group, i.e. also to possible degradation products of MCYST (Zeck et al. 2002).

For this reason the field samples from the transects Wannsee and Tegel were analyzed first by Adda-ELISA and in case of positive signals, also by MCYST ELISA, thus yielding first all substances containing the Adda-group (i.d. MCYST and possible degradation products) and in a second step MCYST only. As only very low concentrations were expected to occur in the groundwater samples, HPLC-analysis was restricted to an intensive sampling campaign at Lake Wannsee in autumn 2004 (see final NASRI Report "algae" part I).

In order to allow analysis with HPLC, higher input levels of MCYST were aimed at in the field scale experiments on the enclosures and SSF of the UBA's experimental field (final NASRI Report "algae", parts IV and V). Thus, the ELISA (in most cases the Adda-ELISA) gave a first impression on the distribution of MCYST in the samples over time (up to 250 samples were taken during one field scale experiment). Subsequently selected samples were analyzed by HPLC yielding further information on the concentrations of the different MCYST variants and higher precision than the ELISA (see above). In most cases the results of the HPLC analysis were used for the modelling and elimination calculations.

In the laboratory experiments (final NASRI Report "algae", parts VI and VII) the small sampling volume was the restricting parameter. For the clogging column and temperature

column experiment this allowed for ELISA analysis only, as realistic MCYST concentrations (< 1 µg/L) were targeted in the effluent. For the batch degradation experiments the input concentrations (about 50 mg/L) were sufficient to conduct HPLC analysis without further concentration by solid phase extraction.

### 1.3.3 Appearance of new peaks in the HPLC Chromatogram

During the experiments the HPLC analyses yielded surprising results concerning the different MCYST variants: While the input solution showed a dominance of demethylated MCYST-RR (dem. [Asp<sup>3</sup>] MCYST RR) which is the main variant produced by the cultured *Planktothrix agardhii* HUB 76, a large number of new peaks appeared in the HPLC chromatogram of the effluent samples with UV spectra characteristic for MCYST (Figure 3).

This phenomenon was observed in all experiments in which an HPLC analysis of the effluent samples was carried out (enclosure and SSF experiments as well as the batch degradation experiments). The number of variants and the exact retention time varied, however, from experiment to experiment as well as between different series of measurements. Therefore, experiments were carried out to clarify whether the filtration process actually leads to shifts in MCYST variants or whether this observation is based on an artefact caused by the analytical method.

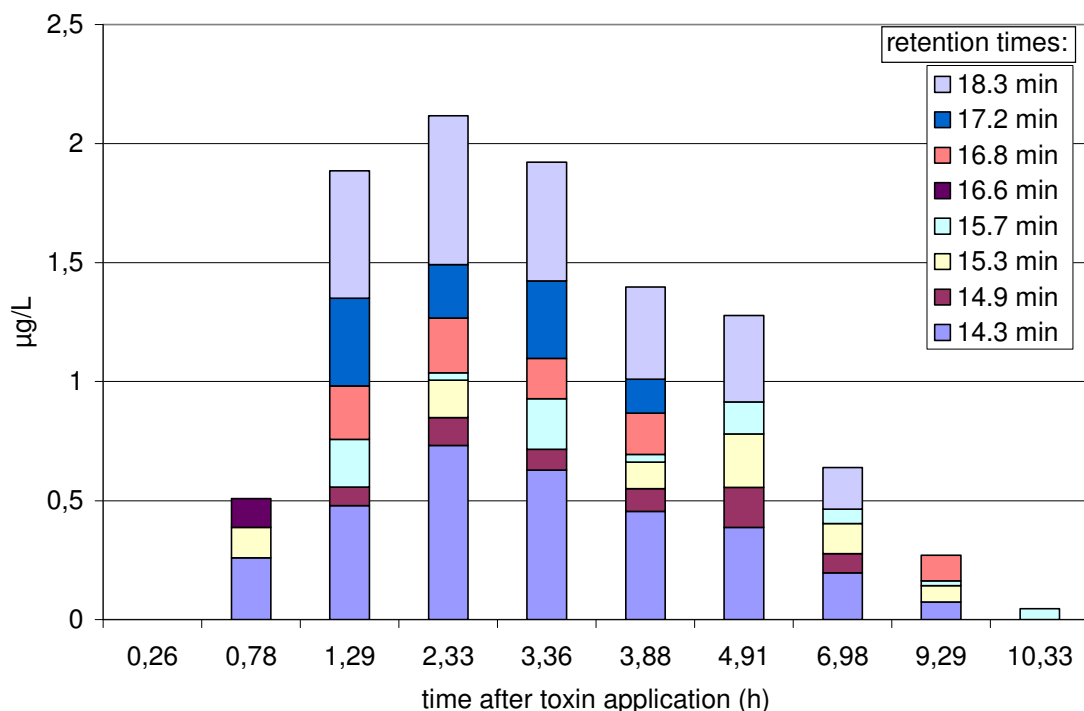


**Figure 3:** Peaks in the HPLC chromatogram with UV spectra characteristic for MCYST in samples from experiment E2 (sampling port in 20 cm depth). The input solution showed only one peak at 13.6 minutes retention time (corresponding to dem. [Asp<sup>3</sup>] MCYST-RR) which was no longer detected in the effluent.

An explanation could be that due to the dominance of dem. MCYST-RR in the input solution other MCYST variants (or substances with similar UV-spectra) were not well separated in the HPLC and thus not detectable (or "hidden"), though present in low concentrations. For this reason, a MALDI-TOF analysis were carried out with the extract from the *Planktothrix agardhii* mass culture, first with the total sample and in a second step with previous separation by HPLC PDA. Then the same analyses were carried out with effluent samples after HPLC-PDA separation. The input solution showed the same molecular masses in the total sample and in the previously separated peaks. These were, however, different from the molecular masses detected in the effluent samples, indeed indicating that the substances present in the effluent samples had not been present in the input samples and that they represent (potentially intermediate) degradation products.

An identification of the substances present in the effluent samples was not possible, as the molecular masses did not correspond to known MCYST variants. Clarification of the mechanisms causing this result is important for understanding MCYST degradation and will have to be subject of further research.

In the field experiments all new HPLC peaks showed similar degradation rates to MCYST so that persistence of these degradation products does not seem likely under the conditions simulated. During the anoxic batch degradation experiments, however, the new substance persisted over a period of more than 20 days (see final NASRI Report "algae", part VII). Here further degradation experiments as well as toxicological tests will be needed in order to assess whether or not this degradation product is of any relevance to human health in bank filtrated drinking water, if it should occur in sufficiently high concentrations.

## 1.4 References

- Botes, D.P., Wessels, P.L., Kruger, H., Runnegar, M.T.C., Santikarn, S., Smith, R.J., Barna, J.C.J. & Williams, D.H. (1985): Structural studies on cyanoginosins-LR, -YR, -YA and YM, peptide toxins from *Microcystis aeruginosa*, J.Chem. Soc, Perkin Transactions, I: 2747 – 2748.
- Fastner J., Erhard M., Carmichael W.W., Sun F., Rinehart K.L., Rönicke H. & Chorus I. (1999): Patterns of different microcystins in field samples dominated by different species of cyanobacteria., Arch Hydrobiol 145 (2): 147 – 163.
- Fastner, J., Flieger, I. & Neumann, U. (1998): Optimised extraction of microcystins from field samples - a comparison of different solvents and procedures. Wat. Res. **32**: 3177 – 3181.
- Harada, K., Kondo, F. & Lawton, L. (1999): Laboratory analysis of cyanotoxins. – in: Chorus, I. & Bartram, J. (eds): Toxic cyanobacteria in water – a guide to their public health consequences, monitoring and management: 369 – 405. E & FN Spon.
- Lawton, L.A., C. Edwards, G.A. Codd (1994): Extraction and high-performance liquid chromatographic method for the determination of microcystins in raw and treated waters, Analyst, 119: 1525 – 1530.

- Sivonen, K. & Jones, G. (1999) Cyanobacterial Toxins, Toxic Cyanobacteria in Water, A Guide to their public health consequences, monitoring and management, I. Chorus & J. Bartram (eds.) The World Health Organization, E &FN Spon, London, p. 41-112.
- Zeck, A., Eikenberg, A., Weller, M.G., & Niessner, R. (2001): Highly sensitive immunoassay based on a monoclonal antibody specific for [4arginine]microcystins. - *Analytica Chimica Acta*, **441**: 1 - 13, Elsevier.
- Zeck, A., Weller, M.G., Bursill, D. & Niessner, R. (2002): Generic microcystin immunoassay based on monoclonal antibodies against Adda. - *The Analyst*, **126**: 2002 - 2007.

## 2 Field Investigations on Transect Lake Tegel

### 2.1 Introduction

Monitoring of Lake Tegel's surface water with respect to cyanobacterial toxins was conducted with the aim of triggering bank filtrate monitoring in case of toxic cyanobacterial blooms. Previous investigations had shown that during the last few years (unpublished data of our own working group) cyanobacterial blooms have no longer been occurring in Lake Tegel (though minor populations have been present every summer, and temporarily increased concentrations of total P in 2000 and 2001 provided a carrying capacity sufficient to sustain major populations).

### 2.2 Results and Interpretation

Figure 4 shows the total and extracellular MCYST-concentrations measured by Adda-ELISA as well as measurements with MCYST-ELISA of total MCYST in 2002. These samples were taken during the monthly sampling campaign of the NASRI project and originate from the lake shore in front of the transect.

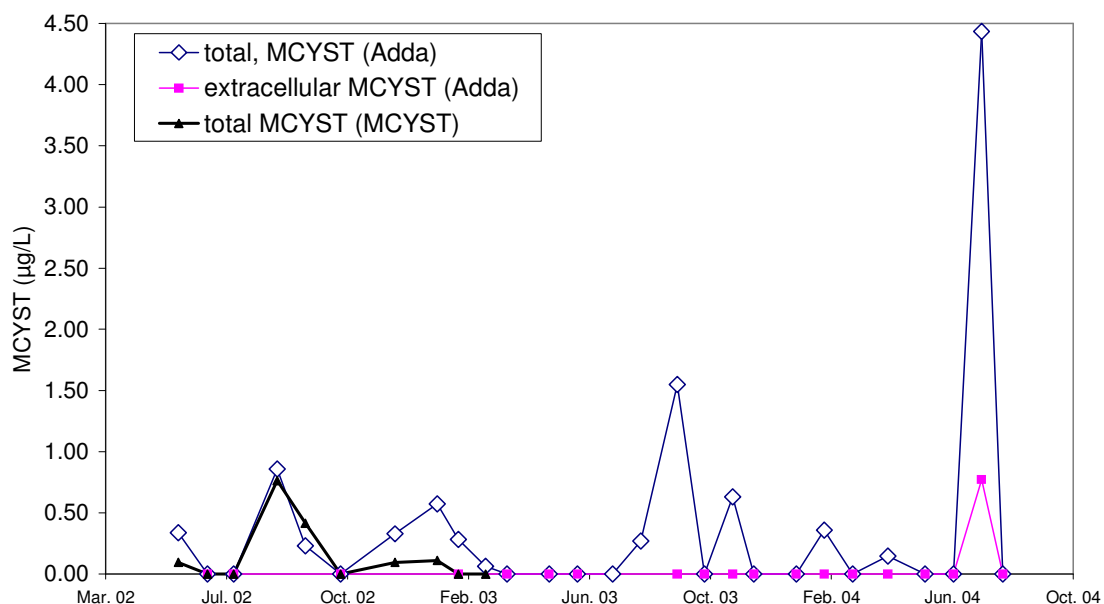


**Figure 4 : Total and extracellular Microcystin (MCYST) concentrations determined with different ELISAs (specifically for ADDA and for the MCYST molecule) in Lake Tegel's surface water 2002 - 2004.**

These results show

- Concentrations measured by MCYST-ELISA are usually lower than those determined by Adda-ELISA. This in accordance with the theory that MCYST degradation products still containing the Adda-group are detected by this ELISA additionally to microcystins themselves. For 2003 and 2004 the analyses therefore were carried out by Adda-ELISA only, giving the worst-case concentration.
- Maximum concentrations were usually measured during July (2004), August (2002) or September (2003), although in winter 2002/2003 traces were also observed in November through January. Measurements carried out by our working group in the context of a different programme in the lake centre (analyses done by HPLC) show a similar pattern although with distinctively lower values (Figure 5). Maximum concentrations measured by HPLC lie around 0.1 µg/L whereas those measured by ELISA reach 1.5 µg/L (2003) and 4.5 µg/L (2004).

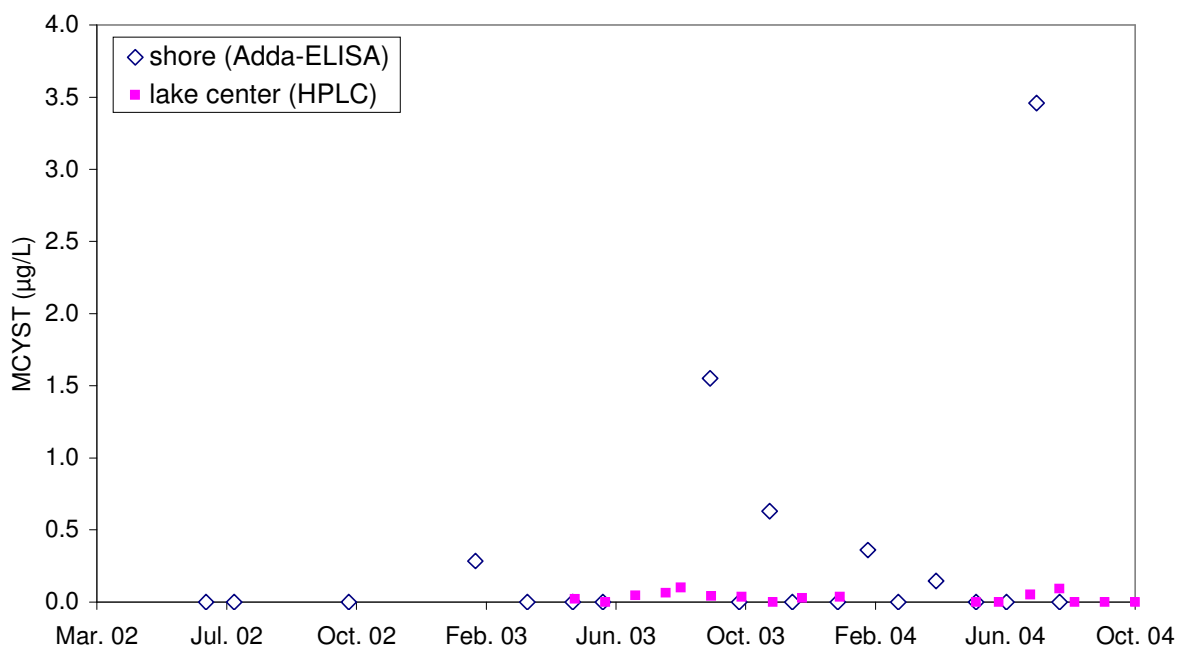


**Figure 5 : Cell-bound MCYST for samples taken from the shore, analysed with ADDA-ELISA, and the lake centre, analysed with HPLC.**

This is most likely to be due to two factors: i) some portion of the MCYST identified by the Adda-ELISA might result from degradation products and ii) due to wind and currents cyanobacteria tend to accumulate near the eastern shore of Lake Tegel, thus leading to higher toxin concentrations.

The reason for elevated MCYST concentrations during the summer months is shown in Figure 6. Usually high densities of toxic cyanobacteria (in Lake Tegel the only toxic species of relevant population density is *Microcystis* spp.) coincide with elevated

microcystin concentrations. This is true for August 2002, August/September 2003 and July 2004. On other occasions however high densities of cyanobacteria did not lead to elevated MCYST concentrations (July 2003). This is true for samples taken from the lake centre as well as from the shore, so regional variability might not be the primary cause. The main reason therefore seems to be that different toxin concentrations per cell or dominance of subspecies with different toxin content can occur throughout the season.

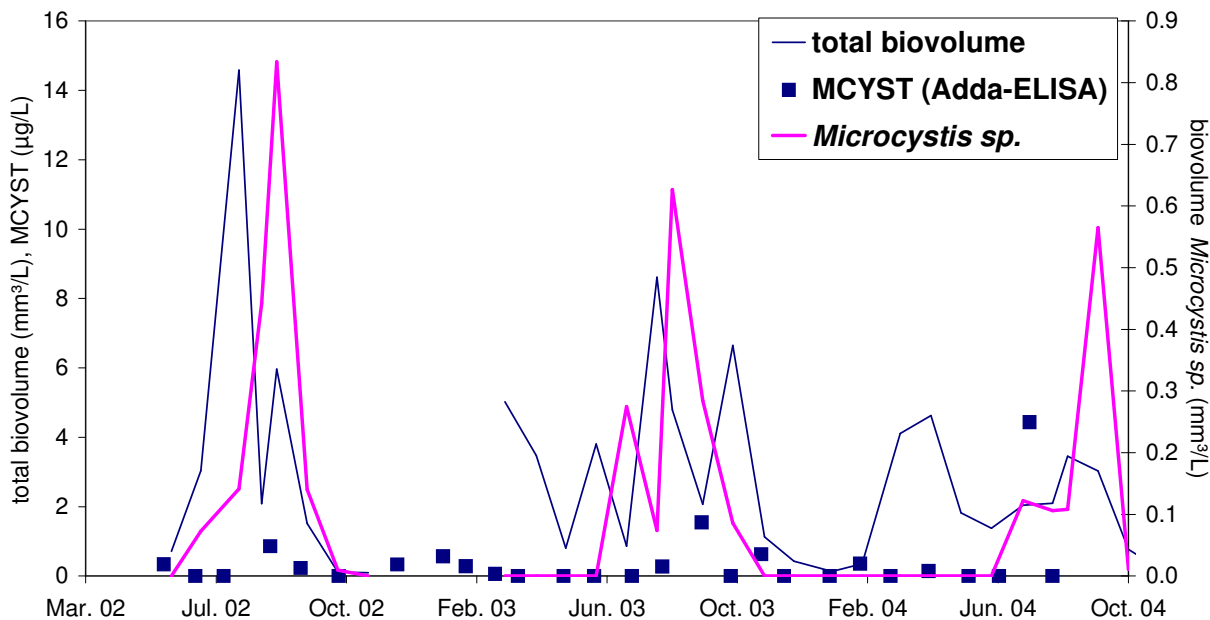


**Figure 6 Total phytoplankton biovolume, total MCYST determined by Adda-ELISA (left axis) and biovolume of toxic cyanobacteria *Microcystis* sp. (right axis) in Lake Tegel.**

- Extracellular MCYST was usually not detected in the surface water samples. The only occasion with detectable extracellular MCYST was in July 2004, when total MCYST reached 4.5 µg/L and extracellular MCYST amounted to 0.77 µg/L (22 %). Although this inverse ratio is unusual (according to Sivonen & Jones, 1999, the share of extracellular MCYST usually amounts to less than 10 %), it is not unlikely that unfavourable conditions (low temperatures, aging population) can trigger some cell lysis and MCYST release from the cells. On the other hand degradation products that are possibly included by Adda-ELISA measurement are likely to occur outside the cyanobacterial cells thus leading to higher extracellular concentrations.

## **2.3            *Conclusions***

Although toxic cyanobacteria occur in Lake Tegel, their share of total biovolume in the years 2002 to 2004 seldom exceeded 10 %. Maximum shares of 20 % to 30 % usually occurred during July, August or September and led to microcystin concentrations measured by Adda-ELISA of less than 1.5 µg/L in 2002 and 2003 on the eastern shore next to the transect. As previous investigations (Chorus et al. 2004) had shown that these concentrations are not high enough to be recovered in the observations wells, groundwater samples from transect Tegel were not analysed during the project.

We recommend, however, to continue surface water sampling in order to ascertain that the input MCYST concentrations for the Lake Tegel bank filtration as well as the artificial recharge site remain on this level.

## **2.4            *References***

- Chorus, I., Grützmacher, G., Wessel, G. & Pawlitzky, E. (2004): BMBF-Forschungsvorhaben: Strategien zur Vermeidung des Vorkommens ausgewählter Algen- und Cyanobakterienmetabolite im Rohwasser – Abschlußbericht - . BMBF-Förderkennzeichen 02 WT9852/7.
- Sivonen K. & Jones G. (1999): Cyanobacterial Toxins, in: Toxic Cyanobacteria in Water, A Guide to their public health consequences, monitoring and management, I. Chorus & J. Bartram (eds.) The World Health Organization, E & FN Spon, London, p. 41-112.

### **3 Field Investigations on the Transects at Lake Wannsee**

#### **3.1 Introduction**

Investigations of cyanobacterial toxin removal at the Lake Wannsee Transects required a detailed monitoring of cyanobacterial biovolume in the surface water because of their high temporal variation. For this reason weekly to fortnightly sampling of surface water was carried out during the summer months in addition to the monthly sampling of ground- and surface water by BWB. The aim was not only to obtain detailed information on cyanobacteria and microcystin concentrations in Lake Wannsee, but also to trigger a weekly sampling campaign for one month during autumn 2003 subsequent to a cyanobacterial bloom with high toxin concentrations.

#### **3.2 Results and Interpretation**

##### **3.2.1 Surface water**

The results of the weekly to fortnightly surface water monitoring conducted by our working group are presented in Figure 7. The data for the biovolume of cyanobacteria show distinct cyanobacterial blooms during summer in all three years. During July and August *Microcystis* sp. prevailed (in 2003 also *Aphanizomenon* sp.), in September and October *Planktothrix agardhii* dominated the cyanobacterial population. Maximum biovolumes ranged from 18 mm<sup>3</sup>/L to nearly 50 mm<sup>3</sup>/L total cyanobacteria which correspond to similar values in the years 1999 - 2002 observed by our own working group (pers. communication Kurmayer). The unusually warm and dry summer of 2003 resulted in a bloom of *Aphanizomenon*, which was not present in the other years. As this species does not produce microcystin (MCYST), concentrations of this toxin during July and August were lower in 2003 than in the other years.

Highest MCYST concentrations were usually found during the *Planktothrix* bloom in September and October, reaching maximum values of 10 µg/L to 14 µg/L of intracellular MCYST (determined by HPLC) in the water body of the lake. Samples taken from scums accumulating near the shore during a bloom on Sept. 15th 2003 showed significantly higher concentrations, i.e. up to 29 µg/L intracellular MCYST (determined by HPLC). At this occasion also extremely high values of extracellular MCYST concentrations were determined (12 µg/L). One week later intracellular concentrations at this spot had decreased to 19 µg/L and extracellular values reached only 1.5 µg/L.

The concentrations measured by ADDA-ELISA also showed peaks during summer. Their time patterns correspond to those determined by HPLC, although generally they tended to be somewhat higher (maximum values reached more than 20 µg/L in 2004). As the ELISA cannot distinguish between pure ADDA and MCYST-breakdown products containing the ADDA-moiety, in the following the signal of this ELISA is interpreted as reflecting concentrations of "ADDA-containing substances" (see also methods). Extracellular ADDA-containing substances occurred in unusually high shares (more than 80% of the total concentrations in September 2003). Although artefacts in sample preparation (see below) cannot totally be excluded, this may be explained by the fact that the ADDA-ELISA responds to MCYST degradation products that are not expected to occur inside the cells.

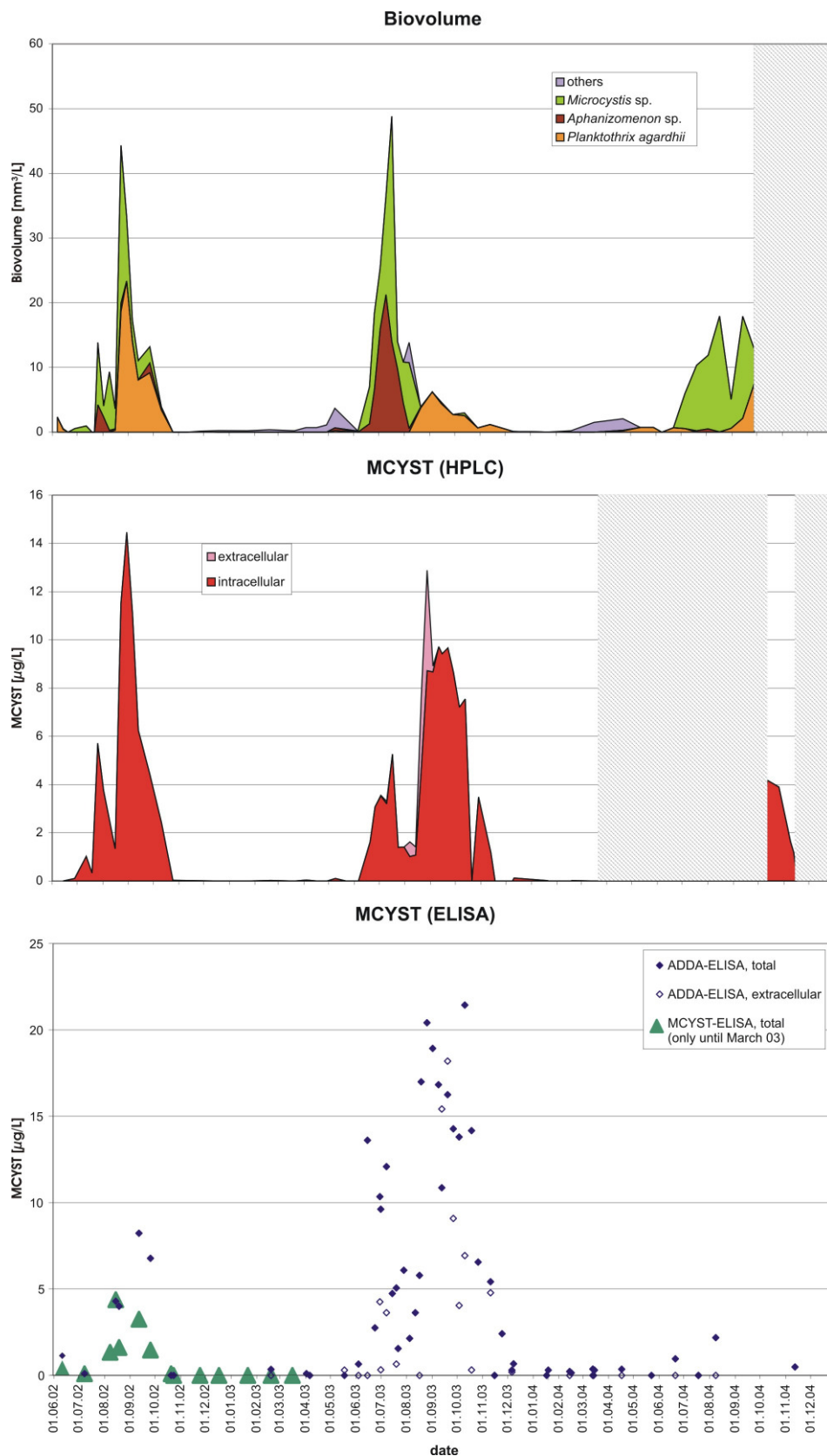


**Figure 7: Results of the surface water monitoring at Lake Wannsee: Biovolume of cyanobacteria and MCYST analysed by HPLC and ELISA. (Mean values of up to 4 samples from different places on one occasion. Shaded areas: no data.)**

For summer (May through October) of all three years, the median input value for MCYST determined by HPLC into the bank filtration system at Lake Wannsee amounted to 3.4 µg/L and < 0.1 µg/L for intra- and extracellular MCYST, respectively (see Table 1). High values for the 90th percentile of 9.6 µg/L for intracellular and 0.6 µg/L for extracellular MCYST reflect the substantial temporal variability. During winter (November through April) the median concentration of intra- and extracellular MCYST amounted to less than 0.1 µg/L.

**Table 1 Median values and 90th percentile for summer and winter concentrations of MCYST in Lake Wannsee's surface water determined by HPLC, MCYST-ELISA and ADDA-ELISA.**

MCYST in µg/L	summer		winter	
	intracellular	extracellular	intracellular	extracellular
HPLC				
median	3.4	< 0.1	< 0.1	< 0.1
90th percentile	9.6	0.6	0.1	< 0.1
number of analyses	42	21	16	10
	total	extracellular	total	extracellular
MCYST-ELISA				
median	0.51		< 0.21	
90th percentile	3.26		< 0.21	
number of analyses	11	0	5	0
ADDA-ELISA				
median	5.1	0.3	0.2	< 0.5
90th percentile	16.9	11.6	0.7	2.5
number of analyses	39	17	21	6

### 3.2.1.1 Groundwater

Figures Figure 8 to Figure 10 give a summary of the results obtained by determination of total and extracellular MCYST with the MCYST-ELISA (Figure 8) and the ADDA-ELISA (Figure 9 and Figure 10).

In transect 1, MCYST determined by MCYST-ELISA was only detected in observation well 3339 which is the well with the shortest travel time (figure 2). Detectable traces (< 0.1 µg/L) were observed in samples taken in September and October 2002, simultaneously to the Planktothrix bloom in the surface water (Figure 7). MCYST and ADDA-containing substances determined by ADDA-ELISA were also detected in the adjacent observation wells 3338 and 3337 with slightly longer travel times (Figure 9). The 90th percentile values of 0.22 µg/L and 0.04 µg/L of extracellular ADDA-containing substances show that there is some migration of MCYST degradation products into the aquifer (Figure 10). These are however retained in the

subsurface as no more values above detection limit were found in the other observation wells nearer to the drinking water production well.

In transect 2, MCYST determined by MCYST-ELISA was found in the one-time samples taken from BEE207OP and BEE207MP1 in January 2003 that are situated in the usually unsaturated zone beneath the lake (Figure 8). In both cases the values cannot be quantified ( $< 0.58 \mu\text{g/L}$  and  $< 0.06 \mu\text{g/L}$ ), but there are, however, clear positive signals above detection limit. The only other observation well on the western side of the drinking water production well with detectable MCYST was BEE202MP2 with a value slightly above detection limit ( $0.02 \mu\text{g/L}$ ) in January 2003. This value was not confirmed with the ADDA-ELISA, however, this might be due to its higher detection limits. A single positive value  $> 0.2 \mu\text{g/L}$  (detection limit) in BEE204OP on the eastern side of the drinking water production well was not confirmed by the ADDA-ELISA. This might have been due to interferences with the groundwater matrix leading to a false positive signal, as usually the trend was towards higher values with the ADDA-ELISA as compared to the MCYST-ELISA.

ADDA-containing substances were detected in the observation wells BEE205, BEE206, BEE207OP, MP1 and UP as well as in BEE202MP1 and MP2 (Figure 9). With exception of a value of  $1.38 \mu\text{g/L}$  measured in BEE207UP in December 2003, no concentrations could be quantified ( $<$  limit of quantification). The number of observation wells with detectable traces is clearly higher than for the MCYST-ELISA. This shows that this ELISA responds to a higher number of substances which are probably MCYST degradation products.

Extracellular ADDA-containing substances could not be detected in the groundwater of transect 2, with exception of one value of  $< 0.6 \mu\text{g/L}$  on the eastern side of the drinking water well. This is most likely a false positive, as it is unlikely that i) degradation products remain inside cyanobacterial cells and ii) cyanobacterial cells can travel this far in the subsurface. The conspicuous absence of concentrations detectable with the ADDA-ELISA may be a methodological artefact. Potentially the ADDA-containing substances are retained on the membrane filter material used for pre-treatment. This could be due to either adsorption on the membrane filter or adsorption on suspended particles. These results show a need for specifically targeted investigations of behaviour of trace concentrations of extracellular MCYST in the laboratory system, which are intended in the context of future research. This uncertainty of the results in these minimal concentration ranges need to be taken into account for data interpretation.

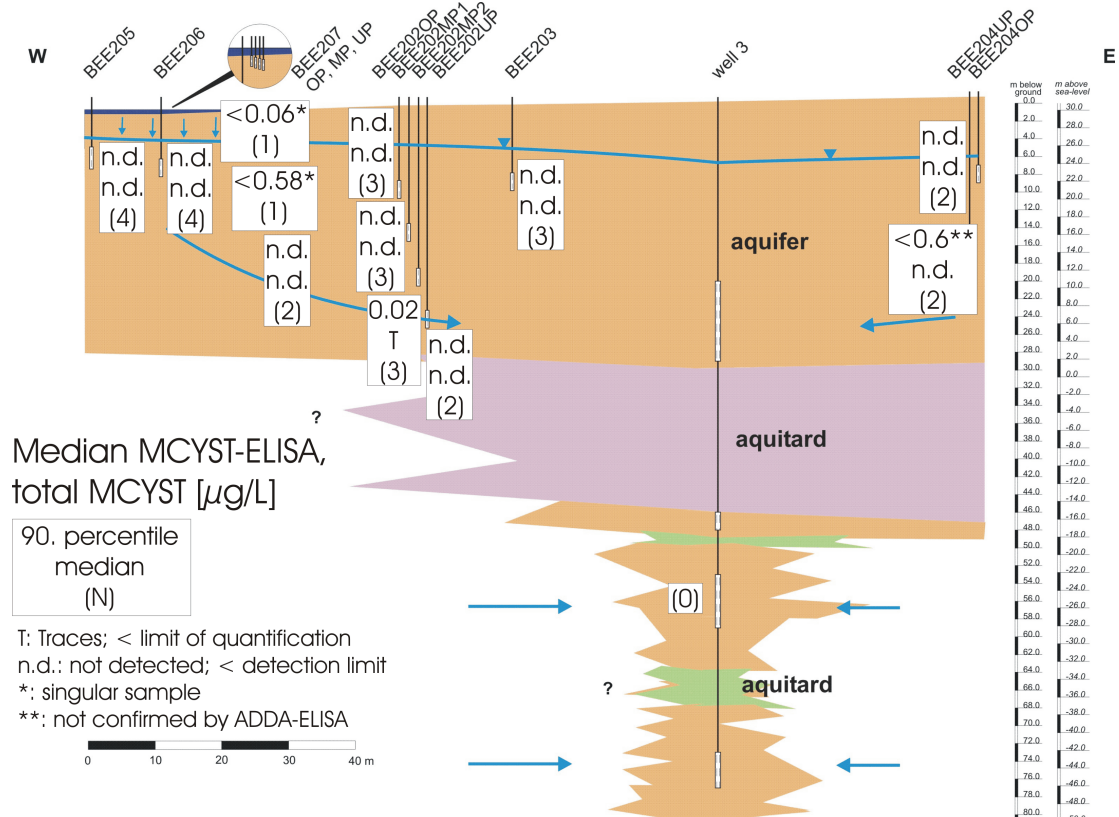
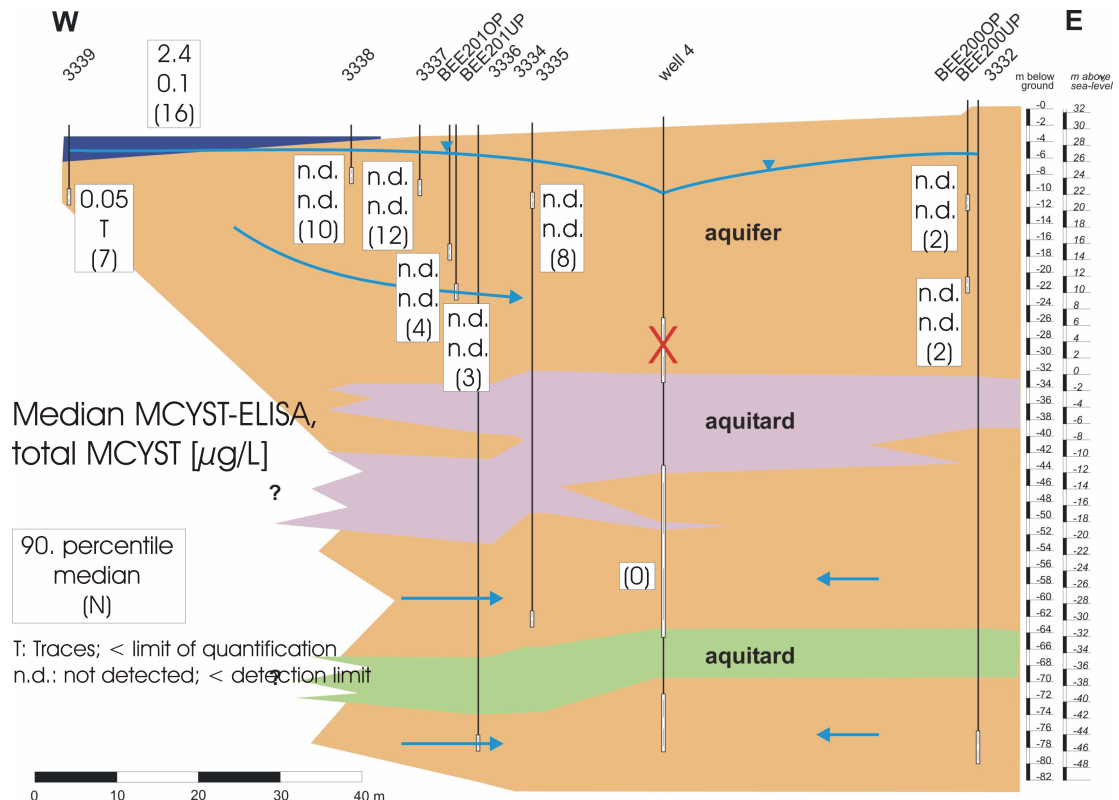


**Figure 8: Results of total MCYST at transect 1 and 2, analysed by MCYST-ELISA (May 2002 to August 2004).**

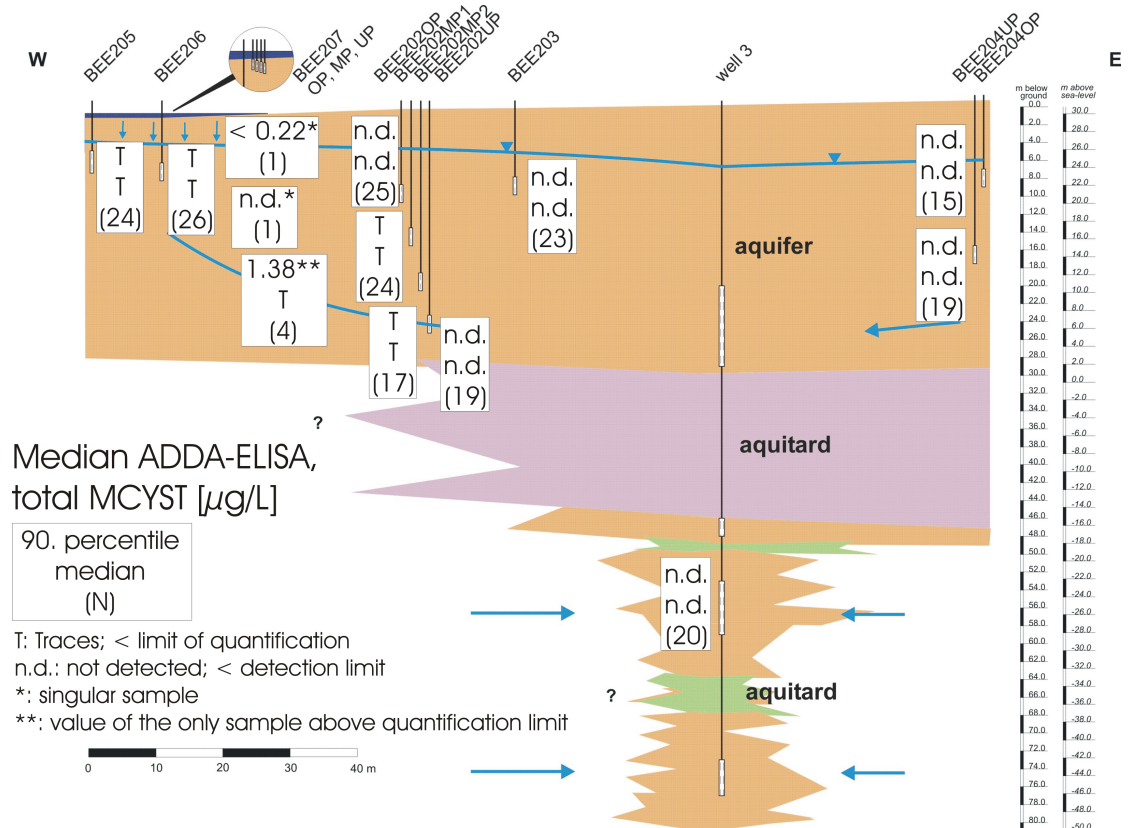
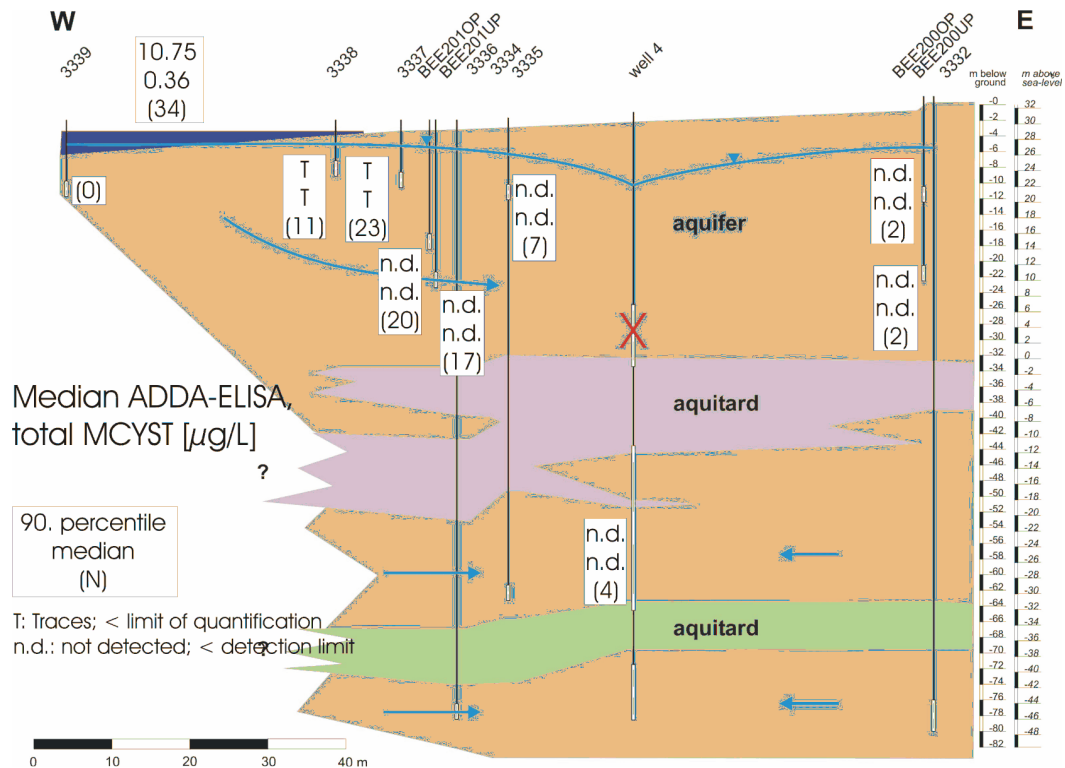


**Figure 9: Results of total MCYST at transect 1 and 2, analysed by ADDA-ELISA (May 2002 to August 2004).**

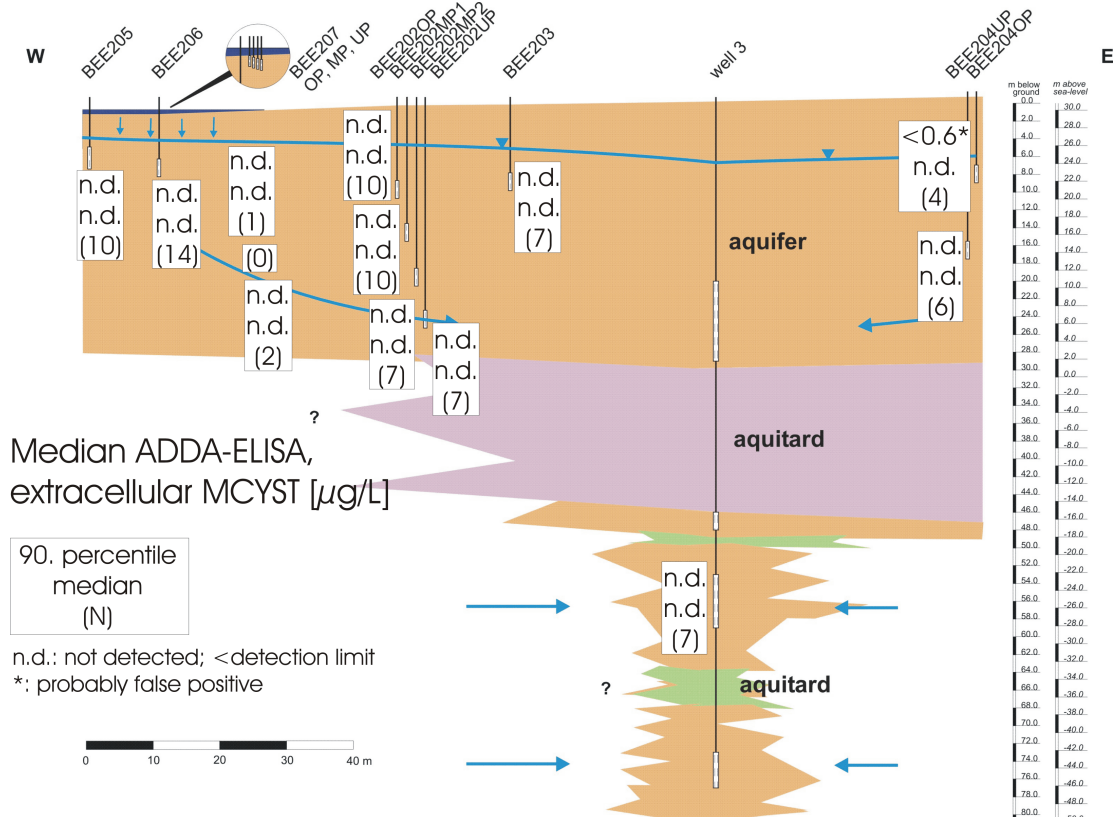
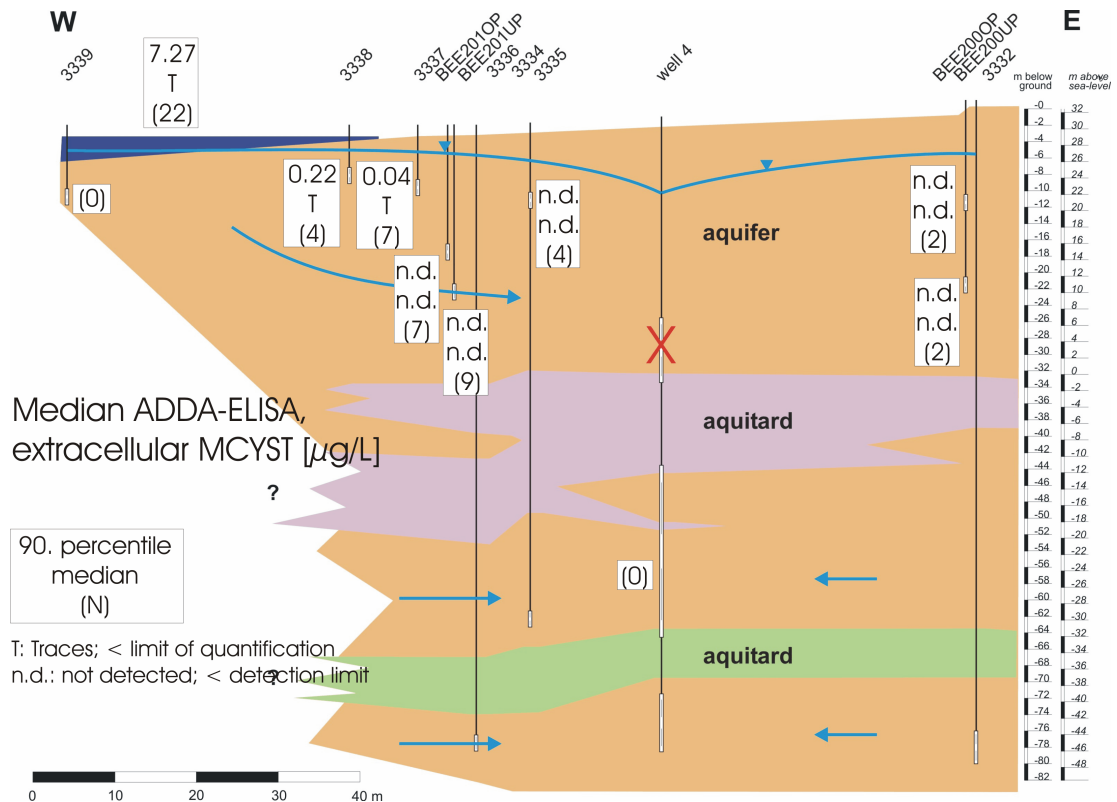


**Figure 10: Results of extracellular MCYST at transect 1 and 2, analysed by ADDA-ELISA (May 2002 to August 2004).**

About one month after a bloom of cyanobacteria in 2003, weekly sampling of selected shallow observation wells of the transects was started to observe potential breakthrough of MCYST. For this campaign, samples were analysed both by HPLC and by ELISA. Figure 11 shows the results of this intensive sampling campaign.

In contrast to other investigations maximum extracellular MCYST concentrations in the surface water were detected during the initial phase of the bloom (until the beginning of September). In this phase nearly one third of the total MCYST was extracellular. The bloom reached maximum values of 8.8 µg/L intracellular MCYST, which is not very high compared to the other years. The bloom, however, prevailed for a month (end of August to end of September) and then slowly broke down. MCYST concentrations around 1 µg/L were observed until the middle of November.

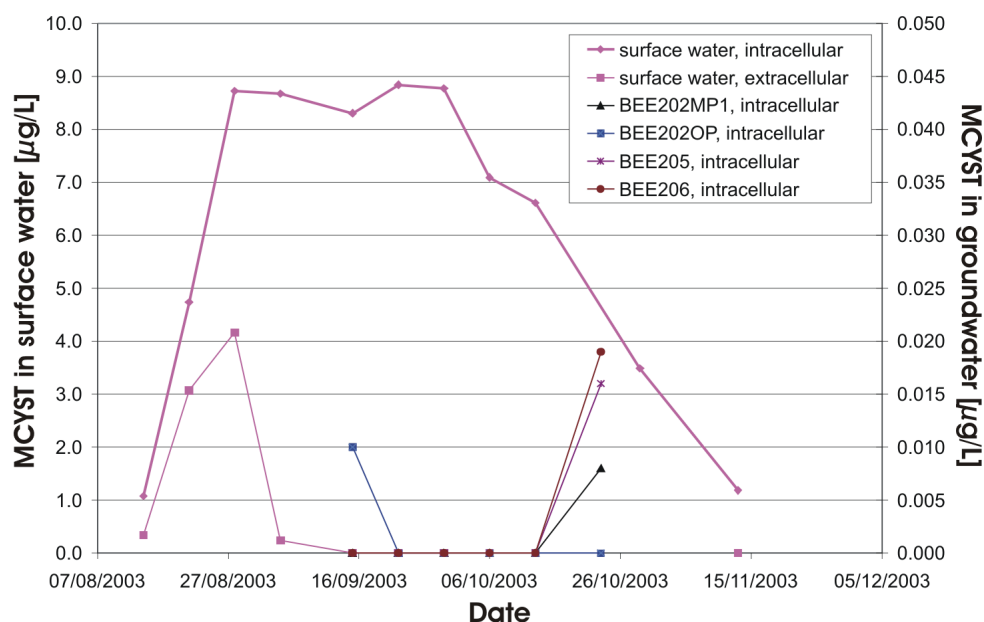


**Figure 11: MCYST concentrations in surface- and groundwater analysed during the intensive sampling campaign in autumn 2003 (extracellular MCYST was not detected in the groundwater samples).**

In the groundwater traces slightly above the limit of quantification were analysed by HPLC for intracellular MCYST. With exception of observation well BEE202OP these occurred a month later than previously assumed (so that only the last sample of this campaign contained MCYST). This as well as the fact that no extracellular MCYST was detected leads to the assumption that processes other than degradation or adsorption of extracellular MCYST might prevail. MCYST occurrence might be a function of a variety of factors including toxin release from the cells, adsorption onto carrier substances, flow velocity etc.

### 3.3 *Conclusions*

Cyanobacteria were present in the surface water every summer during the time period of the investigations. The blooms were similar to those during the last few years, however, not as severe as in other regions, where cyanobacterial densities can reach 10- to 100-fold higher values because of scum accumulation, which is not pronounced at the site of the transects. Highest MCYST concentrations (at times more than 20 µg/L) were observed during the bloom of *Planktothrix agardhii* in September and October 2003. Concentrations determined by ADDA-ELISA were usually higher than those measured by HPLC, and also indicated higher shares of extracellular MCYST. This is probably due to the fact that the ADDA-ELISA also responds to ADDA-containing degradation products of MCYST, which would usually occur outside the cyanobacterial cells.

In the groundwater MCYST and ADDA-containing substances were sometimes detectable in traces by ELISA only in the observation wells closest to the shore. Due to the minimal concentrations and due to the fact that the detection limit of the ELISA varies from analysis to analysis (see methods) the occurrence of positive signals might rather be a function of sensitivity of the ELISA than of input and transport in the groundwater.

Nevertheless some basic conclusions can be drawn:

- maximum elimination of MCYST and ADDA-containing substances occurs during the first few meters of underground passage,
- concentrations after 0.5 to 1 month of underground passage (BEE205, BEE206, 3339) usually lie well below 1 µg/L,
- the only observation well that showed ADDA-containing substances above quantification limit was BEE207UP, where sampling was difficult and no representative sample could be taken.

As quantification of MCYST concentrations in the bank filtrate was limited in face of the extremely low values, degradation rates could not be estimated from these field observations. Therefore, the investigations on this topic focussed on the experiments on UBA's experimental field in Berlin, Marienfelde.

## **4 Artificial Recharge Pond**

### **4.1            *Introduction***

As cyanobacterial biovolume in Lake Tegel did not exceed 1 mm<sup>3</sup>/L (which is less than a tenth of the amount found in Lake Wannsee), it was not expected to find cyanobacteria in large quantities in the artificial recharge pond Tegel (which is fed with surface water from Lake Tegel). To ascertain this, however, the surface water of the pond was monitored for cyanobacteria in the first year of the project and toxins were analysed in case of positive findings.

### **4.2            *Methods and Materials***

Monthly samples of the surface water were first analyzed by microscope according to Lawton et al. (1999) to determine if cyanobacteria were present. In presence of cyanobacteria HPLC-PDA (High Pressure Liquid Chromatography – Diode Array) analyses for cell-bound microcystins were carried out after filtration and extraction according to Fastner et al. (1998).

### **4.3            *Results***

The results of the microscopic examination and the HPLC analyses are shown in Table 2. Only few cyanobacteria were found in the surface water of the AR pond. The highest biovolumes were observed during winter in December and January. During this time cyanobacterial biovolume reached values around 0.3 mm<sup>3</sup>/L. These are normal background concentrations for Lake Tegel and may be due to the fact that the microfiltration unit, which filters lakewater fed to the AR pond, was shut off during winter.

Cell-bound Microcystin concentrations of 0.05 and 0.14 µg/L were detected in the December and January samples, respectively. However, extracellular Microcystin could not be detected in any of these samples.

**Table 2: Results of microscopic and HPLC-analysis of surface water at the artificial recharge pond in Tegel (GWA Tegel).**

Date	Cyanobacteria detected by microscopic analysis	Biovolume (mm <sup>3</sup> /L)	cell-bound Microcystins variants (HPLC) in µg/L
24.05.2002	none	not determined	no analysis
18.07.2002	none	not determined	< 0.01*
15.08.2002	few ( <i>Microcystis</i> sp.)	0,06	< 0.01*
17.09.2002	few ( <i>Microcystis</i> sp.)	0,05	< 0.01*
18.10.2002	very few ( <i>Planktothrix agardhii</i> )	< determination limit	< 0.01*
21.11.2002	very few ( <i>Microcystis</i> sp., <i>Planktothrix agardhii</i> , cf. <i>Limnothrix</i> sp. )	< determination limit	no analysis
12.12.2002	very few ( <i>Planktothrix agardhii</i> , <i>Limnothrix redeckii</i> )	0,35	0,05
16.01.2003	some ( <i>Planktothrix agardhii</i> , <i>Limnothrix</i> sp., <i>Limnothrix redeckeii</i> , <i>Pseudoanabaena</i> sp.)	0,27	0,14
13.02.2003	some ( <i>Planktothrix agardhii</i> , <i>Limnothrix</i> sp., <i>Limnothrix redeckeii</i> , <i>Pseudoanabaena</i> sp.)	0,07	< 0.01*
13.03.2003	very few	< determination limit	< 0.01*
24.04.2003	very few ( <i>Limnothrix redeckeii</i> )	< determination limit	< 0.01*

\* Detection limit for individual MCYST variants.

During a dry phase in July 2003 three cores (10 cm) were taken from the infiltration pond. One core was examined by microscope. The surface layer (1 mm) showed a high content of green algae (*Cladophora* sp.) and diatoms (*Navicula* sp.). Cyanobacteria were not visible. Beneath the surface layer the amount of live organisms decreased rapidly.

Due to these low concentrations no groundwater samples were taken for toxin analysis and the investigations for cyanobacteria and microcystins in the surface water were not continued after April 2003.

#### **4.4            *References***

- Fastner J., Neumann U., Erhard M. (1998): Patterns of different microcystins in field samples dominated by different species of cyanobacteria, In: Chorus I. (ed.): Cyanotoxins – Occurrences, Causes, Consequences., 190 - 199, Springer Verlag Berlin.
- Lawton, L., Marsalek, B., Padisak, J. & Chorus, I. (1999): Determination of cyanobacteria in the Laboratory. - in: Chorus, I. & Bartram, J. (eds): Toxic cyanobacteria in water - a guide to their public health consequences, monitoring and management: p. 347 - 367, E & FN Spon, London.

## **5 Laboratory Experiments: Batch Experiments on MCYST-Degradation**

### **5.1 Introduction**

Previous studies have shown that biological degradation is the most important elimination process for microcystins in porous media without significant clay content as it is usually used for bank filtration or artificial recharge. As part of the research project NASRI (natural and artificial systems for recharge and infiltration) laboratory batch experiments were therefore conducted by the working group "environmental microbiology" of the Technical University Berlin in cooperation with the drinking water section of the Federal Environmental Agency (UBA). The aim was to study the kinetics of microcystin (MCYST) degradation under aerobic and anoxic conditions with the emphasis on the processes that lead to anoxic degradation of microcystins (anoxic meaning in this case that no free oxygen is present).

A preliminary experiment with an aerobic and an anoxic batch aimed to compare degradation under these different conditions and to enrich micro-organisms capable of degrading MCYST under anoxic conditions for further experiments. In the main series all batches were conducted under anoxic conditions with the objective of learning about processes leading to anoxic degradation of MCYST. The preliminary experiment was carried out with the crude extract of the *Planktothrix agardhii* mass culture, the main series with a purified stock solution of demethylated MCYST-RR.

### **5.2 Materials and Methods**

#### **5.2.1 Experimental setup**

##### **5.2.1.1 Preliminary experiment**

The preliminary batch experiment was conducted with a crude extract of a mass culture of *Planktothrix agardhii* HUB 076 cultivated at the UBA's experimental field in Marienfelde (Berlin). Microcystins were extracted by repeated freeze-thawing a cell concentrate obtained by centrifuging the culture. After centrifuging the extract to remove all solid cell contents it contained up to 50 mg/L microcystins amongst other water soluble cell components.

This centrifuged extract was then brought into contact with an inoculum derived from natural sandy bank material from a lake in Berlin with frequent cyanobacterial blooms (Lake Wannsee) together with a fresh sample of the cyanobacterial mass culture in a ratio 5:5:1. The resulting concentration of demethylated MCYST-RR (main variant of *Planktothrix agardhii* HUB 076) was 49.48 mg/L ( $\pm 0.05 \mu\text{g/L}$  variation between the two batches).

One parallel was kept aerobic by allowing contact to the natural atmosphere (A), the other was held anoxic under N<sub>2</sub>/CO<sub>2</sub>-atmosphere (B).

- Aerobic approach (A): 550 ml batch volume incubation on a rotary shaker (120 rpm), at room temperature in the dark,
- Anoxic approach (B): 55 ml batch volume, at room temperature in the dark, serum bottle under N<sub>2</sub>/CO<sub>2</sub> atmosphere.

Samples were taken daily during the first 10 days of the experiment, later weekly, filtered (membrane filter 0.45 µm pore size) and stored deep frozen until analysis.

### 5.2.1.2 Main series of batch experiments

The common basis of all batches run during this series was:

- 50 mL sulfide reduced anoxic medium, reduced by volume of added solutions, prepared according to Widdel & Bak (1992) and Tschech & Pfennig (1984),
- 1 mL demethylated MCYST-RR stock solution, about 800 mg/L and 600 mg/L in sum in the first and second series, respectively,
- 0.5 mL anoxic pre-culture (obtained in the anoxic preliminary experiment),
- 0.5 mL *Planktothrix agardii* HUB 076 culture.

The redox indicator resazurin was added to indicate oxidizing conditions by pink colour (Figure 12) and dithionite (reductive agent) was added when needed.

Three parallels were run for each of the following compounds in order to study the microorganisms and metabolic pathways involved in the transformation of microcystin with different electron acceptors/donators:

- KNO<sub>3</sub> (0.1 mM), in order to find out if nitrate can serve as electron donator,
- glucose (0.03 mM), in order to simulate high nutrient conditions (and thus co-metabolism as the prominent degradation process),
- casaminoacids (0.5 %), in first series only, in order to find out if MCYST is degraded simultaneously to chemically similar substances.

The experiments were carried out with a purified dem. MCYST-RR extract that was prepared in order to rule out co-metabolism as a degradation process. The purification was carried out by semi-preparative HPLC application (appendix VII-1). During the second main series an additional control without pre-culture and *Planktothrix agardhii* culture as inoculum was carried out.



**Figure 12:** Screw cap tubes filled with sulfide reduced anoxic medium supplemented with KNO<sub>3</sub>. The pink bottle shows an example of oxidized medium.

Samples were taken every 2 to 3 days and glass beads were added to the tubes in exchange in order to compensate for the loss in batch volume (Figure 12). The samples were then stored frozen in glass test tubes until analysis by HPLC.

### **5.2.2 Analytical Methods**

MCYST-analyses were carried out by HPLC (High Performance Liquid Chromatography) with a photodiode array detector according to Lawton et al. (1994). The samples were thawed, diluted with methanol (1:1) and analyzed directly, without further pre-treatment.

## **5.3 Results**

### **5.3.1 Preliminary experiment**

The results of the two batch experiments (Figure 13) show complete transformation of microcystins (< 40 µg/L) under aerobic as well as under anoxic conditions with more rapid degradation under aerobic conditions. A lag phase of 2 days with only little degradation (10 %), however, can even be observed under aerobic conditions. Nevertheless, after the 2nd day 99.9 % of the microcystin present was degraded within 2 days. Under anoxic conditions the MCYST concentrations remained on a high level (> 44.85 mg/L) for the first nine days of the experiment. A sample taken on day 21 after the beginning of the experiment, however, showed complete degradation (MCYST-RR < 40 µg/L).

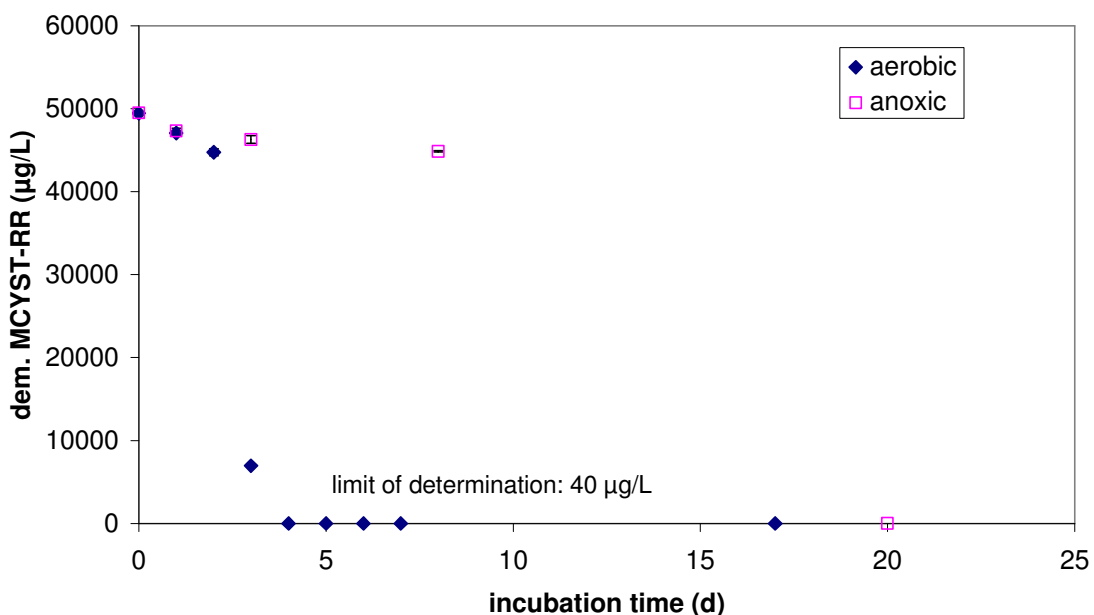


**Figure 13:** Degradation of dem. MCYST-RR under aerobic and anoxic conditions during first batch series.

These results show that transformation is also possible under anoxic conditions, although the lag phase seems to be distinctively longer. A contamination with oxygen during sampling, however, can not be ruled out completely so we decided to change the experimental setup and use an anoxic sulfide reduced medium with a redox indicator in further experiments.

### 5.3.2 Main series of batch experiments

The sum of MCYST analysed in the samples of the first batch series is given in Figure 14. All three different experiments showed a similar trend in MCYST concentration: Starting from values around 10 to 12 mg/L there is an immediate decline until values around 1 mg/L are reached on day 15. After this the MCYST concentration remains constant in all batches.

The residual concentrations of MCYST are, however, not demethylated MCYST-RR but are composed of substances that show different retention times in the HPLC chromatogram (Figure 15) but can be identified as MCYSTs due to their characteristic UV-spectra (see final NASRI Report working group algae, part IIX). Dem. MCYST-RR is reduced to below detection limit after 5 to 8 days.

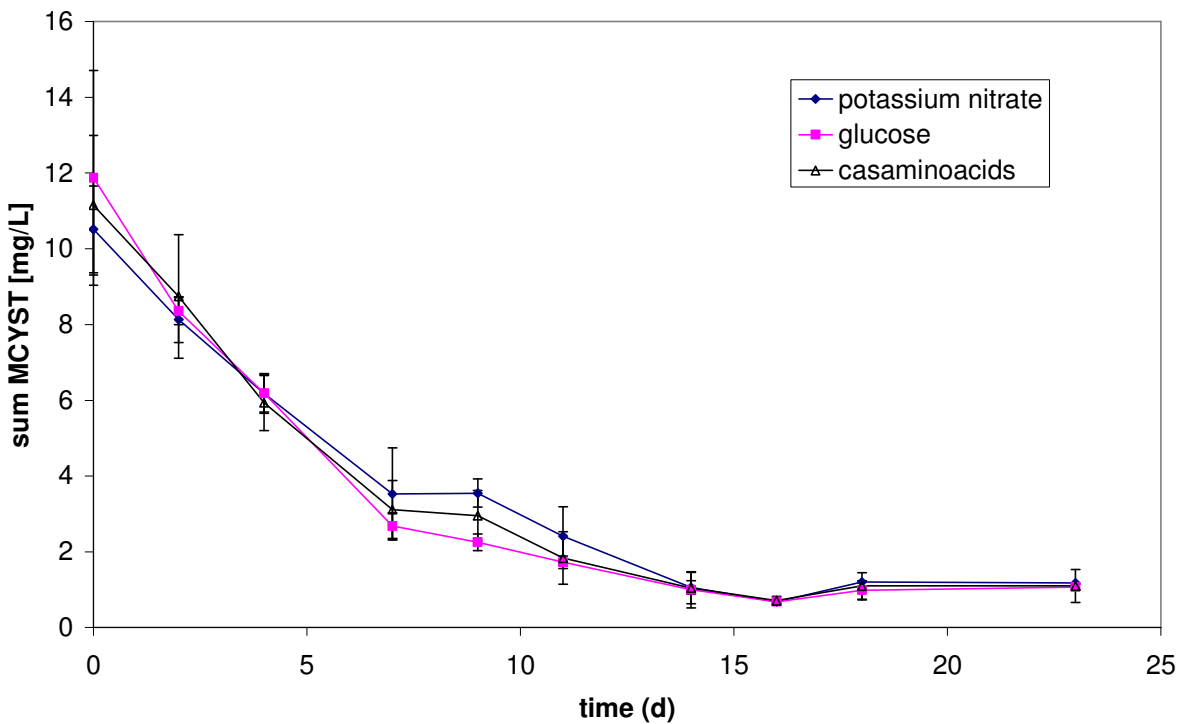


**Figure 14:** MCYST (sum of all variants) during the first main series of degradation experiments under anoxic conditions with addition of KNO<sub>3</sub>, glucose and casaminoacids (average values and standard deviation of three parallels each).

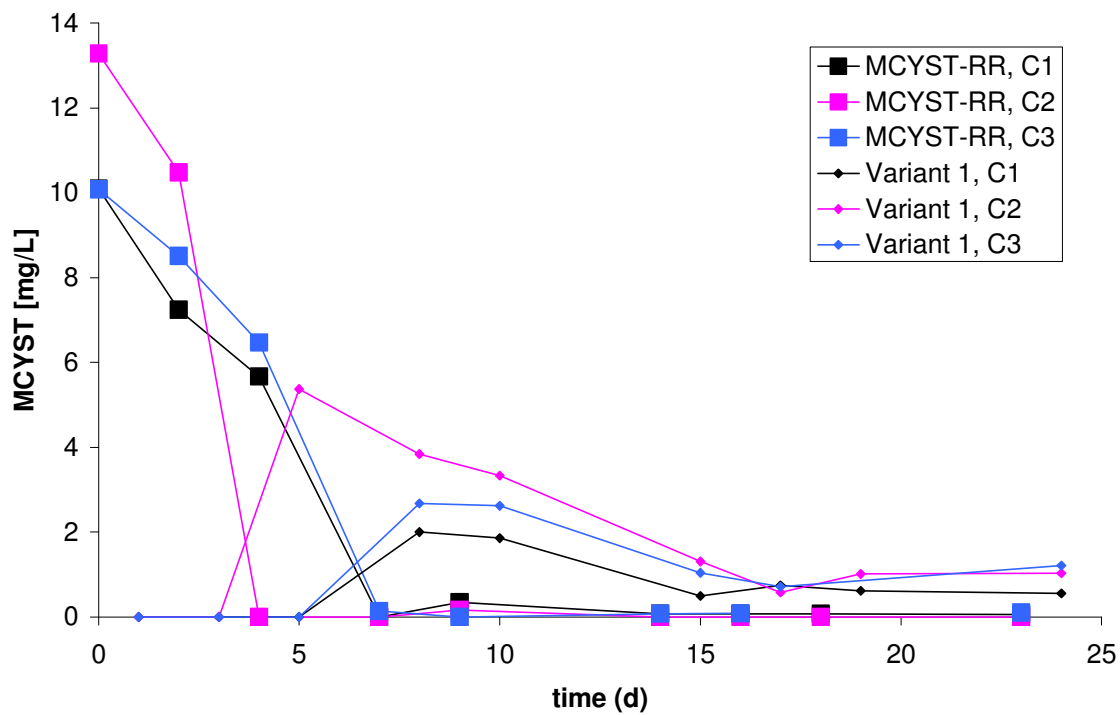


**Figure 15:** Concentrations of dem. MCYST-RR (full squares) and an unidentified MCYST variant (retention time: 10.5 min, small diamonds) during the three parallel experiments with casaminoacids in the first main series.

The HPLC analysis of the stock solution used for the second series already showed traces of other MCYST peaks: additionally to 98.7 % dem. MCYST-RR, 1 % was found at a retention time of 11.8 min and 0.3 % at 10.2 min. This indicates that transformation might have already taken place in the stock solution prior to the beginning of the experiment.

The results of the MCYST analyses of the second batch series are shown in Figure 16. In this series the drop in MCYST concentrations in all batches is even more rapid than in the first series (compare Figure 14). This might be due to lower initial concentrations (11.2 mg/L average in the first and 3.2 mg/L in the second series). Like in the first series, however, a residual concentration of about 1 mg/L is remained all batches with exception of those without inoculum and additional substances.

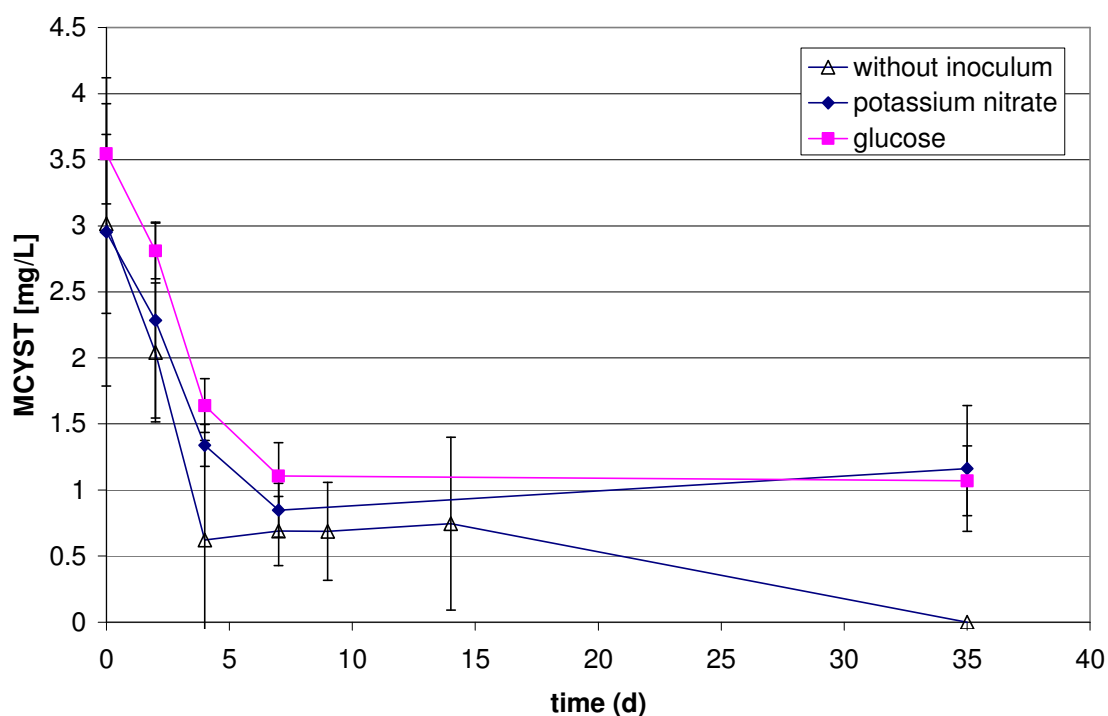


**Figure 16:** MCYST (sum of all variants) during the second main series of degradation experiments under anoxic conditions with addition of KNO<sub>3</sub>, glucose and without inoculum (average values and standard deviation of three parallels each).

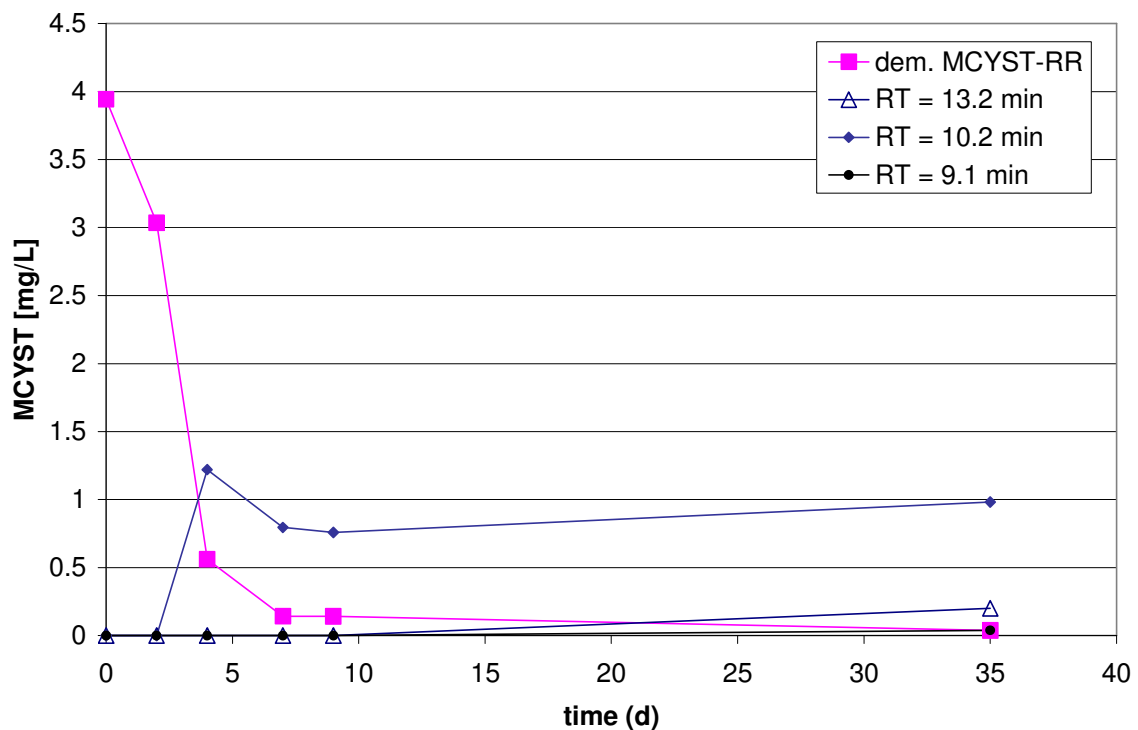


**Figure 17:** Concentrations of dem. MCYST-RR and unidentified MCYST variants during one series with glucose in the second main series (RT = retention time).

A closer look at the different peaks of the HPLC chromatogram (Figure 17) reveals that the concentration of the main MCYST variant (dem. MCYST-RR) declined to values below 0.2 mg/L after day 8 and to around 0.04 mg/L (limit of determination) on day 36. Other substances with a typical MCYST-spectrum and other retention times were not detectable in the beginning of the experiment. For the variants previously identified in the undiluted stock solution this is in agreement with the theoretical concentration calculated from the dilution factor, which would be less than 0.01 mg/L whereas the detection limit is clearly higher (0.04 mg/L). After five days one variant with a retention time of 10.2 min appeared in concentrations around 1.2 mg/L. This had a molecular mass of  $m/z$  1106  $[M+H]^+$  (identified by LC-MS), some fragments characteristic for MCYSTs and remained detectable until the experiment was terminated at concentrations around 1.0 mg/L.

### **5.3.3        *Summary of the Results***

In summary, the batch experiments carried out on MCYST degradation showed the following results:

In the preliminary experiment aerobic degradation was more rapid than anoxic degradation due to a shorter lag phase. (However, as mentioned above, it could not be ruled out that degradation in the further course of the experiment was due to oxygen contamination).

In strictly anoxic experiments of the main batch series with pure MCYST and the anoxic pre-culture no lag phase was observed. This was, however, also true for a batch without any pre-culture - this indicates that the lack of adapted microorganisms was not the limiting factor in the preliminary series. Another possibility might be that degradation is not due to biological processes.

Addition of KNO<sub>3</sub>, glucose or casaminoacids did not accelerate or retard anoxic degradation of pure MCYST.

Surprisingly, during MCYST-transformation additional peaks appeared in the HPLC chromatogram, that showed a typical MCYST UV-spectrum and characteristic fragments. These appeared to be more stable than the variant present initially (dem. MCYST-RR) and are detectable at constant concentrations around 1 mg/L from day 5 until the end of the experiment (after 36 days).

## **5.4            *Interpretation and Discussion***

Taking these results of the preliminary and the main batch series into account the following conclusions can be drawn:

- Demethylated MCYST-RR can be transformed under aerobic and anoxic conditions.
- The presence of other, possibly more readily degradable substances (BDOC) in the crude extract seems to promote a lag phase before rapid degradation commences.
- Under the conditions used in the preliminary experiment (presence of high amounts of BDOC) the lag phase is shorter under aerobic than under anoxic conditions.
- Pure demethylated MCYST-RR is degraded rapidly (without lag phase) under anoxic conditions in the main series with half lives of less than 5 days.
- Under these conditions other substances with UV-spectra and mass fragments characteristic of MCYST emerged.
- These substances are less easy to degrade under the conditions mentioned above and are still present in solution 36 days after the beginning of the experiment.

Although a number of investigations on the aerobic degradation of MCYST have been published (e.g. Bourne et al. 1996, Christoffersen et al. 2002, Cousins et al. 1996, Jones et al. 1994, Lahti et al. 1997, Saitou et al. 2002, Welker et al. 2001), experiments on anoxic degradation are limited (Holst et al. 2003).

Holst et al. (2003) postulated that degradation of MCYSTs (in their case MCYST-LR) was restricted to situations in which a strong electron acceptor such as oxygen or nitrate was present. This was shown in batch experiments under microaerophilic conditions ( $O_2 < 0.3\%$ ), where degradation was only observed if  $NO_3$  and / or glucose was added. Although this seems to contradict our own experimental results, there are two important differences: a) the MCYST variant used by Holst et al. (2003) was mainly MCYST-LR, while our experiments were carried out with demethylated MCYST-RR and b) the conditions in our experiments were strictly anoxic (-51 mV, at pH 7), whereas Holst et al. (2003) stated microaerophilic conditions.

In conclusion, these findings leave the following open questions:

- Which are the factors influencing the occurrence of a lag phase prior to rapid MCYST degradation (adapted microbiology, presence of BDOC or others?)
- Apart from the lag phase, is there a difference in aerobic and anoxic degradation rate?
- Do degradation rates differ between MCYST variants? Are there variants that are persistent?
- Can degradation transform MCYSTs from one variant to another?
- Which bacteria are involved in MCYST degradation?

In order to assess the rate and reliability of anoxic MCYST degradation under the conditions commonly occurring during infiltration, a broader, systematic approach to further experiments is needed. This is important as in most cases microaerophilic, anoxic and anaerobic conditions prevail during artificial recharge or bank filtration.

## 5.5 References

- Bourne D.G., Jones, G.J., Blakeley R.L., Jones A., Negri A.P. & Riddles P. (1996): Enzymatic Pathway for the Bacterial Degradation of the Cyanobacterial Cyclic Peptide Toxin Microcystin LR., Appl. Env. Microbiology, 62 (11): 4086 – 4094.
- Christoffersen K., Lyck S. & Winding A. (2002): Microbial activity and bacterial community structure during degradation of microcystins., Aq. Microb. Ecology, 27: 125 – 136.
- Cousins I.T., Bealing D.J., James H.A. & Sutton A. (1996): Biodegradation of Microcystin-LR by Indigenous Mixed Bacterial Populations., Wat. Res., 30(2): 481 – 485.
- Holst, T., Jørgensen, N.O.G., Jørgensen, C. & Johansen, A. (2003): Degradation of microcystin in sediments at oxic and anoxic, denitrifying conditions. - Wat. Res. 37: 4748 - 4760.
- Jones G.J., Bourne D.G., Blakeley L. & Doelle H. (1994): Degradation of cyanobacterial hepatotoxin microcystin by aquatic bacteria., Natural Toxins, 2: 228-235

- Lahti K., Rapala J., Färdig M., Niemelä M., Sivonen K. (1997): Persistence of cyanobacterial hepatotoxin, microcystin-LR, in particulate material and dissolved in lake water, *Wat. Res.*, 31 (5): 1005 – 1012.
- Lawton, L.A., C. Edwards, G.A. Codd (1994): Extraction and high-performance liquid chromatographic method for the determination of microcystins in raw and treated waters, *Analyst*, 119: 1525 – 1530.
- Saitou T., Sugiura N., Itayama T., Inamori Y., Matsumura M. (2002): Degradation of Microcystin by Biofilm in Practical Treatment Facility., *Wat. Sci. Techn.* 46(11-12): 237 – 244.
- Tschech, A. & Pfennig, N. (1984) Growth yield increase linked to caffeate reduction in *Acetobacterium woodii*. *Arch. Microbiol.* 137, p 163-167.
- Welker M., Steinberg C. and Jones G. (2001): Release and Persistence of Microcystins in Natural Waters, In: (I. Chorus ed.): *Cyanotoxins - Occurrence, causes, consequences.*, Springer Verlag Berlin, 83-101
- Widdel, F. & Bak, F. (1992) Gram-negative mesotrophic sulfate-reducing bacteria. In: *The Prokaryotes: a handbook on the biology of bacteria: ecophysiology, isolation, identification and applications*, 2nd ed. (Balows, A., Trüper, H. G., Dworkin, M., Harder, W. and Schleifer, K.-H. Eds.) p 3353-3378. Springer-Verlag, New York.

## **6 Column Experiments to assess Effects of Temperature on MCYST-Degradation**

### **6.1            *Introduction***

In order to transfer the results of laboratory and field experiments to the field setting, the influence of temperature on substance removal has to be regarded closely, as this is one of the physico-chemical parameters that varies distinctively throughout the year in natural settings. Concerning the elimination of cyanobacterial toxins, only few publications have so far addressed this topic.

Some publications suggest that a reduced degradation of microcystins (MCYST) could be the result of lower temperatures as biodegradation is known to decrease with sinking temperatures. This was the result of field experiments in late autumn for example (Grützmacher et al. 2002). Holst et al. (2003) carried out experiments with two different temperatures, 10 and 21 °C, showing that elimination was better at 21 °C. In order to confirm these findings experiments with MCYST were carried out on columns run by the NASRI working group “organics” (Technical University of Berlin) as part of a diploma thesis by Charlotte Garing, supported by the working group “algae” under supervision of Dr. Birgit Fritz and Prof. Behra (ENSIACET, France).

### **6.2            *Materials and Methods***

#### **6.2.1        *Microcystin extract***

The microcystins were extracted from a mass culture of *Planktothrix agardhii* HUB 076, currently run by UBA, by centrifugation and freeze-thawing. The extracts were homogenated, centrifuged and stored frozen. The undiluted microcystin extract had a concentration of 61.85 mg/L.

#### **6.2.2        *Soil column experiments***

##### **6.2.2.1      *General characteristics***

Three acryl glass columns with a diameter of 0.14 m and height of 0.5 m were filled with an industrial sand, consisting mainly of quartz sand with a grain size ranging from 0.7 to 1.2 mm and with a poor organic content (loss on ignition = 0,13%). Water from Lake Tegel and microcystin were pumped into the column. The flow rate was estimated to be about 840 mL/d for each column and the pore velocity about 0.2 m/d. The installation is summarized in Figure 18 and Figure 19 gives an illustration of one of the columns. Further details can be taken from the final report of the NASRI working group “organics”.

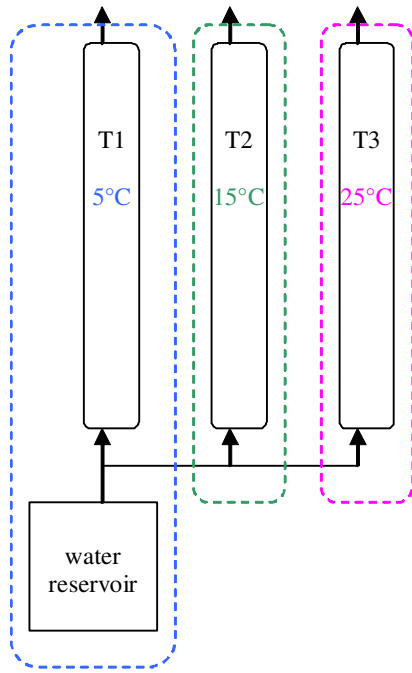


**Figure 18 Simplified diagram of the installation.**

The columns were kept at different temperatures: 5°C for the first column, 15°C for the second one and 25°C for the third one (see Table 3 for details on average temperatures of the columns during both experiments).

**Table 3 Average temperature of each column during experiment 1 (a) and experiment 2 (b). The number of measurements was 23 and 7 for a) and b), respectively.**

a)	T1 (°C)	T2 (°C)	T3 (°C)
mean	4,83	15,65	25,67
deviation	1,12	0,89	0,81

b)	T1 (°C)	T2 (°C)	T3 (°C)
mean	5,30	15,28	26,34
deviation	0,83	0,46	0,48

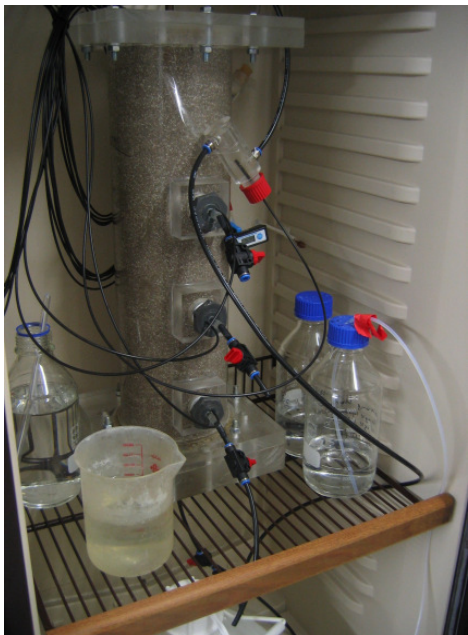


**Figure 19** Photograph of one of the columns.

#### **6.2.2.2      Experiment 1**

For the first experiment, 5 mL of the microcystin extract and about 20 L of Lake Tegel water were added to the water reservoir each week in order to maintain a microcystin input concentration of around 15 µg/L.

The experiment lasted 47 days. The water reservoir was sampled daily, to check the development of its microcystin content. During the first four days, two samples of the effluent from each column were taken per day and then one per day until the end of the experiment. The samples were kept frozen in glass test tubes until analysis.

#### **6.2.2.3      Experiment 2**

In the second experiment, the diluted extract (40.5 mL in 1000 mL Lake Tegel water) was injected directly into each column just after having been mixed with Lake Tegel water from the water reservoir with a dilution factor of 1/50. This different mode of application was chosen in order to avoid variations in the input concentration due to degradation and / or incomplete mixing as observed in experiment 1. The resulting concentration was targeted at 50 µg/L.

The experiment lasted 35 days. The effluent of each column was sampled daily. Samples from the microcystin input solution were also taken, approximately once a week, in order to check the correct microcystin input concentration. The samples were kept frozen in glass test tubes until analysis.

#### **6.2.2.4 Analytical methods**

All samples were analyzed by ELISA in order to determine their total microcystin content. During the second experiment, one sample from the output water of each column and one from the input microcystin solution were additionally analyzed by HPLC to check the microcystin concentration and to distinguish the different microcystin variants present in the water. Further details on MCYST analysis can be taken from the final NASRI Report of the working group "algae" part IIX.

#### **6.2.2.5 ELISA**

The concentration of microcystin in the samples was quantified by a competitive ELISA (enzyme-linked immunosorbent assay). This method is based on the reaction between microcystins and antibodies. It is an efficient method in detecting concentrations down to 0.1 µg/L with only a small volume of solution and no need for sample pre-treatment.

The ELISA used was a generic microcystin immunoassay based on monoclonal antibodies against the unusual Adda group characteristic for microcystins, nodularins and certain peptide fragments (Zeck et al. 2001). The range of determination lies between 0.1 µg/L and 1.0 µg/L, and thus samples from the water reservoir had to be diluted with deionized water. Each value was determined as the average of two parallels taken from the same sample.

#### **6.2.2.6 HPLC**

The microcystin variants and their concentrations were analyzed by HPLC with photodiode array detection. The samples were first filtered by membrane filters RC 55 with a pore size of 0.45 µm. They were then enriched by solid phase extraction over C18-cartridges: three cartridges were filled with the three samples from the column water outflow and one cartridge with the sample of the microcystin input solution. After one day the cartridges were submitted to washing, elution and evaporation (details are given in final NASRI Report working group "algae" part IIX).

#### **6.2.2.7 Numerical methods**

Retardation and degradation rates were estimated by fitting a numerical model to the measured values obtained from the column experiments. The model used was an inverse model created by E. Holzbecher (IGB, Berlin), using basic MATLAB package in connection with the optimization toolbox. This model is represented in Appendix VIIb-1.

The function representing degradation was modified in order to obtain a better description of the processes in the columns:

$$\text{for } c \neq 0, \quad \lambda = 1 / [\exp(-cT) - 1] * [(\lambda_2 - \lambda_1)\exp(-ct) + \lambda_1 \exp(-cT) - \lambda_2]$$

$$\text{for } c = 0, \quad \lambda = \lambda_1 + (\lambda_2 - \lambda_1) t / T$$

$\lambda$  : loss rate [1/d]

t: time [d]

T: duration of the experiment [d]

$\lambda_1$ ,  $\lambda_2$  and c: parameters of  $\lambda$  [1/d]

Figure 20 shows the evolution of  $\lambda$  with the time, for different values of c, as calculated by this model.

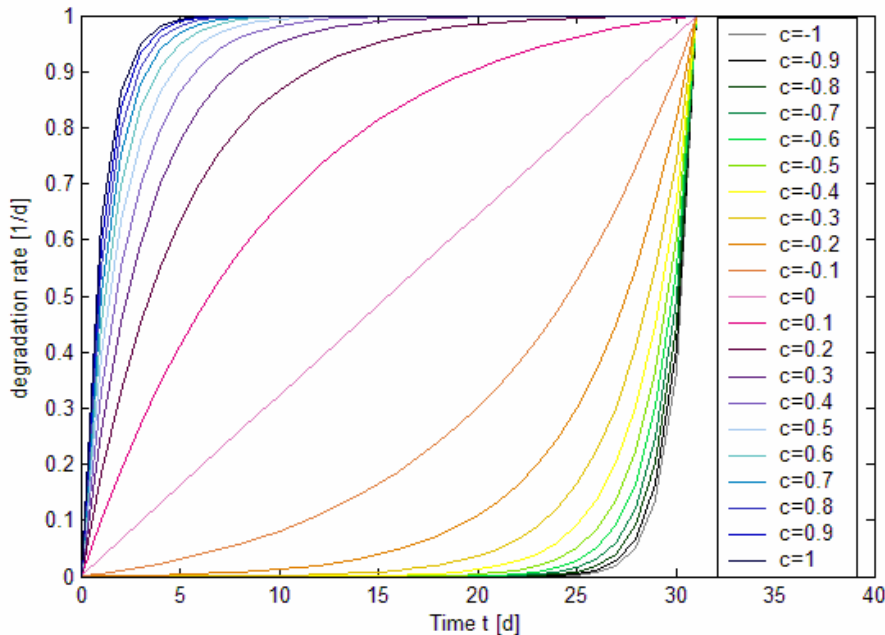


**Figure 20 Evolution of loss rate ( $\lambda$ ) with the time for c from -1 to 1. Parameters for the given situation are:  $\lambda_1 = 1e-10$ ,  $\lambda_2 = 1$  and  $T = 31$ .**

The modelling was done with a pore velocity of 0.2 m/d and a value of the longitudinal dispersivity assumed equal to 0.05 m.

For the first experiment, a constant input microcystin concentration of 19.18 µg/L was taken and the modelling was done with the first 31 points.

For the second experiment, the model used a constant input microcystin concentration of 63.5 µg/L.

## 6.3 Results

### 6.3.1 Experiment 1

#### 6.3.1.1 Soil column results

Although the evolution of microcystin input concentration was quite unstable, it could be separated into two main phases: the first 31 days the concentration in the water reservoir had an average value of 19.2 µg/L ( $\pm 4.7$ ) and then from day 31 to day 47 the average concentration was around 7.6 µg/L ( $\pm 2.8$ ) (Figure 21).

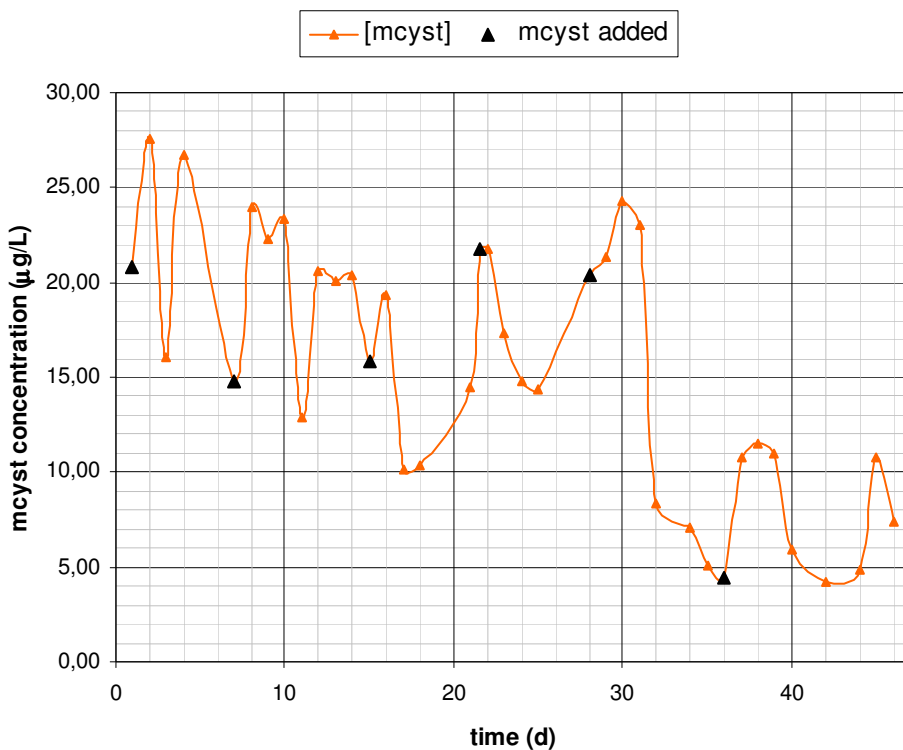


**Figure 21 Microcystin concentration in the water reservoir.**

The concentration of microcystin in the output water had the same tendency for each column, regardless of the experimental temperature, i.e. 5°C, 15°C and 25°C (Figure 22).

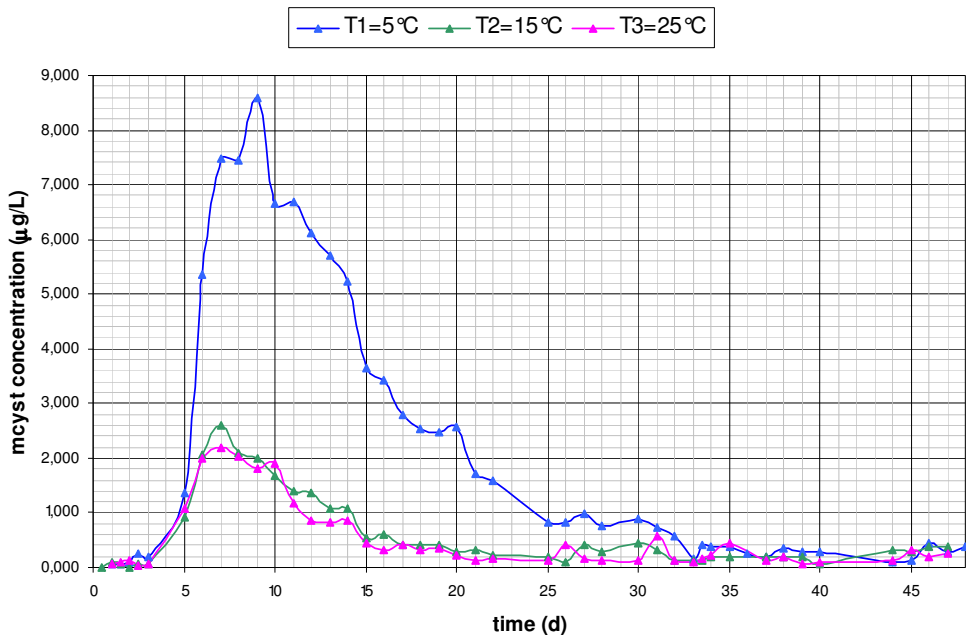


**Figure 22 Microcystin concentrations at column outlets investigated at three experimental temperatures, T1 = 5°C, T2 = 15°C and T3 = 25°C for an input concentration around 19.2 µg/L.**

During the first 3 to 4 days, no microcystin was observed in the outlet. Then the microcystin concentration increased rapidly until reaching a maximum value at day 7 for column 2 and 3, with 2.61 and 2.18 µg/L respectively, and at day 9 at 5°C in column 1 with 8.6 µg/L. Then it decreased in all columns until the end of the experiment. The concentration of microcystin in the output water reached values under detection limit after day 21 for column 3 at 25°C, day 26 for column 2 at 15 °C and day 44 for column 3 at 5 °C, and all the values after day 25 remained lower than 1 µg/L, the provisional WHO guideline value for MCYST-LR in drinking water (WHO 1998). From day 35 until day 47, the end of the experiment, the microcystin concentration was between 0.05 µg/l and 0.455 µg/L for all the columns.

In terms of elimination, the percentage of microcystin eliminated at the end of the columns compared to the input, column 1 at 5 °C showed an average elimination of 88.3%, whereas in the columns both at 15 and at 25 °C it amounted to 96.6% (Figure 23).

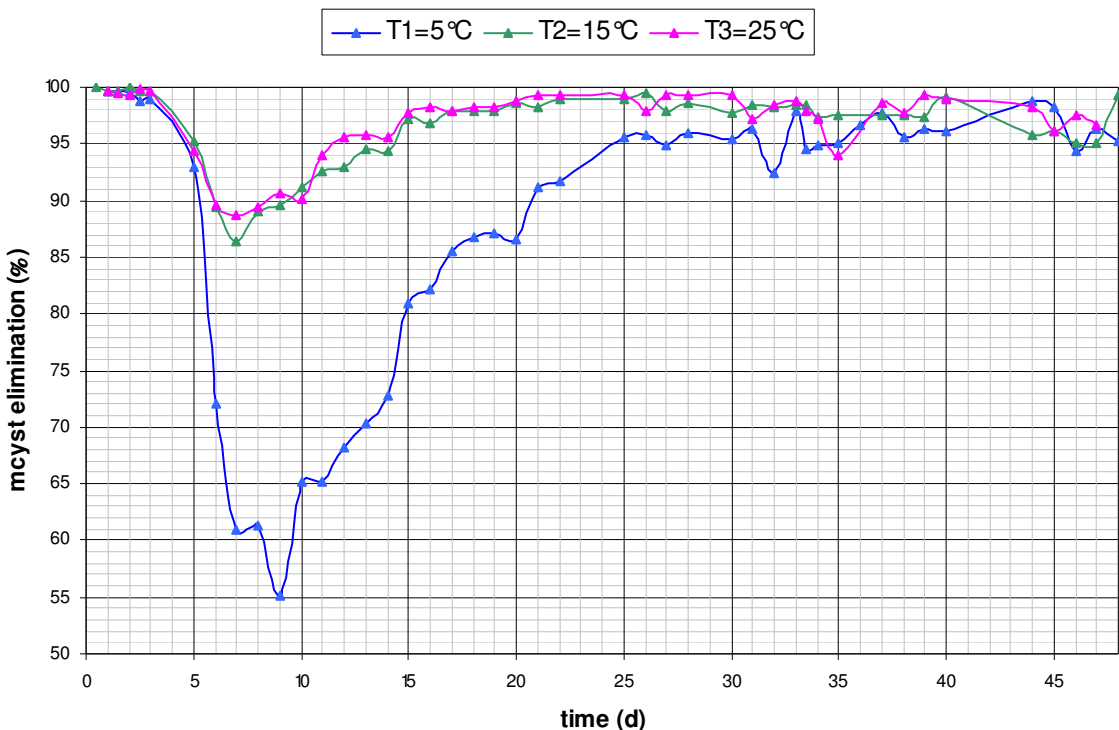


**Figure 23 Microcystin elimination during experiment 1 (input concentration 19.2 µg/L for days 0 to 31 and 7.6 µg/L for days 32 to 47).**

### 6.3.1.2 Modelling Results

For the first column at 5°C, the best fit of the microcystin outlet concentration curve was achieved with the set of parameters represented in Table 4. The modelled curves are shown Figure 24 and the corresponding degradation rates in Figure 25.

**Table 4 Fitting parameters for experiment 1 ( $v = 0.2 \text{ m/d}$ ,  $\alpha L = 0.05 \text{ m}$ ,  $T = 31 \text{ d}$ ).**

	5 °C	15 °C	25 °C
R	3.44	4	4
$\lambda_1 [\text{d}^{-1}]$	2.e-9	2.e-10	2.e-10
$\lambda_2 [\text{d}^{-1}]$	0.8	0.86	0.9
c [ $\text{d}^{-1}$ ]	-0.029	0.043	0.039

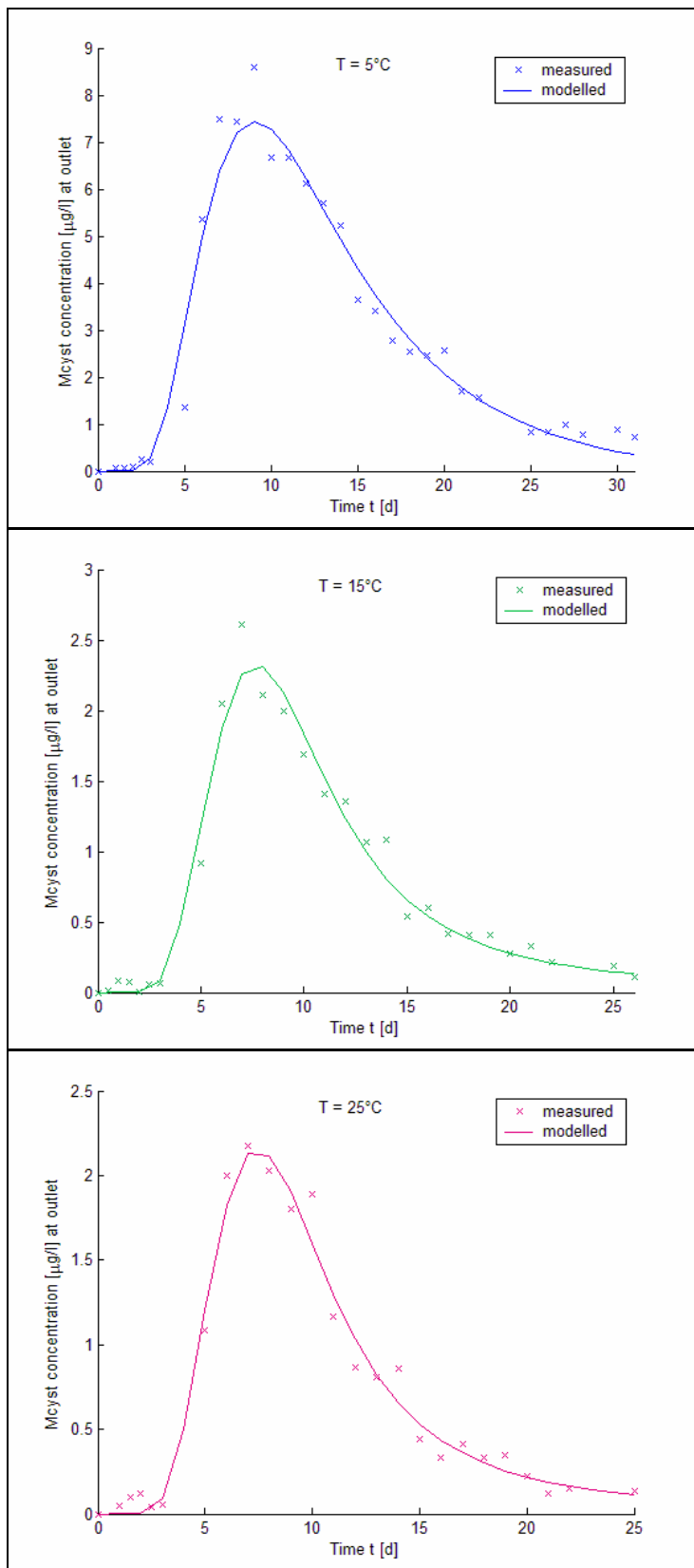


**Figure 24 Measured and modelled microcystin outlet concentration for experiment 1.**

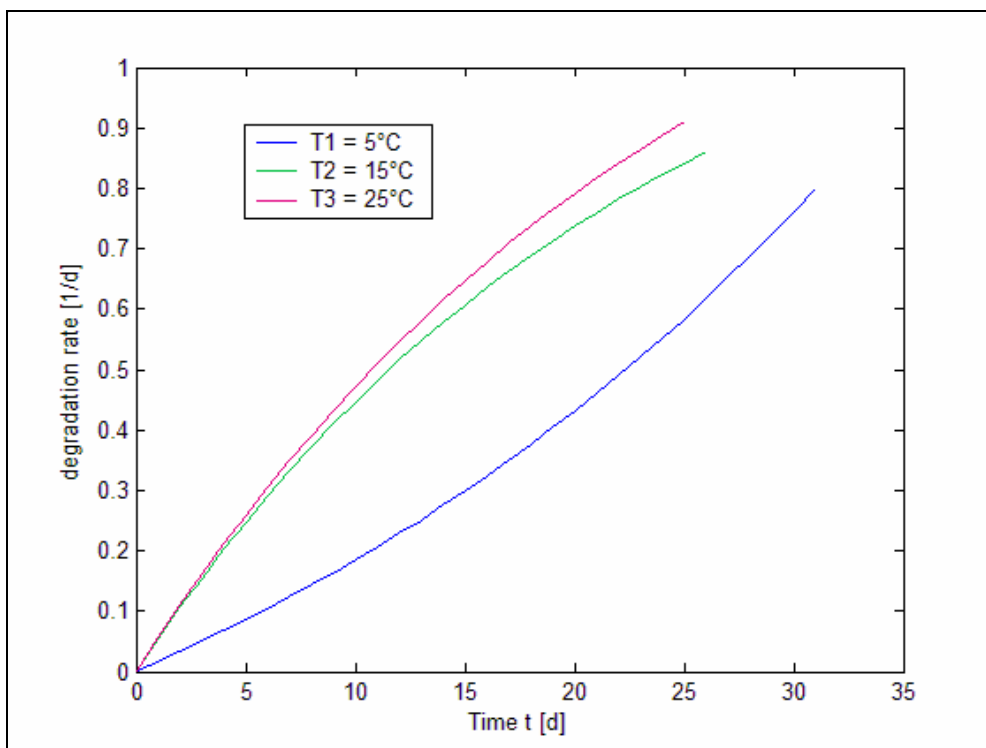


**Figure 25 Microcystin degradation rates over time at 3 different temperatures.**

### 6.3.2      *Experiment 2*

#### 6.3.2.1      Soil column results

An HPLC analysis of the microcystin input solution was carried out at day 26. Eight different peaks corresponding to three types of microcystin variants (Table 5) were detected, amounting together to an overall microcystin input concentration of 96 µg/L.

**Table 5 Microcystin variants in the input solution with their concentration in the solution and the calculated concentration injected into the column (dilution of 1/50).**

MCYST variant	Concentration in MCYST-solution	MCYST input concentration
	µg/L	µg/L
LR 237.0	3583.55	71.67
YR 229.9	1219.64	24.39
MC_Try p	4.53	0.09

Throughout the experiment, the ELISA analyses detected input concentrations ranging from 30 to 78 µg/L, with an average of 63.5 µg/L ( $\pm 20.8$ ). The concentration of microcystin in the output water had the same tendency for each column (Figure 26).

During the first 5 to 7 days, microcystin was not present in the outlet samples. Then the concentration increased rapidly until a maximum value was reached at day 11 for all the columns, with 60.3 µg/L for column 1, 18.1 µg/L for column 2 and 30 µg/L for column 3. Then the microcystin concentration decreased until the end of the experiment. For the first column the decrease of the concentration showed some fluctuations. The concentration of microcystin in the effluent reached values under 1 µg/L after day 14 for column 2, day 15 for column 3 and day 34 for column 1. For the column 2 and 3, from day 21 until the end of the experiment, the microcystin concentration stayed between 0.17 µg/l and 0.40 µg/L, which was very low but still above the detection limit of the ELISA. However, the HPLC analyses made by day 26 showed no microcystin in the effluent of any of the columns, not even for even for column 1.

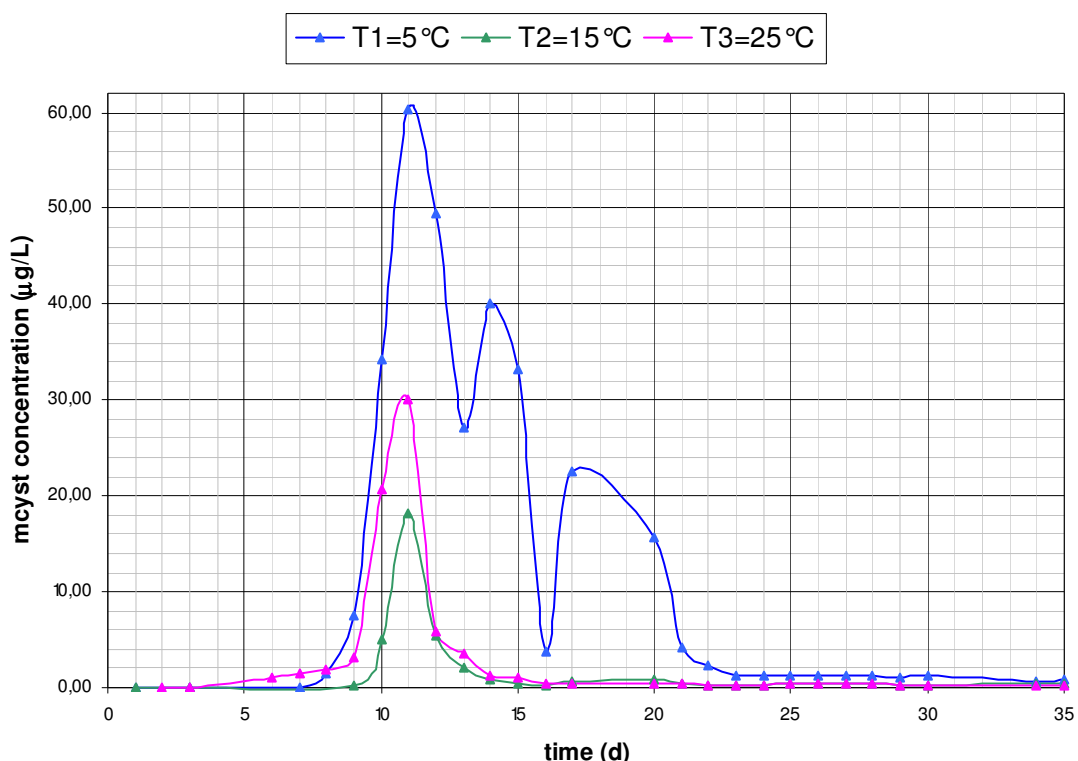


**Figure 26 Microcystin concentration at T1 = 5°C, T2 = 15°C and T3 = 25°C for an input concentration of about 63.5 µg/L.**

In the first column (5 °C), the microcystin was eliminated by 81% in average. The mean value of microcystin elimination for columns 2 (15 °C) and 3 (25 °C) were 97.5% and 95.6%, respectively (Figure 27).

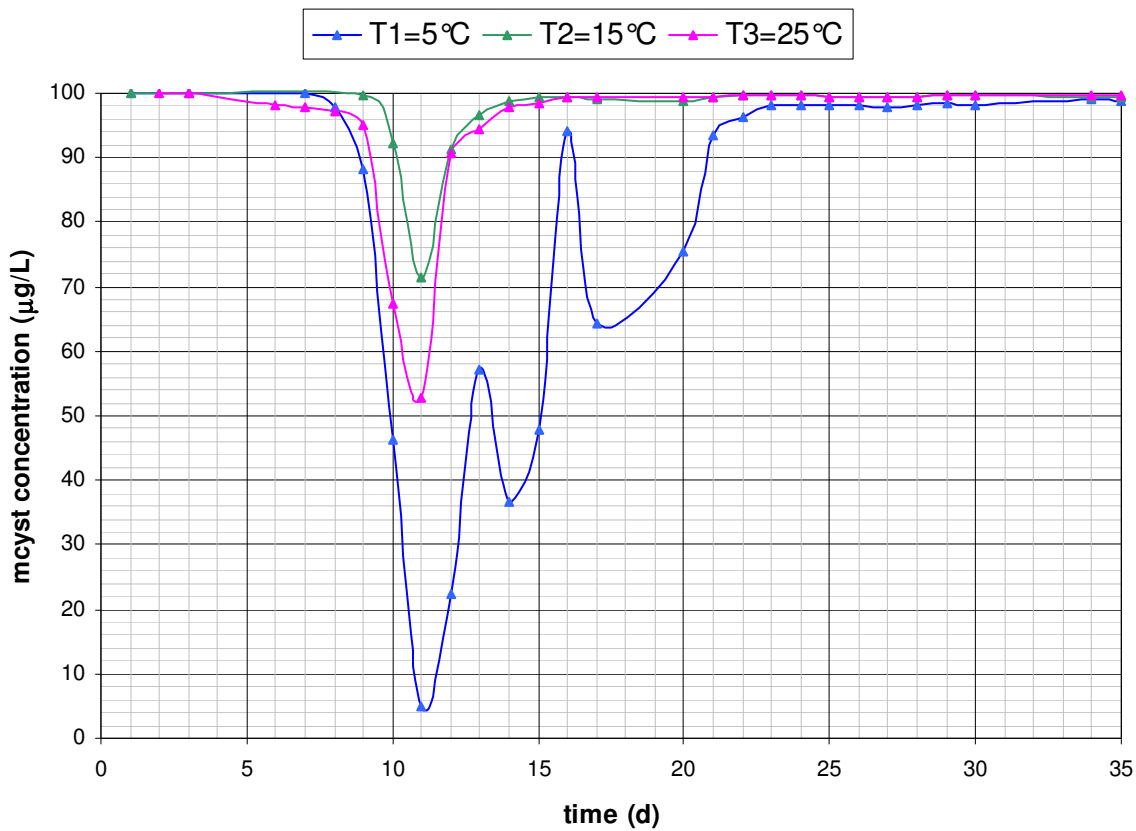


**Figure 27 Microcystin elimination during the time of the experiment for each column (input concentration about 63.5 µg/L).**

### 6.3.2.2 Modelling results

The parameters estimated for the first experiment were tested on the second one, changing the input microcystin concentration to 63.5 µg/L and the time of the experiment to 35 days. The three resulting curves are shown in Figure 28.

On the basis of these results, an adjustment of the parameters was attempted, in order to fit the microcystin outlet concentration curve better. However, no satisfactory fitting was achieved with this model: The major breakthrough peak for all columns was far too tight to be fitted closely.

The introduction of a lag phase  $T_0$  in the  $\lambda$  function managed to yield better results but was still not satisfactory. The results for columns 2, with the addition of a lag phase of 5 days, are presented in Figure 29. This was the best fitting achieved for this column.

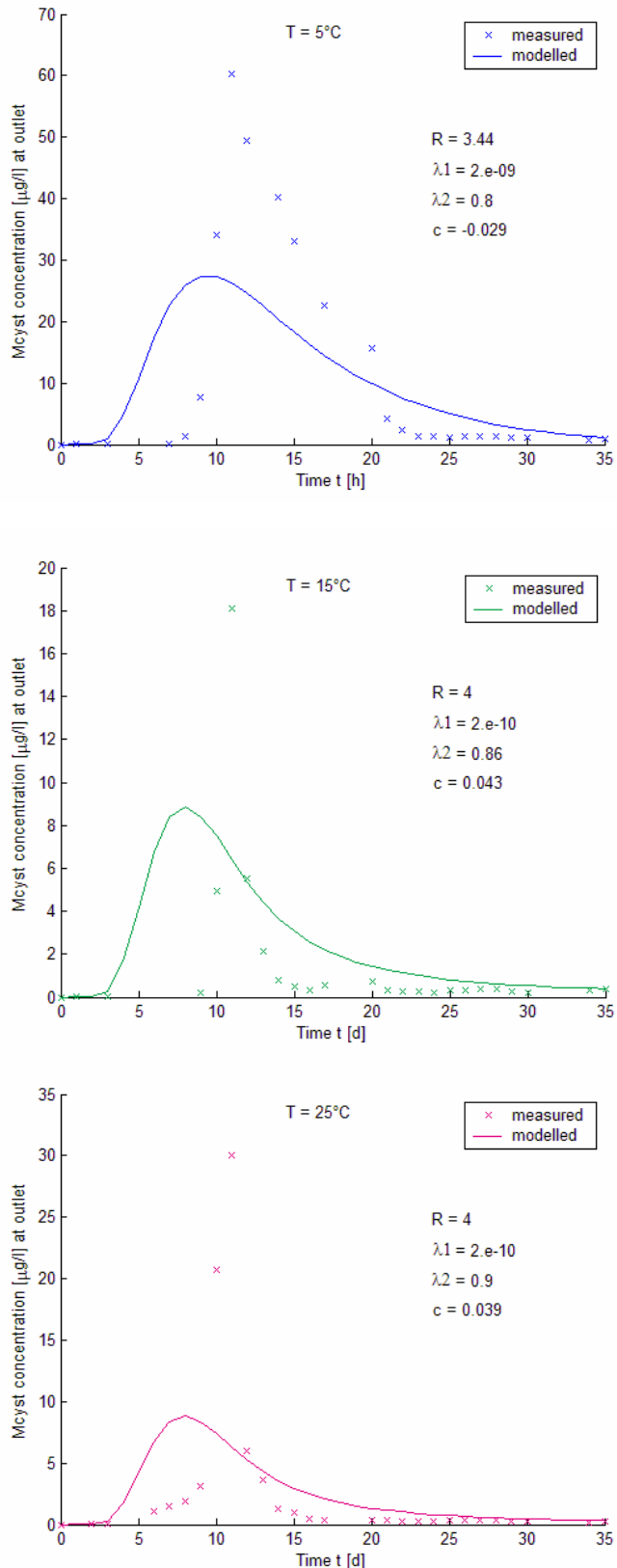


**Figure 28 Measured and modelled microcystin outlet concentration for experiment 2 with the parameters estimated for the experiment 1.**

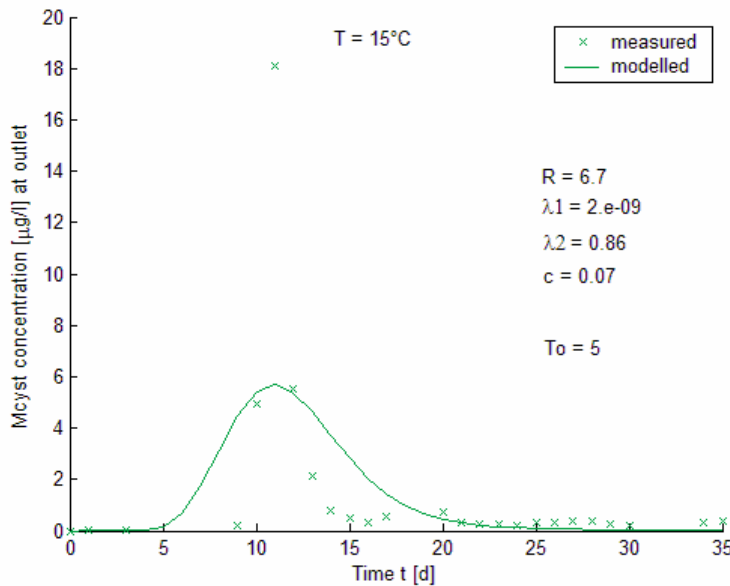


**Figure 29 Measured and modelled microcystin outlet concentration for experiment 2 (column 2 at 15°C) with a lag phase for the degradation  $T_0 = 5$  d.**

## 6.4 Interpretation and Discussion

### 6.4.1 Elimination

The following table summarizes the mean value for the elimination obtained in both experiments.

**Table 6 Mean value of the elimination for each temperature and experiment.**  
**Experiment 1: MCYST added to the water reservoir feeding the columns,**  
**Experiment 2: MCYST injected directly on column.**

MCYST input concentration	Experiment 1      Experiment 2	
	19.2 µg/L	63.5 µg/L
elimination (%)		
5 °C	88.3	81
15 °C	96.6	97.5
25 °C	96.9	95.6

In the second experiment MCYST was still detectable after 35 days by ELISA. The HPLC analysis detected no microcystin after 26 days for all columns. The difference between both results can be explained by two methodological aspects: (i) The Adda-ELISA does not distinguish between microcystins and degradation products. When microcystin is degraded, it is transformed into a linear substance (Bourne et al. 1996) which also contains the Adda-

group. Thus some of the microcystin detected by the ELISA might result from degradation products. (ii) Differences between both methods may be due to differences in sensitivity of detection, particularly as the ELISA reacts to all microcystin variants in a sample in unison, whereas HPLC detects individual peaks for each variant.

The values found for microcystin elimination are in the same order of magnitude as those reported by Holst et al. (2003), who found an elimination of 93 % at 10 °C and 97.5 % at 21 °C for a 66 days experiment for an input concentration of 70 µg/L. In the experiments conducted by Lahti et al. (1998) with soil and sediment columns consisting mainly of gravel, an elimination of 97.9 % was achieved with two soil columns at 14 °C during 7 days with an input microcystin concentration of 0.7 µg/L to 3.1 µg/L.

So far microcystin elimination was usually reported to increase with rising temperature (eg. Holst et al. 2003, see above). In both our experiments also, the rise in temperature from 5 to 15 °C increased the percentage of microcystin eliminated. However, there was no significant difference between 15 and 25 °C: in the first experiment column 3, run at 25 °C, showed a slightly better elimination, however, in the second experiment the tendency was the opposite with a better elimination for column 2 at 15 °C. This can be explained by different processes influencing the degradation rate between the two experiments. In the first experiment the rise in degradation was surely due to the adaptation of the bacteria degrading microcystin. When a higher input concentration was applied, the bacteria may have first been overstrained, leading to the observed breakthrough in all columns. The rapid acceleration of degradation which then occurred is not likely to be due to further adaptation, but rather to population growth and / or higher activity of the bacteria in order to cope with this higher microcystin concentration. A growth optimum around 15 °C for the microbial population in the Lake Tegel water would then explain the better elimination occurring at 15 °C in the second experiment.

#### **6.4.2      *Degradation rates***

In the first experiment, the degradation rates increased during the runtime of the experiment for all columns, with values ranging from 0 to 0.8 d-1, 0.86 d-1 and 0.9 d-1 for column 1, 2 and 3, respectively, with an average of 0.34 d-1 for column 1 (5 °C), 0.51 d-1 for column 2 (15 °C) and 0.52 d-1 for column 3 (25 °C) as shown in figure 8.

For an input microcystin concentration of 10 µg/L at 17 °C and during 12 days, Cousins et al. (1996) reported a degradation rate of 0.17 to 0.23 d-1. These results are very similar to those of our experiment, where the mean value of the degradation rate on 12 days was 0.17 d-1 for 15 °C and 0.18 d-1 for 25 °C. For 4 °C, during 7 days, Jørgensen (2001) found a degradation rate of 0.027 d-1, which is also quite similar to the value of the degradation rate at 5 °C for 7 days that we estimated as 0.05 d-1.

The first experiment also showed that the degradation rate increased with the temperature. Like for the elimination, there was almost no difference between the degradation rate at 15 °C and the one at 25 °C compared to the much lower degradation rate found for 5 °C. One conclusion from these results is that 20 °C ± 5 °C makes no substantial difference for the microbiology to degrade MCYST quite rapidly. For lower temperature such as 5 °C, the

activity of the bacteria may be hindered, lengthening the time necessary to degrade the microcystins as efficiently as with higher temperatures. Holst et al. (2003) also reported a higher microcystin degradation at 21°C than 10°C. Schoenheinz et al. (2005) studied the DOC degradation at 5, 15 and 25°C and found a similar influence of temperature on DOC removal, with degradation rates of 0.9, 1.1 and 1.3 d<sup>-1</sup> for 5, 15 and 25°C respectively.

#### **6.4.3 Retardation factor**

In the first experiment retardation coefficients varied between 3.44 (5°C) and 4 (15 and 25 °C), see table 2. Few retardation coefficients for MCYST are mentioned in the literature. Miller et al. (2001) determined retardation coefficient from breakthrough curves constructed from column experiments for different soil: 1.07 for a high sand soil, 4.40 for a high clay soil and 5.87 for an intermediate soils. Those values have the same order of magnitude as the one found by fitting the microcystin outlet concentration of the first experiment, maybe a little higher than what would have been expected with sand.

The influence of the temperature on the retardation factor was noticeable between 5 °C and 15 °C but the same value was obtained for 15 and 25°C. Thus, higher temperatures may lead to higher retardation coefficients.

No retardation factors were calculated for the second experiment but the plot of the modelled curves with the fitting parameters of experiment 1 and the microcystin input concentration of experiment 2 showed that a much higher retardation coefficient would be appropriate. From the fitting tried on column T2 = 15°C, with the introduction of the lag phase in the  $\lambda$  function, a retardation factor of 6.7 was calculated instead of 4 for the first experiment. The tendency would be the same for the other temperatures as well. These results are surprising, taking into account that the flow rate was the same than for the first experiment. The microcystin outlet concentration curves showed that the breakthrough of microcystin appeared by day 8 or 9. The results and data available did not suggest any explanation for these observations.

### **6.5 Conclusions**

The experiments conducted on three soil columns at different temperatures (5, 15 and 25°C) with two different microcystin input concentrations (19.2 and 63.5 µg/L) yielded the following conclusions:

Concerning reversible adsorption microcystin was quite mobile in the soil used, with higher mobilities at lower temperatures (retardation factor of 3.4 at 5°C instead of 4 at 15°C and 25°C). However, degradation was the most important process for microcystin elimination. This was also the conclusion of Bartel & Grützmacher (2002) and Lahti et al. (1998). Thus residence time is an important factor for MCYST removal during bank filtration.

Degradation rates increased during continuous application of microcystin, suggesting an adaptation and / or growth of the bacteria capable of degrading microcystin.

Microcystin elimination and degradation increased with temperature but for temperatures above 15°C, a rise in temperature had no relevant further impact on microcystin removal

processes. Microcystin degrading bacteria may have optimal conditions in the range of 15 – 25 °C.

With an input microcystin concentration of about 20 µg/L, a complete removal of microcystin was achieved in 21, 26 and 44 days at 25°C, 15°C and 5°C respectively. With a higher MCYST input the concentrations reached very low levels by day 35.

These results show that the use of underground passage in order to remove microcystin from water may be very effective, especially at moderate temperatures. However the efficiency of the toxin elimination strongly depends on many different factors such as the properties of the soil, the concentration of toxin applied, the behaviour of bacteria and microbiology and the filtration distance. Therefore, local validation of these results is important for candidate bank filtration sites.

## 6.6 References

- BARTEL H., GRÜTZMACHER G., 2002: Elimination of Microcystins by slow sand filtration at the UBA Experimental Field, C. RAY (ed): Understanding Contaminant Biogeochemistry and pathogen Removal, 123-133, Kluwer Academic Publishers.
- BOURNE D.G., JONES G.J., BLAKELEY R.L., JONES A., NEGRI A.P., RIDDLES P., 1996: Enzymatic Pathway for the Bacterial Degradation of the Cyanobacterial Cyclic Peptide Toxin Microcystin LR, Applied and Env. Microbiology, 62 (11): 4086-4094.
- COUSINS I.T., BEALING D.J., JAMES H.A., SUTTON A., 1996: Biodegradation of microcystin-LR by indigenous mixed bacterial populations, Wat. Res., 30 (2): 481-485.
- GRÜTZMACHER G., BÖTTCHER G., CHORUS I., BARTEL H., 2002: Removal of microcystins by slow sand filtration, Environm. Tox, 17: 386-394, John Wiley & Sons.
- HOLST T., JØRGENSEN N.O.G., JØRGENSEN C, JOHANSEN A., 2003: Degradation of microcystin in sediments at oxic and anoxic, denitrifying conditions, Wat. Res. 37: 4748-4760.
- JØRGENSEN C., 2001: Removal of algae toxins during artificial recharge – column and batch studies, Artificial Recharge of Groundwater, EC project ENV4-CT95-0071, Final report, 6.6: 133-135.
- LAHTI K., VAITOMAA J., KIVIMÄKI A.L., SIVONEN K., 1998: Fate of cyanobacterial hepatotoxins in artificial recharge of groundwater and in bank filtration, Artificial Recharge of Groundwater, Peters et al. (eds), Balkema, Rotterdam.
- MILLER M.J., HUTSON J., FALLOWFIELD H.J., 2001: An overview of the potential for removal of cyanobacteria hepatotoxin from drinking water by riverbank filtration, Env. Health, 1 (1): 82-93.

SCHOENHEINZ D., BÖRNICK H., WORCH E., 2005 : Temperature effects on organics removal during river bank filtration, Proceedings of the 5th International Symposium on Management of Aquifer Recharge, ISMAR-5, Berlin, 12-17 june 2005.

World Health Organisation, 1998: Guidelines for drinking water quality, 2nd edition, Addendum to Volume 2, Health criteria and other supporting information, WHO, Geneva.

ZECK A, WELLER M.G., BURSILL D., NIESSNER R., 2001: Generic microcystin immunoassay based on monoclonal antibodies against Adda, Analyst, 126: 2002-2007.

# **7 Clogging Column Experiments**

## **7.1 *Introduction***

The experiments carried out on the clogging column by the working group „algae“ had the aim to examine the elimination of dissolved and extra-cellular microcystin (MCYST) in a setting typical for the Berlin situation. Experiments carried out on the UBA’s experimental field (see final NASRI Report working group algae, part IV and part V) had covered the setting relevant for many artificial recharge and bank filtration sites with mostly sandy sediments. These left a gap regarding settings with fine to medium grained sand with some portions of silt and clay as well as organic material, as are found partially in Berlin and elsewhere. Also, the observation wells at the transects with contact times of 2 weeks minimum did not cover the time span relevant for elimination of microcystins in detail (maximum half life only a few days). Therefore, experiments using the clogging column set up at the FU Berlin provided the opportunity to fill this gap.

Two experiments were carried out with MCYST:

- CC1: Continuous dosing of dissolved MCYST over 9 days, sampling water at different depths,
- CC2: Pulsed application of cyanobacterial cells with subsequent sampling of water and sediment.

## **7.2 *Materials and Methods***

### **7.2.1 *Sediment chemistry***

Further descriptions can be taken from the final NASRI Report working group FUB, part I (see chapter 1.2.2).

### **7.2.2 *Water chemistry***

Further descriptions can be taken from the final NASRI Report working group FUB, part I (see chapter 1.2.3)

### **7.2.3 *Experimental Methods***

#### **7.2.3.1 *Column setup***

Further descriptions of the experimental design can be taken from the final NASRI Report working group FUB, part I (see chapter 1.2.3)

### **7.2.3.2 Experiment with dissolved MCYST (CC1)**

The crude extract of MCYST obtained from the UBA's mass culture (extract # 5 with 62 mg/L MCYST) was diluted 1: 500 with water from Lake Wannsee (see final NASRI Report working group FUB, part I). Prior to the experiment the water reservoir at the top of the column as well as all tubing was emptied and filled with the prepared MCYST solution. The inlet was then connected to a water reservoir with MCYST solution that was permanently stirred (for oxygen saturation) and the bottle was wrapped with aluminium foil to avoid photochemical decay of MCYST.

A tracer experiment with NaCl was carried out in parallel to the first application of MCYST with continuous measurement of the electrical conductivity (EC) at the outlet (see final NASRI Report working group FUB, part I, chapter hydraulics). The experiment commenced on 8th Dec. 2004. On 17th Dec. dosing with MCYST solution was terminated and the column was flushed with lake water. The last sampling was carried out on 27th Dec. 04. Thus, the experiment was carried out 246 to 265 days after column setup.

During the experiment the flow rate through the column amounted to 350 to 550 mL/d, corresponding to a filtration velocity of 0.091 m/d to 0.142 m/d and a flow velocity (considering an effective pore volume of about 30 %) of 30 cm/d to 48 cm/d (see final NASRI Report working group FUB, part I).

Samples for MCYST analysis by ELISA were taken from the water reservoir (before and after the reservoir was exchanged every 2 to 3 days) as well as from the sampling ports at 4, 8, 12, 25, 60, 80, 90 and 99 cm every 2 to 3 days. The samples were stored frozen in glass test tubes and analysed using the Adda-ELISA (see chapter MCYST analyses).

### **7.2.3.3 Experiment with cyanobacterial cells (CC2)**

The experiment with cyanobacterial cells was carried out together with the working group "microbiology" of the TU Berlin, which applied fluorescent particles ( $d = 2.44 \mu\text{m}$ ) simultaneously. The particles and the cyanobacterial cells (taken from the UBA's mass culture of *Planktothrix agardhii* HUB 076) were applied in a pulse by exchanging the water above the column with Lake Wannsee water (300 mL) to which the substances had been added beforehand (200 mL mass culture, 10 mL NaCl solution and 10  $\mu\text{L}$  particle suspension). The resulting initial concentration in the water reservoir was 165  $\mu\text{g/L}$  total MCYST of which 39  $\mu\text{g/L}$  (or 24 %) were extracellular. The biovolume amounted to 34  $\text{mm}^3/\text{L}$ , which is about the maximum concentration of cyanobacteria found in Lake Wannsee during 2002 to 2004 (see final NASRI Report working group algae, part I).

The column was then flushed with water from Lake Wannsee at a constant flow rate of 600 mL/d which corresponds to a filtration velocity of 15.6 cm/d ( $1.8 \times 10^{-6}$  m/s) and a flow velocity of 52 cm/d ( $6 \times 10^{-6}$  m/s). The experiment commenced on 3rd March 2005 and was terminated on 17th March 2005 (331 to 345 days after start of operation).

Similarly to the procedure for the dissolved microcystins, samples for MCYST analysis by ELISA were taken from the water reservoir and from the sampling ports in 4, 8, 12, 25, 60,

80, 90 and 99 cm depth twice a week. Parallel samples were taken for total MCYST (i.e. cell-bound and extra-cellular) and for extra-cellular MCYST (sample filtered by membrane filter, pore size 0.45 µm). The samples were stored frozen in glass test tubes and analysed using the Adda-ELISA (see chapter MCYST analyses). Biovolume of cyanobacteria was additionally determined in the samples from the water reservoir by microscope according to Utermöhl (1958).

After the experiment had been terminated the sediment was extracted from the column and samples were taken on 19th April 2005, 33 days after the last water samples had been taken, for biovolume determination and MCYST analysis. Biovolume of cyanobacteria in the sediment was determined by suspending a known volume of sediment (previously conserved with formolaldehyde) with deionized water with a ratio of 1:10, shaking and centrifuging for homogenisation and sedimentation of the particulate anorganic matter. The supernatant was then examined by microscope following the method described by Utermöhl (1958). The ELISA was carried out from a parallel sample that had been deep frozen and thawed in order to release cell-bound MCYST and also brought into suspension with a known volume of deionized water. This method detects the sum of cell-bound MCYST released from cells trapped within the sediment together with MCYST adsorbed to the sediment and desorbed by addition of deionized water.

## 7.3 *Results*

### 7.3.1 ***Experiment with dissolved MCYST (CC1)***

Samples from the water reservoir were taken directly after preparation of the MCYST solution and before it was disconnected 2 to 3 days later. The results given in Figure 30 show a dramatic drop in concentration over the 2 to 3 days during which the water reservoir was connected to the column (the lines mark samples taken from the same flask, concentration developments would surely follow an exponential decay curve). This drop is most probably due to degradation in the water reservoir. This had not been expected, as previous experience during field experiments had never shown this rapid decline in concentration. The reason for this may lie in the constantly high temperatures of 20°C to 22°C, well above those reached during the field experiments. Hence the input concentration for the experiment was highly variable, making it difficult to draw quantitative conclusions.

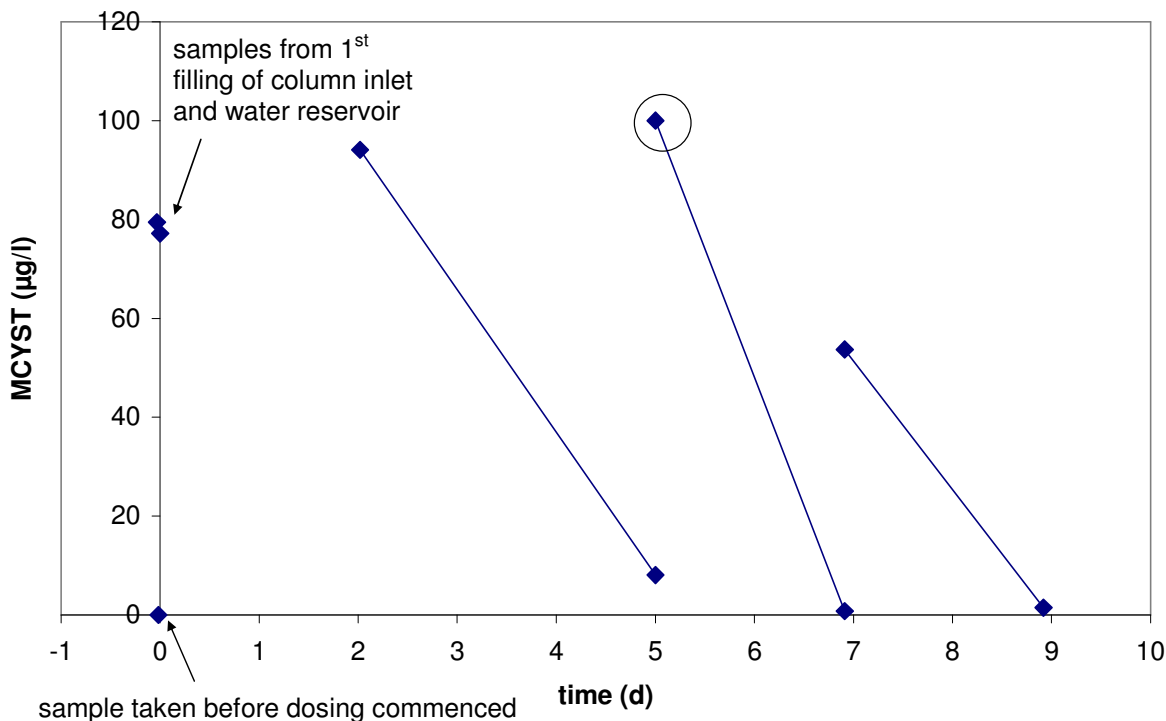


**Figure 30:** Concentrations of MCYST in the water reservoir during the experiment with dissolved MCYST. Lines indicate samples taken from the sample flask, not concentration developments (circle marks MCYST concentration calculated from extract concentration and dilution factor).

The concentrations at the different sampling ports during the experiment are given in Figure 31. Due to the highly variable input (see above) the results are limited to the following points:

Concentrations of initially about 78 µg/L (water reservoir, day 0) decrease to 16 µg/L in 25 cm depth after 2 days (although higher values cannot be ruled out between 25 and 60 cm), a conservative tracer would be expected to reach 61 to 96 cm during this time (see chapter 7.2.3.1). This would imply a retardation coefficient roughly between 1.0 and 3.9.

After additional 3 days (5 d after first toxin application) a maximum in concentration was observed in 80 cm and 90 cm depth with 7.9 µg/L in both of the sampling ports. This maximum most probably traces back to the high concentrations in the water reservoir after it had been exchanged 3 days before. On the basis of these data, retardation coefficients amount roughly to values between 1.0 and 1.7.

After additional 2 days (7 d after first toxin application) a concentration peak of 4.5 µg/L was observed in 80 cm and 90 cm depth. Considering a water reservoir maximum 2 days prior to this sampling event retardation coefficients reach about 0.6 to 1.1. As values < 1 are not likely to occur for MCYST these low MCYST concentrations in 80 to 90 cm may be due to toxins originating from the peak applied on day 2 and only slowly desorbing from the fine particles occurring at the basis of the column (compare final NASRI Report working group FUB, part I). This would also mean that the peak applied on day 5 has been degraded to values < 0.1 µg/L by this time.

Without taking dispersion and retardation into account the elimination rates amount to values between 80 % in two days (1st peak) and 92 % in three days (2nd peak). For peaks 3 and 4 (applied on day 5 and day 7) these rates lie well over 99 % in two days.

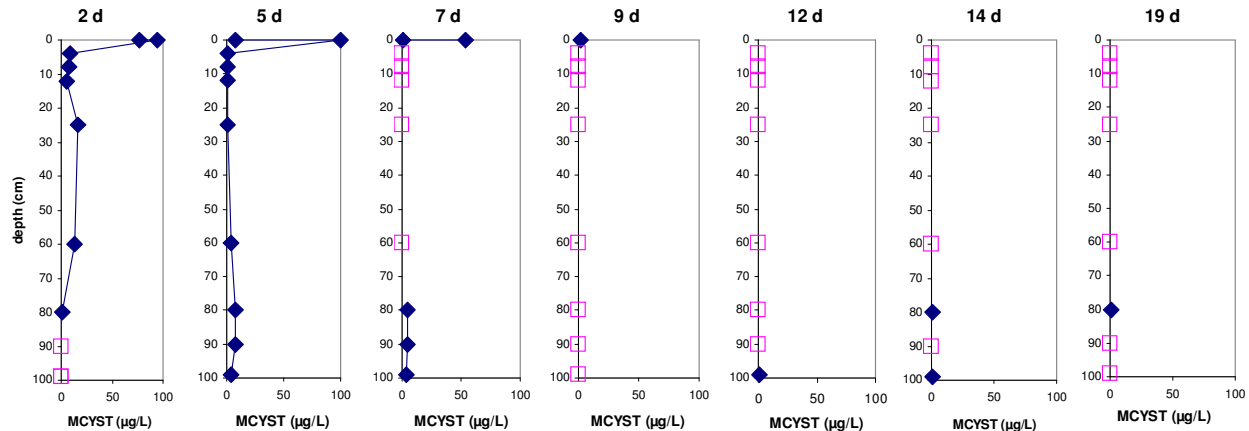


**Figure 31:** MCYST concentrations in the water reservoir (depth = 0) and in the sampling ports during experiment CC1 (two values at depth = 0 correspond to two samples taken before and after exchange of reservoir; open squares: values below detection limit).

These figures show that in spite of very high input concentrations (5 fold higher than the maximum total (i.e. extra-cellular and cell-bound) concentrations in Lake Wannsee during 2002 to 2004) only traces were detectable at the column effluent in 1 m depth, and elimination must be assessed as highly effective. This underpins the field observations of the concentrations measured along the transects at Lake Tegel and Lake Wannsee which were usually below detection limit.

### 7.3.2 Experiment with cell-bound MCYST (CC2)

Experiment CC2 carried out with live cells of *Planktothrix agardhii* had the aim to assess the elimination of cyanobacterial cells through lake Wannsee shore sediment and the possible release of cell-bound MCYST from the strained cells. The biovolume of *Planktothrix agardhii* as well as the MCYST concentrations (total and extracellular) determined in the water reservoir are shown in Figure 32. There is a sharp drop in biovolume and total MCYST during the first day of the experiment. A comparison with the dilution curve calculated on the basis of a constant flow rate of 600 mL/d (Figure 32), which drops even more steeply than the measured values of biovolume, shows that there must be some resuspension of the cells from the sediment surface as growth is unlikely to occur in darkness.

The absolute concentration of extracellular MCYST decreased only slightly during the first day of the experiment, and the relative share of extracellular MCYST increased from 24 % directly after application to 87 % and 86 % on day one. These initially high values might

already be an indication of cell stress or lysis, during which MCYST is released, as usually more than 90 % of the MCYST is cell-bound. This is indicated by changes in concentrations of MCYST per mm<sup>3</sup> of cell volume, i.e. cellular MCYST content, decreased by 60 % from 3.7 µg/mm<sup>3</sup> to 1.45 µg/mm<sup>3</sup> during this time. It could, however, also be due to preferential sedimentation of the cyanobacterial cells, in contrast to extracellular, dissolved MCYST.

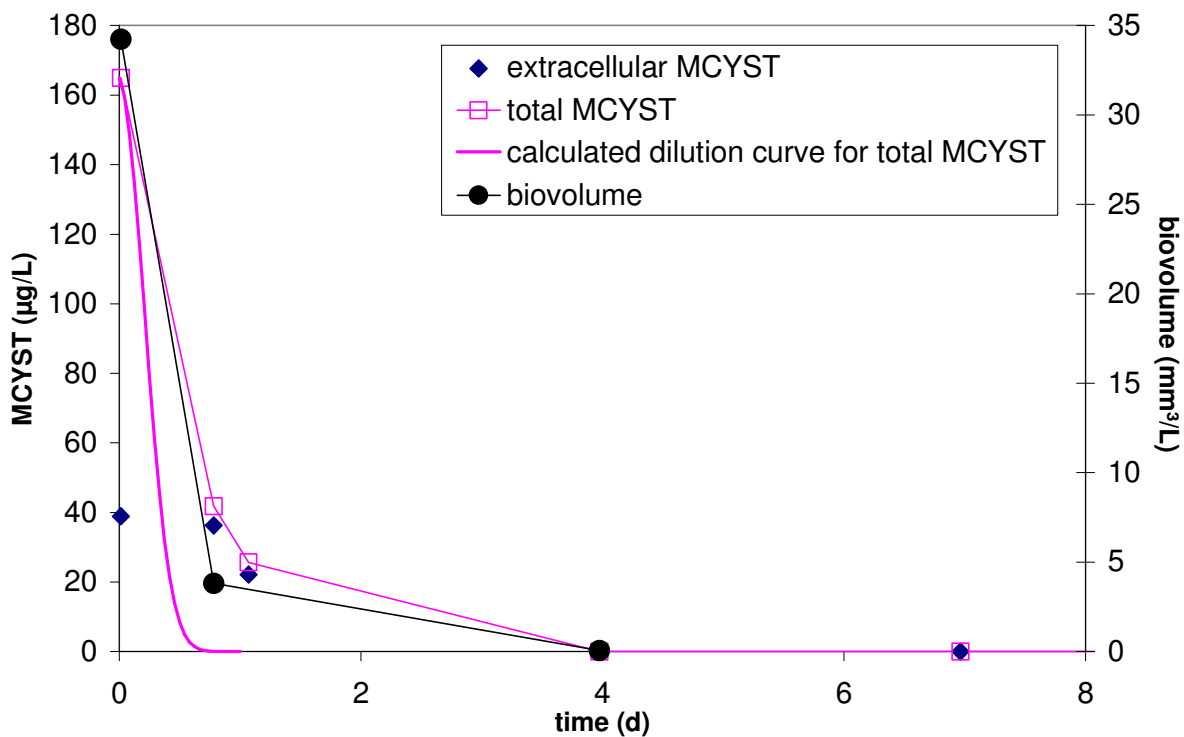


**Figure 32:** Total and extracellular MCYST as well cyanobacterial biovolume in the water reservoir during experiment CC2.

The extracellular MCYST concentrations measured and the cell-bound MCYST concentrations calculated from total and extracellular MCYST in the sampling ports are given in Figure 33 for day four after application. The curves show an increase of both concentrations with depth. No MCYST can be detected in the first 12 cm of sediment passage, cell-bound MCYST is not detectable in the uppermost 50 cm. From 50 cm on downwards extracellular MCYST was determined at concentrations between 0.43 µg/L and 0.48 µg/L. Cell-bound MCYST increases constantly with depth from 70 cm on downwards with a maximum of 1 µg/L in 99 cm depth. From the next sampling event (day 7) on, no MCYST was detectable in the sampling ports.

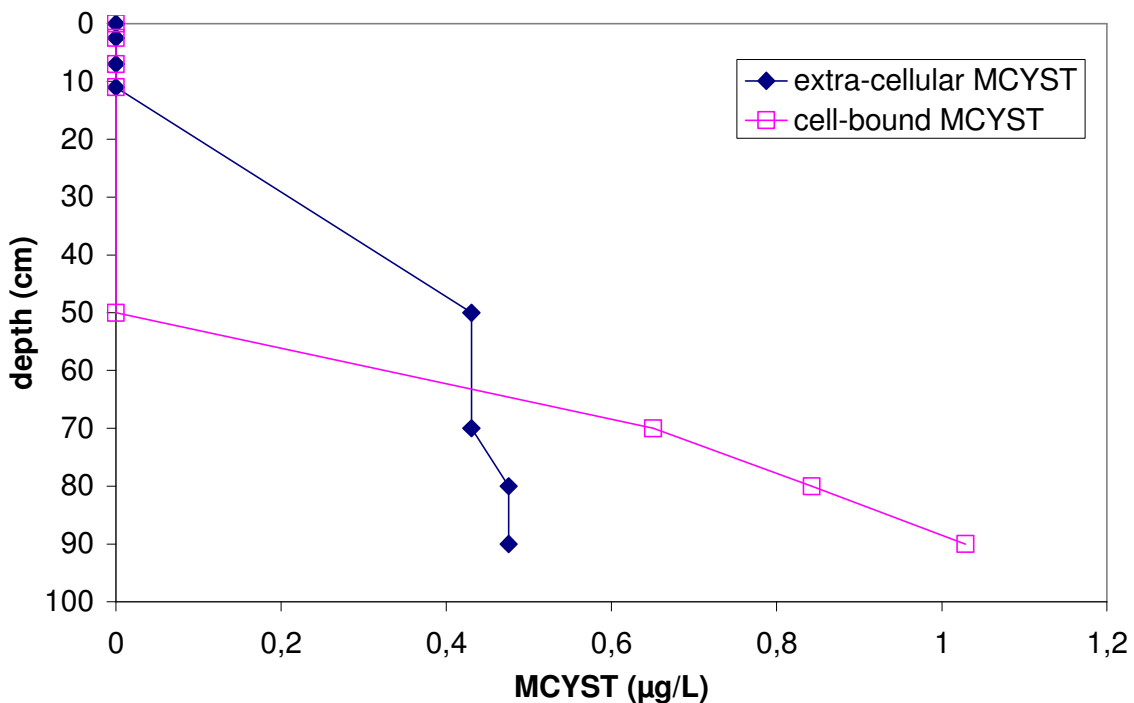


**Figure 33:** Cell-bound and extra-cellular MCYST in the sampling ports on day 4 after application.

Microscopic examination of the sediment after the column was sacrificed showed no filaments of *Planktothrix agardhii* throughout the column. The ELISA revealed low concentrations of extracellular MCYST (< 0.9 to 1.4 µg/L) in the pore water. As no MCYST had previously been detectable in the water samples these traces are probably due to MCYST released from particulate matter either by desorption or from lysed cells. The concentrations, however, are very low and distributed evenly across the entire depth of the column so that remobilisation does not seem to be a factor to be considered in the field setting.

#### 7.4 Interpretation and Discussion

The experiment with dissolved MCYST in the clogging column (CC1) showed two important results:

In repeated pulsed applications retardation coefficients between 1.0 (no retardation compared to a conservative tracer) and 3.9 were observed. This is in agreement with field experiments carried out by our own working group (see final NASRI Report working group algae, part IV and part V) as well as laboratory experiments carried out by Miller (2000).

Degradation could be observed, even under low oxygen conditions (no totally anoxic conditions were achieved during the experiment) and the elimination rates increased with time (from 80 % in the beginning to 99 % during the fourth pulsed application). Similar values

have also been published by other working groups (Lahti et al. 1996, Jørgensen 2001, Miller 2000). Although the adaptation of MCYST degrading bacteria with repeated contact has so far only been shown with lake water and without sediment contact (Christoffersen et al. 2002), this is the most likely mechanism causing enhanced elimination rates over time.

The second experiment with initially mostly cell-bound MCYST on the clogging column (CC2) showed the following results:

During the first day of application the ratio of extracellular MCYST in the water reservoir increased from 24 % to 86 % probably due to cell lysis under unfavourable conditions and / or sedimentation of cells. The assumption that release of MCYST from the cells is the main mechanism is supported by the fact that the concentrations of MCYST per mm<sup>3</sup> of cell volume, i.e. cellular microcystin content, decreased by 60 % during this time.

After four days the uppermost 12 cm showed no detectable MCYST in the aqueous phase. This leads to the assumption that the cells accumulated on the sediment surface do not act as a continuous source for MCYST.

In greater depth, however, extracellular as well as cell-bound MCYST was detectable, mostly with greater cell-bound than extracellular concentrations. This shows that a breakthrough of cells may well be possible and has to be regarded more closely in further experiments.

In summary, the experiments with MCYST on the clogging column showed results that complement the observations on the transects at Lake Wannsee and support the field results observed at these sites: Extracellular MCYST is degraded rapidly in the lake sediments even under conditions of low oxygen concentrations. Thus even maximum MCYST concentrations of 20 µg/L (greatest extracellular concentrations measured in Lake Wannsee surface water) would be reduced to at least 4 µg/L during the first day of sediment contact. Field observations showed that maximum values in observation wells with residence times of about 2 weeks amounted to less than 1 µg/L.

Concerning the complex question of interaction between extracellular and cell-bound MCYST the experiments still leave some uncertainties. Although an accumulation and subsequent continuous release of MCYST from sedimented cells could not be confirmed, the transport of cell-bound (possibly particle bound) MCYST through sediment has to be observed more closely in future experiments.

## 7.5 References

- Christoffersen K., Lyck S. & Winding A. (2002): Microbial activity and bacterial community structure during degradation of microcystins., *Aq. Microb. Ecology*, 27: 125 – 136.
- JØRGENSEN C., 2001: Removal of algae toxins during artificial recharge – column and batch studies, Artificial Recharge of Groundwater, EC project ENV4-CT95-0071, Final report, 6.6: 133-135.
- Lahti, K., J. Silvonen, A-L. Kivimäki and K. Erkoma (1996) Removal of cyanobacteria and their hepatotoxins from raw water in soil and sediments columns in Artificial Recharge

of Groundwater, Proceedings of an international symposium, A-L. Kivimäki and T. Suokko (eds.) Finnish Environment Institute, Helsinki, 187-195.

Miller M.J. (2000): Investigation of the removal of cyanobacterial hepatotoxins from water by river bank filtration . PhD Thesis, Flinders University.

Utermöhl H. 1958. Zur Vervollkommnung der quantitativen Phytoplanktonmethodik. Mitt Int Ver Limnol 9: 1 – 38.

## 8 Slow sand filter experiments

### 8.1 Introduction

The slow sand filter (SSF) experiments on the UBA's experimental field were carried out in order to investigate elimination processes during relatively short contact times and high flow velocities in comparison to the bank filtration sites. This was necessary especially for those substances that are usually readily removed by sediment contact (e.g. algal toxins, viruses and bacteria). For these substances the observation wells at the transects with contact times of 2 weeks minimum did not cover the time of interest. A second reason for conducting SSF experiments was the opportunity to observe substance removal during underground passage in settings likely to occur in other regions of the world and / or during artificial recharge. This was necessary as the bankfiltration sites in Berlin are not typical for most other settings and some of the investigated substances were not present in the artificial recharge basin at Tegel at sufficient level for detailed investigation. Additionally the slow sand filter offered the opportunity to investigate the formation of a clogging layer under well defined conditions by hydraulic, geochemical and microbiological methods.

Figure 34 gives an overview of all investigations and experiments carried out on the slow sand filter during the NASRI project.

	Jan.	Feb.	March	April	May	June	July	Aug.	Sept.	Oct.	Nov.	Dec.
	<b>2002</b>											
technical modifications												
	<b>2003</b>											
technical modifications												
average filtration velocity												
microbiol. Investigations												
experiments												
	<b>SSF1</b>	<b>SSF2</b>	<b>SSF3</b>	<b>SSF4</b>	<b>SSF5</b>							<b>SSF6</b>
date of experiments			19.3.03	15.4.03	23.04.03	26.5.03	17.6.03					19.11.03
applied substances			NaCl, phages	MCYST	NaCl, drugs	NaCl, phages	NaCl, MCYST, phages, drugs					NaCl, MCYST, phages, bact., drugs
	<b>2004</b>											
technical modifications												
average filtration velocity												
microbiol. Investigations												
experiments												
date of experiments												
applied substances												
Legend:	SSF dry SSF flooded (little or no clogging) SSF flooded (visible clogging layer)											

Figure 34: Overview of the investigations and experiments carried out on the SSF.

The aim of the series of experiments conducted with MCYST was to test elimination under a combination of 3 worst-case conditions (experiment SSF2: virgin sand that had no previous contact to MCYST, missing clogging layer and with 2.4 m/d high filtration velocities) in order to test whether lower filtration velocities (experiment SSF5: 1.2 m/d and experiment SSF6: 0.6 m/d) and enhanced clogging can lead to better removal rates.

## 8.2 Materials and Methods

### 8.2.1 Technical scale slow sand filter on the UBA's experimental field

The slow sand filter (SSF) is fed with surface water from a storage pond of the facility and has a surface area of 73 m<sup>2</sup> (Figure 35). As the pond narrows towards the bottom the average area of the filter sand is 60.4 m<sup>2</sup>. The water reservoir above the filter bed has a depth of 30 cm to 60 cm and a volume of approximately 40 m<sup>3</sup>, depending on the water level adjusted for the respective experiment. Water percolates through the filter following gravitational flow. The filter bed has a depth of 80 cm with a gravel layer of 15 cm depth at the bottom and 65 cm of filter sand above. The drainage pipes form a double-H (Figure 36), ensuring almost vertical flow.

The filter sand was replaced in autumn 2002 in order to carry out experiments with virgin sand for the simulation of worst case conditions (Figure 37).

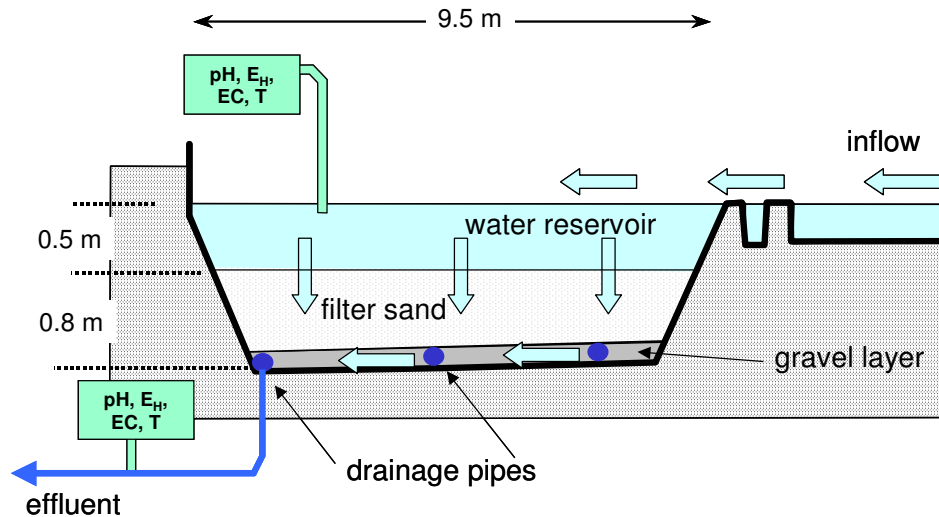


**Figure 35:** Schematical cross section of the slow sand filter



**Figure 36:** Drainage pipes on the basis of the slow sand filter during sand exchange.



**Figure 37:** Preparation of the filter sand during sand exchange.

## 8.2.2 Characterization of the virgin filter material

The filter sand is medium to coarse sand with small amounts of fine sand. Silt and clay are not present. The gravel layer consists of fine gravel with large amounts of medium grained gravel (Figure 38).

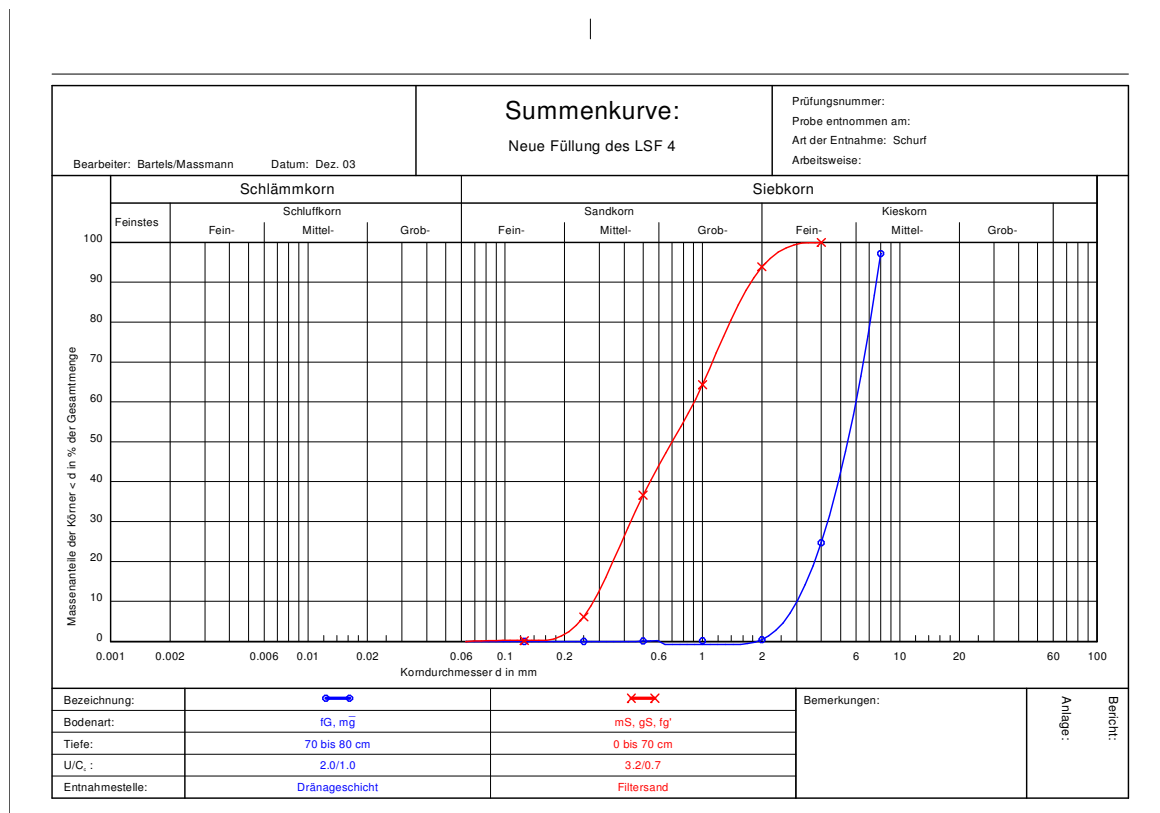


Figure 38: Grain size distribution of the filter material in the SSF (data by FU Berlin).

Table 7: Geochemical properties of the virgin SSF sand in comparison to sand from Lake Wannsee's shore (data by FU Berlin).

Parameter	virgin SSF sand	sand from Lake Wannsee shore (average of two samples taken by FU Berlin $\pm$ standard deviation)
Fe-ox [mg/kg]	275	457 ( $\pm$ 140)
Fe-red [mg/kg]	850	838 ( $\pm$ 88)
Fe-total [mg/kg]	1125	1295 ( $\pm$ 52)
Mn-ox [mg/kg]	11.0	30 ( $\pm$ 24)
Mn-red [mg/kg]	17.5	16.3 ( $\pm$ 8.8)
Mn-total [mg/kg]	28.5	46 ( $\pm$ 16)
C-org [weight %]	0.022	0.37 ( $\pm$ 0.29)
C-inorg [weight %]	0.118	0.36 ( $\pm$ 0.13)

The geochemistry resembles that of sand taken from the shore of Lake Wannsee fairly well (Table 7), with exception of the total Fe content (13 % less in the filter material) and the cation exchange capacity (CECeFF: 82 % less in the filter material). This is probably due to the coarser grain size of the filter material (Massmann et al. 2004).

### **8.2.3        *Hydrochemistry under normal operating conditions***

The surface water used for the experiments originates from the surrounding aquifer and is treated for iron and manganese removal in the water works of the experimental field before being fed into the storage pond. Its high electrical conductivity (about 950 µS/cm) is due to relatively high concentrations of salts ( $\text{HCO}_3^-$ : 140 mg/L,  $\text{SO}_4^{2-}$ : 230 mg/L,  $\text{Cl}^-$ : 95 mg/L,  $\text{Ca}^{2+}$ : 130 mg/L and  $\text{Na}^+$ : 45 mg/L, average of 3 samples taken during 2002 and 2003, data is given in appendix IV-1). The DOC ranges from 5.5 mg/L in summer to 2.4 mg/L during winter. Calculations with PHREEQC show that in relation to the atmosphere the surface water is slightly oversaturated with  $\text{CO}_2$  and  $\text{O}_2$  (partial pressures 0.08 % and 28 %, respectively), probably due to biological activity of algae and water plants. This might also be the reason for the slightly alkaline pH in the water reservoir (pH 8.2 in average).

During sand passage a slight reduction of pH (to pH 7.9),  $\text{O}_2$  (to a partial pressure of 20 %) and DOC (40 % reduction in summer and 15 % reduction in winter) can be observed. On the other hand, nitrate can be detected at values around 0.4 mg/L, while it cannot be detected in the surface water, due to nitrification inside the filter.

### **8.2.4        *Experimental Methods***

In preparation of the experiments the flow rate was adjusted to the desired amount, corresponding to the filtration velocities. The tracer and the trace substances were applied by spraying them evenly across the water reservoir with a hose from a barrel containing the concentrated substances diluted with 100 L of tap water. The tracer applied was sodium chloride ( $\text{NaCl}$ ) so that the sampling intensity in the different sampling points could be adjusted by observing the electrical conductivity (EC). Care was taken not to increase the electrical conductivity by more than 10 %.

The MCYST applied was extracted from a mass culture of *Planktothrix agardhii* HUB 076 by centrifugation and freeze thawing in order to release the mainly cell-bound, highly water soluble microcystins. The freeze thawed extract was homogenized and then centrifuged to remove the cell debris and stored frozen. One day prior to each experiment the extract was thawed and partitioned into the required volume. The application to the water reservoir was carried out as mentioned above. The resulting MCYST concentrations in the water reservoir amounted to  $10 \mu\text{g/L} \pm 2 \mu\text{g/L}$ .

## 8.3 Results

Quantification of clogging by different methods

Hydraulic conductivity

Figure 39 gives the development of hydraulic conductivity ( $k_f$ ) determined by hydraulic head ( $i$ ) and flow rate ( $Q$ ) according to (1).

$$k_f = v_f / i = Q / (A * h / l) \quad (1)$$

With A: average area of the SSF ( $60.4 \text{ m}^2$ ),

h: head loss between water reservoir and effluent,

l: height of filter bed (0.8 m).

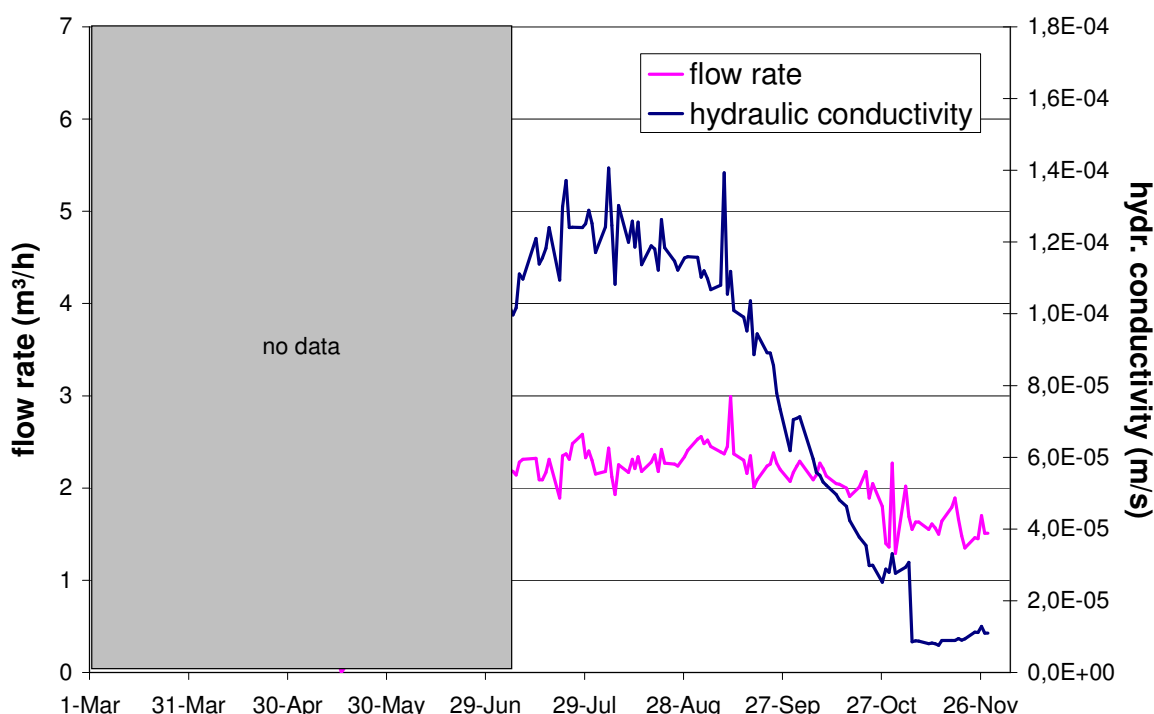


**Figure 39:** Flow rate and hydraulic conductivity in the slow sand filter used for the SSF experiments during 2003 (time scale corresponding to Figure 41).

The filter showed a substantial increase of clogging between August and November 2003. During this time hydraulic conductivity was reduced from  $1.2 * 10^{-4}$  to  $0.5 * 10^{-4}$  m/s. Due to missing water table measurements before July 2003 no hydraulic conductivities could be calculated. As the observed water table was lower than during summer and the flow rate higher (up to  $6 \text{ m}^3/\text{h}$ ), we can conclude that the hydraulic conductivities must have been substantially higher.

In August 2004, after all SSF experiments had been carried out, the superficial layer of the slow sand filter was destroyed by raking. As can be seen on the picture taken during this

procedure (Figure 40), gas bubbles emerged, indicating that clogging had lead to partially unsaturated conditions due to trapped gas in the upper centimeters of the filter.



**Figure 40:** Photograph taken during raking of the SSF in order to destroy the superficial clogging layer.

### 8.3.1.1      Organic substance determined by loss on ignition (LOI)

The LOI-results of the 5 cm cores sampled weekly during 2003 (Figure 41) show high variations (minimum: 0.26 %; maximum: 4.4 %) in time and depth. The variations between different depth increased over time, as did some absolute values. In the beginning of 2003 when the measurements started the differences in LOI between the layers sampled did not exceed 0.5 %. In autumn 2003 the difference on some occasions reached 2 %. The highest values of LOI were measured in the uppermost millimeter of the filter in some samples taken during summer and autumn 2003. In other samples of this layer taken during that time, however, no relevant increase was observed compared to the values measured in March 2003. It was supposed that this may be due to a high spatial inhomogeneity. In order to test this, six samples from different places distributed over the filter surface were taken on one occasion and analysed by the same method.

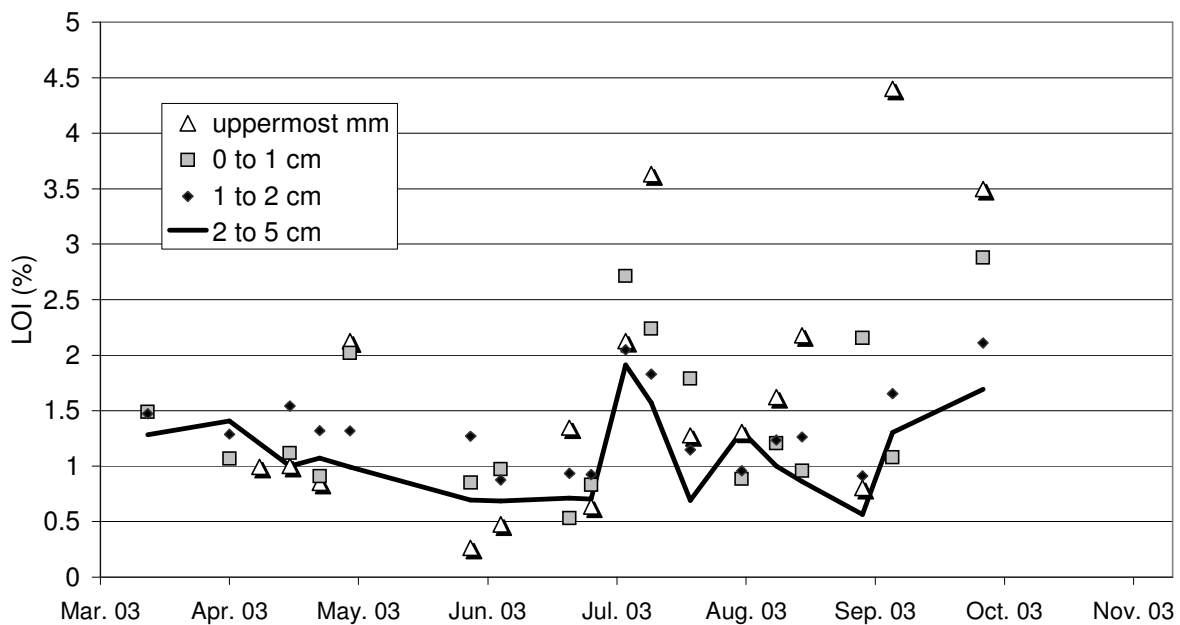


**Figure 41:** Loss on ignition (LOI) as measure for organic substance in the filter bed of the SSF.

The results show a regional variation of up to 1 % LOI (95 % confidence interval) with highest variations in the uppermost centimeter (Figure 42). These variations, however, do not explain the differences of up to nearly 4 % between the different sampling events in 2003.

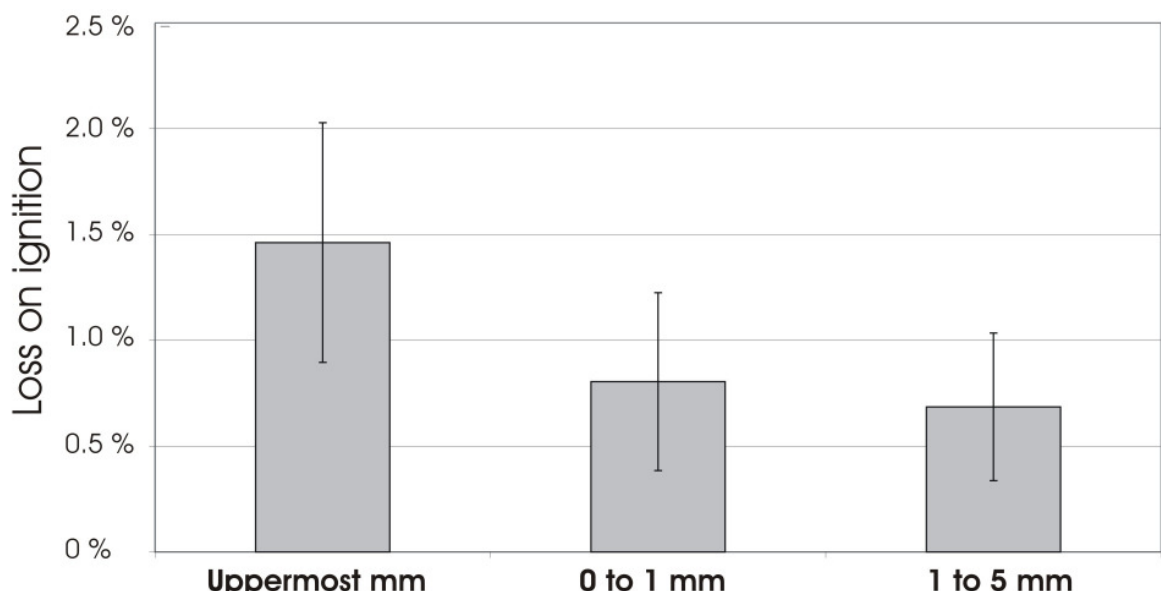


**Figure 42:** Variation of LOI during one sampling event (error bars indicate the 95 % confidence interval, n = 6).

### 8.3.1.2 Geochemistry of the clogging layer

Table 8 gives the geochemical properties of the clogging layer in comparison to the values determined in the virgin SSF sand. The results show a clear increase of all the parameters measured. This is due to the accumulation of organic substance (debris and biomass lead to a 10-fold increase of Corg). There is, however, also a distinctive increase in inorganic carbon concentration (also more than 10-fold) as well as iron and manganese, probably due to the relative increase of fine mineral material.

**Table 8:** **Geochemical properties of the clogging layer in comparison to virgin SSF sand. (Massmann et al. 2004).**

Parameter	virgin SSF-material	clogging layer
Fe-ox [mg/kg]	275	605
Fe-red [mg/kg]	850	1700
Fe-total [mg/kg]	1125	2305
Mn-ox [mg/kg]	11.0	68.8
Mn-red [mg/kg]	17.5	100.0
Mn-total [mg/kg]	28.5	168.8
C-org [weight %]	0.022	0.343
C-anorg [weight %]	0.12	1.40

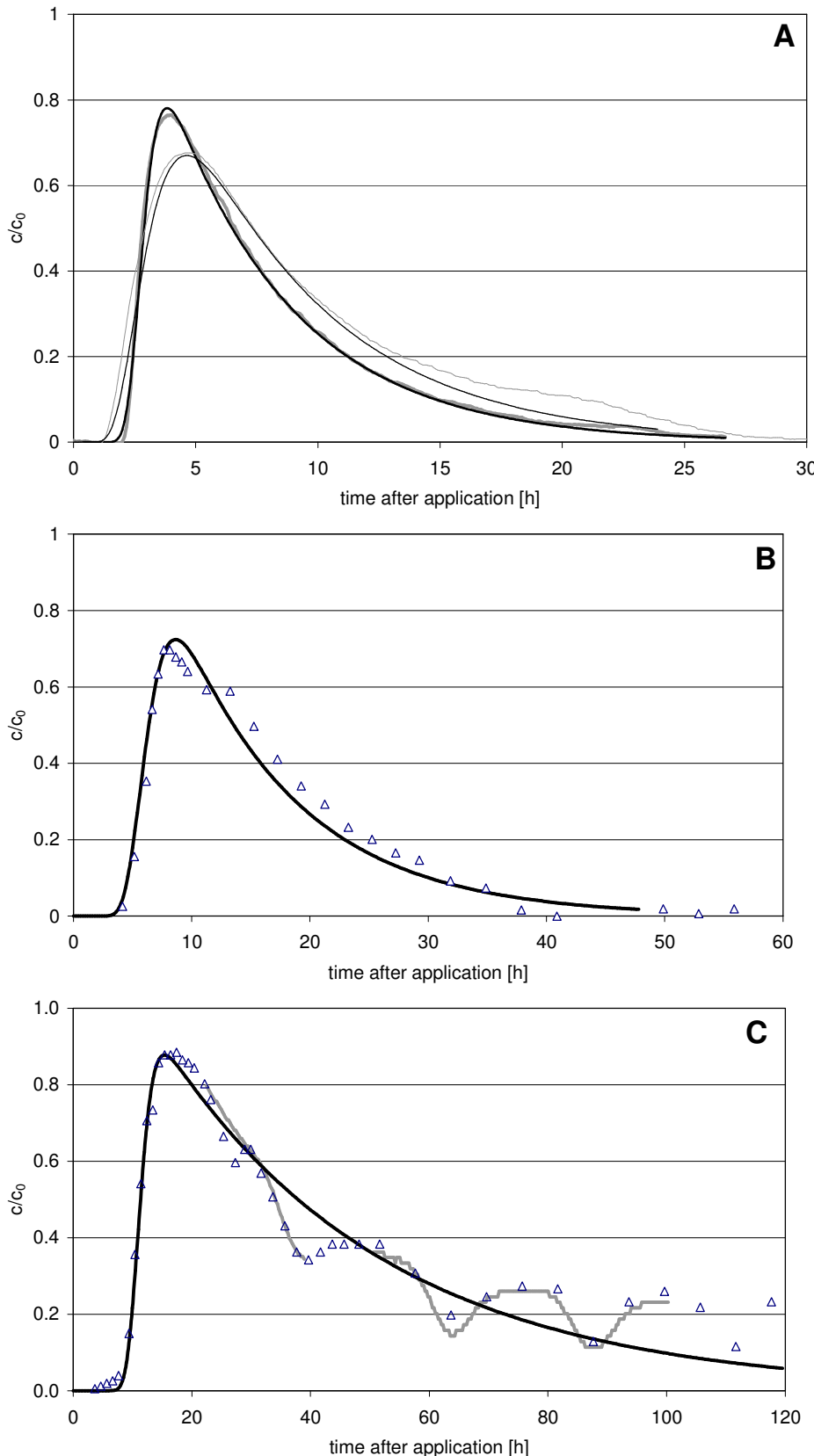
### 8.3.1.3 Hydraulic properties determined by tracer experiments

Figure 43 gives the conductivities measured in the effluent as well as the curves modelled by using Visual CXTFIT for all tracer experiments carried out in the course of 2003. Table 9 lists the modelled pore velocities, dispersion lengths as well as the filter resistance for each of the experiments conducted on the slow sand filters and enclosures.

**Table 9:** **Pore velocities, dispersion lengths, effective pore volumes and hydraulic conductivities during the tracer experiments on slow sand filter.**

Experiment No.	Filtration velocity	Pore velocity	Dispersion length	Eff. Pore-volume (ne)	Hydraulic conductivity
	[m/d]	[m/d]	[m]		[m/s]
SSF1	2.4	6.24	0.012	0.385	n.d.
SSF3	2.58	6.48	0.05	0.37	n.d.
SSF5	1.43	3.12	0.023	0.385	1.4*10-4
SSF6	0.59	1.68	0.01	0.357	7.4*10-6

The slow sand filter experiments were conducted with three different filtration velocities (about 2.5 m/d, 1.4 m/d and 0.6 m/d). Therefore pore velocities changed correspondingly. The reduction of the dispersion length between SSF3, SSF5 and SSF 6 can also be explained by the decline of flow velocities. A substantial disturbance of one part of the filter due to installation of microbial slide holders before SSF3 (see Figure 35) may be the reason for the increase in dispersion length between SSF1 and SSF3 with otherwise similar conditions. Effective pore volumes vary between 0.357 and 0.385, with a trend to smaller values with time. This is in line with the overall increase of hydraulic resistance. As to be expected average hydraulic conductivities dropped during 2003 due to clogging (see chapter 3.1).



**Figure 43:** Measured electrical conductivity and modelled output function for SSF tracer experiments. Symbols: hand measurements, grey lines: online measurements, black lines: modeled curves. A: SSF1 (thick lines) and SSF3 (thin lines); B: SSF 5; C: SSF6 (note different time scales on x-axis for A, B and C).

### **8.3.1.4 Assessing the clogging situation of the slow sand filter during the experiments**

Different methods were used to assess the clogging situation of the slow sand filter in 2003:

- Calculating hydraulic conductivities from daily measurement of water table and flow rates,
- Calculating effective porosities from pore velocities obtained by modelling breakthrough curves during tracer experiments,
- Measuring the organic content in the upper centimeters of the filter bed from weekly sampling,
- Determining the biomass by total cell count in weekly samples from the upper centimeters of the filter bed,

The hydraulic conductivities showed a clear and constant decrease in the course of September ( $1.2 \times 10^{-4}$  m/s) to November 2003 ( $0.2 \times 10^{-4}$  m/s) with previous short term variations (probably due to higher flow rates during rainfall) of  $0.2 \times 10^{-4}$  m/s between June and September (Figure 39). Effective porosities, calculated from tracer breakthrough curves, show a similar pattern of quite constant values between 0.37 and 0.385 during the first few experiments (SSF1 through SSF 5) until June 2003. No tracer tests were performed from July to October, but in November the effective porosities had decreased significantly to 0.357 (Table 9).

The bio- and geochemical processes leading to this decrease in hydraulic conductivity (or clogging) were assessed with the two other methods mentioned above (LOI measurement and total cell count).

As expected, the measured values for organic content (loss on ignition, LOI) showed an increase from values around 1.5 % ( $\pm 0.5$  %) in March, April and May to 2 % ( $\pm 1$  %) after July (Figure 41). There are, however high temporal variations in all layers sampled (uppermost millimeter, 0 to 1 cm, 1 to 2 cm and 2 to 5 cm) with the temporal variations increasing in time and exceeding the vertical and horizontal spatial variations. These results imply that high organic content usually concurs with lower hydraulic conductivities. Lower organic content, however, does not necessarily mean high conductivities.

An indication of which processes take place during clogging can be derived from the observation of gas bubbles during raking of the filter surface (Figure 40). The formation of gas bubbles is due to biological activity inside the filter bed without the possibility of escaping to the water surface (which may be due to physical clogging by fine organic and inorganic particles).

During the enclosure experiments carried out with the same filter material, substances and water quality further results concerning clogging processes in this setting were obtained. They will be discussed in part V of this report.

### 8.3.2 *Changes in general hydrochemistry during the experiments*

Table 10 shows the results of the main cation and anion analysis carried out by the FU Berlin on samples taken during SSF 5.

**Table 10:** Main anions and cations during TV 6 (data by FU Berlin).

Time after application	Sodium	Potassium	Calcium	Magnesium	Chloride	sulfate	Nitrate	Phosphate
	Mmol/L							
Water reservoir	-0.6	2.02	0.11	3.13	0.74	2.82	2.46	0.005 < 0.001
	0.1	4.67	0.12	3.25	0.75	5.61	2.50	0.005 < 0.001
	5.1	3.61	0.12	3.20	0.74	4.51	2.35	0.005 < 0.001
	25.1	2.22	0.11	3.25	0.74	3.05	2.38	0.006 < 0.001
Effluent	0.7	2.02	0.11	3.30	0.77	2.82	2.36	0.006 < 0.001
	6.1	2.94	0.12	3.40	0.81	4.09	2.35	0.006 < 0.001
	34.9	2.27	0.10	3.15	0.74	3.07	2-43	0.006 0.003

In the course of the experiment no relevant change in inorganic hydrochemistry can be seen with exception of sodium and chloride that were added for tracer reasons together with the trace substances. The slight increase in calcium and magnesium in the effluent compared to the water reservoir before the experiment may indicate some cation exchange with the sodium added.

Simultaneously, DOC was analysed in a few representative samples. The results are shown in Figure 44. They indicate an increase in DOC removal during the course of the experiment that may be due to the addition of highly biodegradable polysaccharides together with the algal extract.

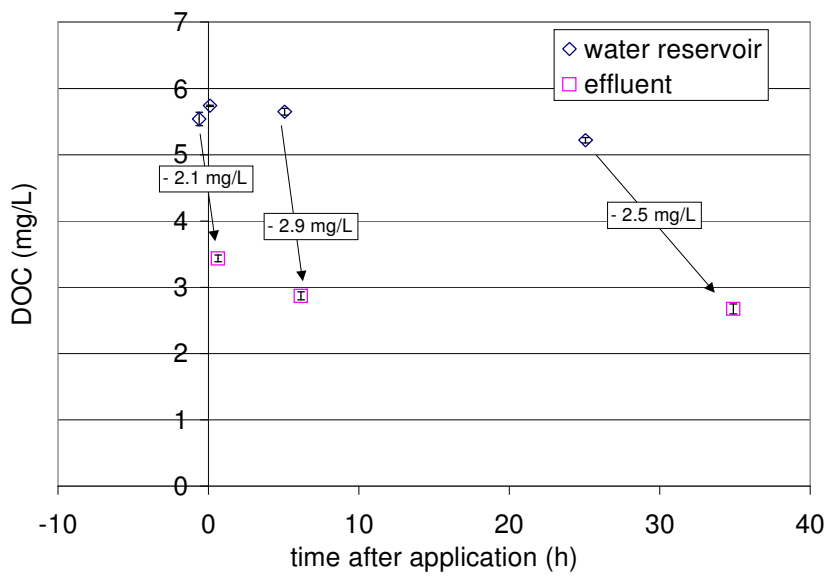


**Figure 44:** DOC values during SSF5 (data by TUB). Polysaccharides were reduced substantially through the filtration process, as indicated by the pronounced reduction of the peak at 39 min. in LC-OCD chromatograms (Fig. 12).

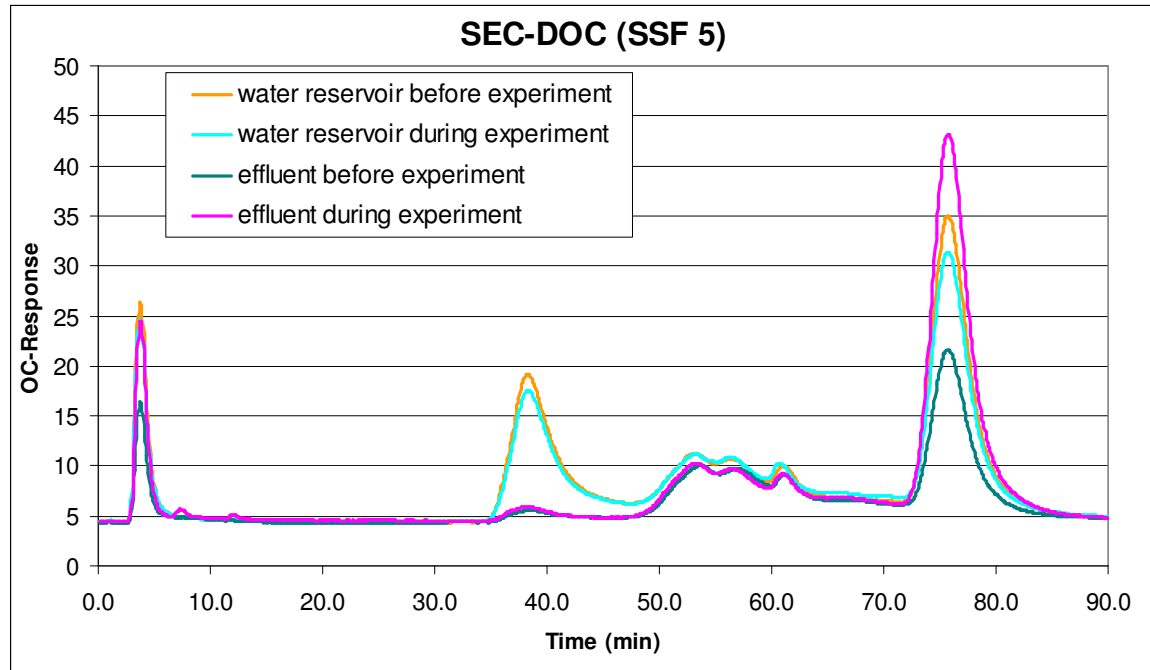


**Figure 45:** LC-OCD Chromatogram of samples taken before and during experiment SSF 5 (data by TUB).

### 8.3.3 *Elimination of trace substances during the experiments*

#### 8.3.3.1 Cyanobacterial Toxins

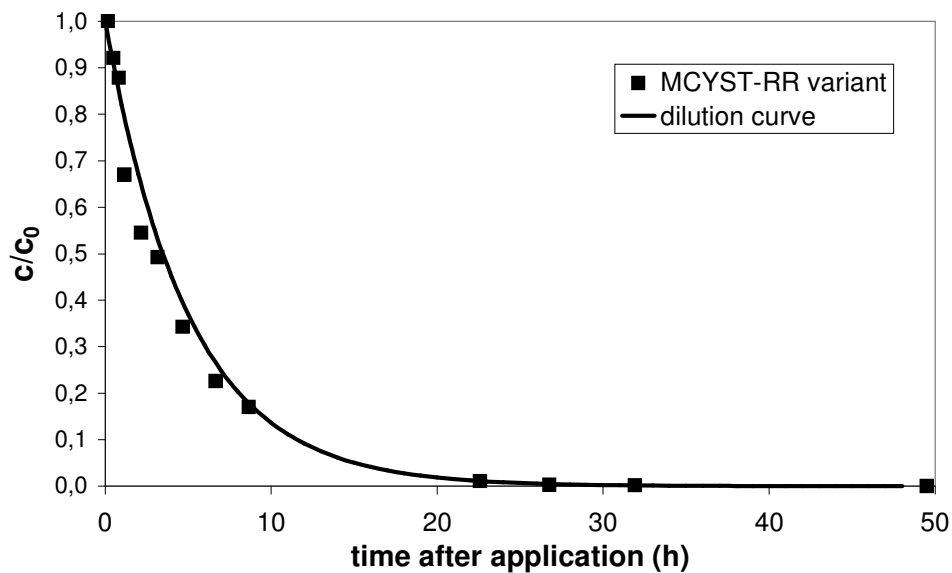
Table 11 gives a summary of the initial parameters during the three SSF experiments conducted with MCYST. The MCYST concentrations were determined by HPLC and refer to the main MCYST variant (demethylated MCYST-RR). Two other peaks with UV spectra characteristic for MCYST were visible in some the HPLC chromatograms of water reservoir samples at retention times of 21.7 min and 14.2 min during SSF2 and SSF6. The concentrations, however, were below the limit of quantification (< 0.1 µg/L).

The mean residence times in Table 11 were obtained by modelling the tracer experiments conducted before and after the MCYST experiments (for SSF2) or simultaneously (for SSF5 and SSF6). They represent the half life of the fitted exponential decay function.

**Table 11:** Initial parameters of the SSF experiments with MCYST.

Experiment no.	Minimum and maximum air temp. [°C]	Average filtration velocity [m/d]	Clogging layer visible?	MCYST applied [mg] determined by HPLC	Initial concentration of MCYST determined by HPLC [µg/L]	Mean residence time in water reservoir [h]
SSF2	8 – 19.5	2.49	No	462	10.5	3.6
SSF5	14.7 – 25	1.43	Yes	301	8.6	6.3
SSF6	4.8 - 13	0.59	Yes	190	5.95	16.8

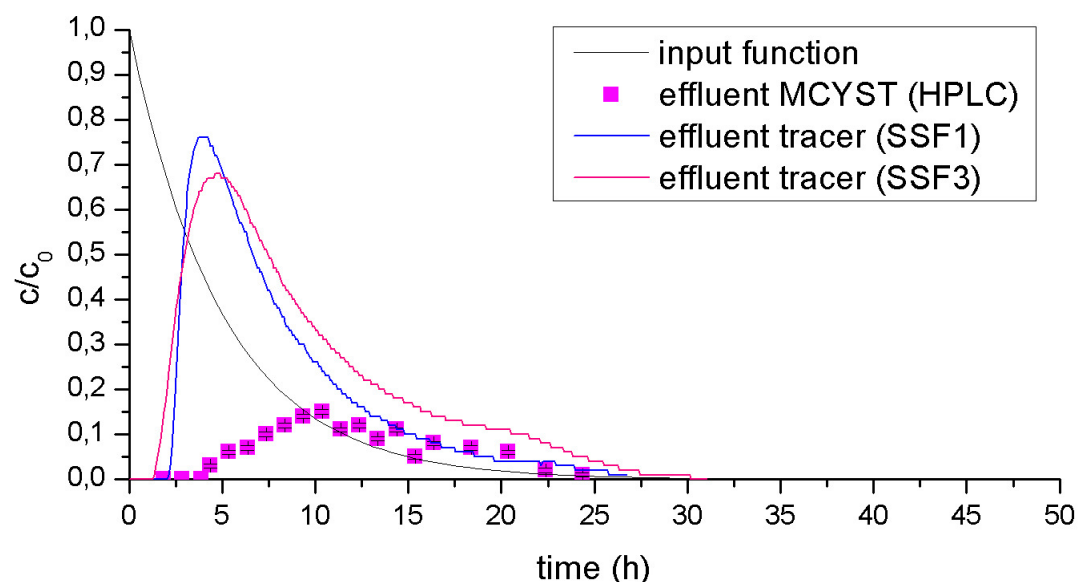
The relative concentrations of the main MCYST variant (demethylated (dem) MCYST-RR, determined by HPLC) measured in the water reservoir during SSF2 as well as the calculated dilution curve (confirmed by two tracer tests) are shown in Figure 46. These data confirm that there is no relevant degradation of this MCYST-variant in the water reservoir during the mean residence time of about 3 hours. Similar results were obtained in SSF5 and SSF6 with mean residence times in the water reservoir of 6.3 h and 16.8 h, respectively (see appendix IV-1).



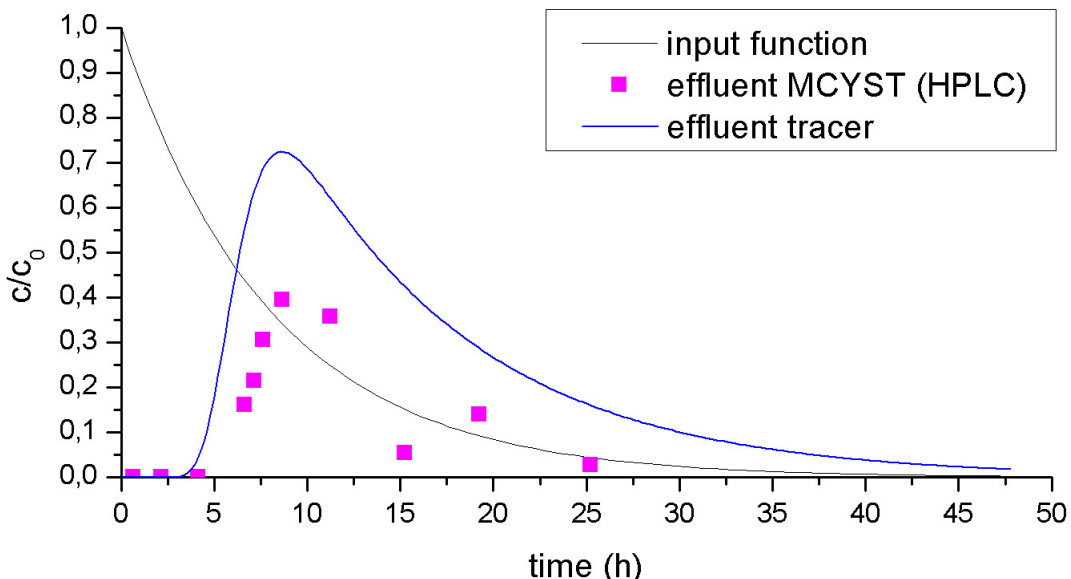
**Figure 46:** Concentration of demethylated MCYST-RR (main MCYST variant of mass culture) in the water reservoir during the slow sand filter experiment SSF2.

Figure 47 through Figure 49 show the effluent concentrations of MCYST during the three experiments (as sum of all MCYST variants determined by HPLC) in relation to the calculated dilution curve for the water reservoir concentrations and the tracer breakthrough curves (obtained by modelling the tracer results with VCXTFIT).

Compared to the tracer peak MCYST shows a clear retardation and decrease in concentration in all three experiments.



**Figure 47:** Effluent concentrations of MCYST in experiment SSF2 (tracer results refer to separate tracer experiments, before and after SSF2).



**Figure 48:** Effluent concentrations of MCYST in experiment SSF5.

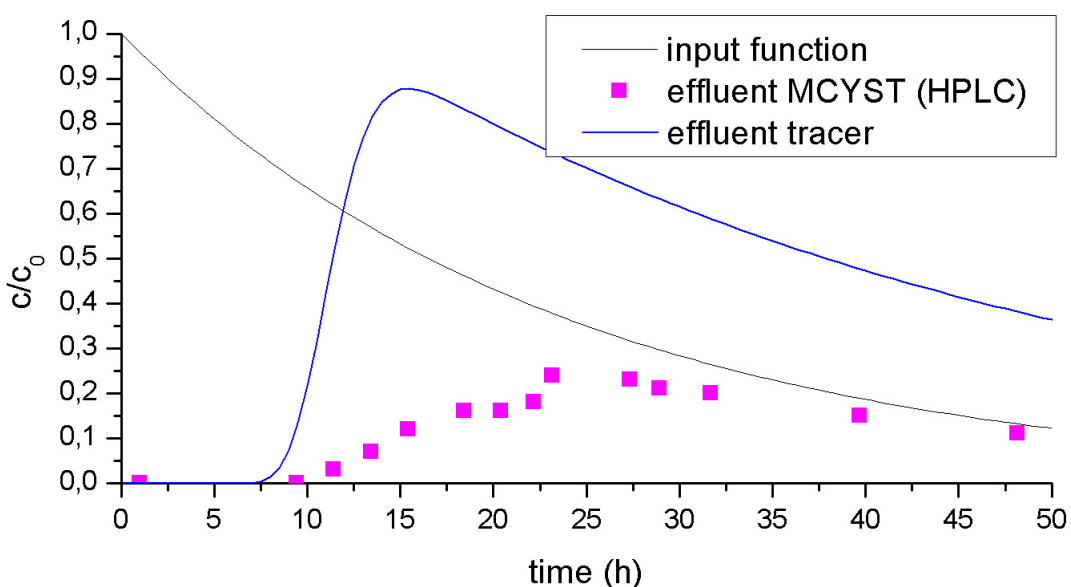


**Figure 49:** Effluent concentrations of MCYST in experiment SSF6 (after 50 h MCYST concentrations were no longer detectable).

Table 12 gives the amounts of MCYST recovered in the effluent during the SSF experiments. Concerning the recovered shares of MCYST there is a distinctive difference between SSF2 and SSF5 on the one hand (22.5% and 26.5%, respectively) and SSF6 on the other hand with a higher recovered share of 37.2 % of the initially applied MCYST. This shows that higher residence times in the filter do not necessarily lead to higher removal rates. Other parameters like temperature, see final NASRI Report part V (enclosures) and part VII

(laboratory experiments) may have a far stronger influence. Surprisingly, the results also indicate that the worst case conditions simulated in SSF2 (virgin sand, no visible clogging layer, high flow velocity) did not lead to lower removal rates.

**Table 12: Recovered amounts of MCYST the experiments SSF2, SSF5 and SSF6.**

Experiment no.	Minimum and Maximum air temperature [°C]	Measured mean filtration velocity [m/d]	Clogging layer visible?	Mean residence time in filter [h]	MCYST recovered by HPLC [mg]	Share of recovered MCYST by HPLC [mg]
SSF2	8 – 19.5	2.49	No	3.0	104	22.5 %
SSF5	14.7 – 25	1.43	Yes	6.2	79,9	26.5 %
SSF6	4.8 - 13	0.59	Yes	11.4	70,7	37.2 %

In the HPLC chromatograms of the effluent samples up to 7 different peaks of substances were identified that show UV-spectra typical for microcystins. Figure 50 shows the distribution of the different peaks in effluent samples from SSF2, characterized either by MALDI-TOF (as  $[\text{Asp}^3]\text{MCYST-RR}$  and  $[\text{Asp}^3]\text{MCYST-LR}$ ) or by their retention time (RT). Of these only the  $[\text{Asp}^3]\text{MCYST-RR}$  had been detected in the water reservoir. Similar results, however with some different MCYST-peaks in the effluent, were observed in SSF5 and SSF6 as well as in the enclosure and laboratory experiments. The reasons for this are still unclear and will be discussed in part IIX (analytics).

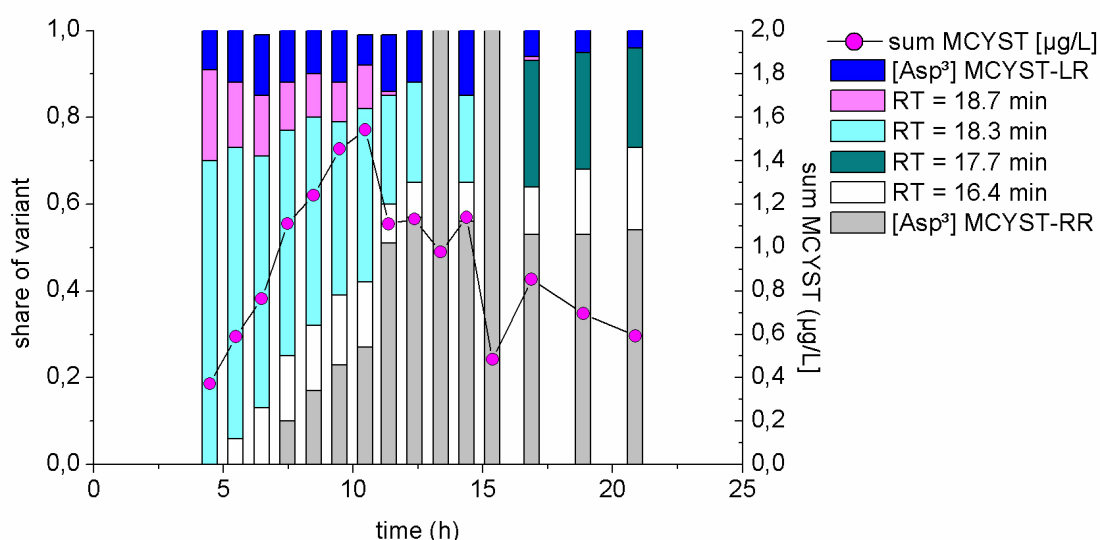


**Figure 50: HPLC chromatogram peaks identified as microcystins in the SSF2 effluent samples (RT: retention time). Columns refer to left y-axis and represent the relative shares of the different peaks in relation to the sum of MCYST (dots, right y-axis).**

The MCYST breakthrough curves were subsequently modelled with VCXTFIT with the hydraulic parameters (pore velocity and dispersion coefficient) obtained from the tracer breakthrough curves (Table 9). The resulting retardation coefficients and degradation rates are given in Table 13. While the retardation coefficients and degradation rates in SSF5 and SSF6 are similar ( $R = 1.3$  to  $1.5$  and  $\lambda = 0.04$  to  $0.05 \text{ h}^{-1}$ ), those obtained from experiment SSF2 are substantially higher ( $R = 2.6$  and  $\lambda = 0.17$ ).

**Table 13:** Retardation coefficients (R) and degradation rates ( $\lambda$ ) obtained by modelling SSF experiments with MCYST.

Experiment #	filtration velocity [m/d]	R	$\lambda$ [h $^{-1}$ ]	remarks
SSF2	2.4	2.6	0.17	virgin sand, no clogging
SSF5	1.2	1.3	0.04	some clogging
SSF6	0.6	1.5	0.05	clogged

## 8.4 Interpretation and Discussion

The slow sand filter experiments had the aim to compare MCYST elimination under assumed worst case conditions with elimination under optimal conditions on a field scale in order to assess which parameters are crucial to prevent toxin breakthrough.

The first experiment (SSF2) was carried out under conditions assumed to be quite unfavourable for degradation, i.e. virgin sand and high flow velocity (pore velocity: 6.2 to 6.5 m/d, filtration velocity: 2.4 to 2.6 m/d). The results did not show a reduced elimination of MCYST compared with the other scenarios tested in SSF 5 and SSF 6 (preconditioned sand, and lower filtration velocities with 1.4 and 0.2 m/d). In contrast, under the presumably unfavourable conditions, higher elimination was observed (recovered amounts: 22.5 % in SSF2 and 26.5 to 37.2 % in SSF 5 and SSF 6, respectively).

Modelling the MCYST breakthrough yielded a possible reason for this unexpected result: Retardation coefficients and degradation rates in SSF 5 and 6 amounted to similar values ( $R = 1.3$  to  $1.5$  and  $\lambda = 0.04$  to  $0.05 \text{ h}^{-1}$ ) and are comparable to the values obtained by modelling the effluent data of the enclosure experiments (see final NASRI Report, part V, table 11). In experiment SSF 2, however, with virgin sand and high flow velocity the retardation coefficient was 2.6 and the resulting degradation rate  $0.17 \text{ h}^{-1}$ , i.e. 2 to 4 times the values obtained in the two other experiments. Thus, elimination processes during this first experiment seem to differ from those that occurred during the following experiments on the SSF and the enclosures.

A possible explanation might be irreversible sorption of MCYST onto the virgin grain surfaces and subsequent saturation, so that no or little further adsorption can occur. While the original working-hypothesis was that MCYST-elimination would be lower due to the lack of adapted bacteria (leading to lower degradation rates in virgin filter material), these results indicate that this effect is more than compensated by irreversible adsorption processes that can only occur with virgin filter material. Differentiation between irreversible adsorption and degradation is difficult to verify in experiments and has so far not been investigated. Further studies could therefore comprise laboratory experiments addressing this topic, e.g. with radio-labelled MCYST.

Enclosure experiments with MCYST were carried out subsequently to the SSF experiments in order to assess the influence of varying conditions (clogging, temperature, redox potential) onto MCYST elimination (see final NASRI Report working group “algae” part V).

## **8.5            *References***

Massmann, G., Taute, T., Bartels, A. & Ohm, B. (2005): Characteristics of sediments used for Batch- Enclosure and Column-Studies. – NASRI Report by the Free University of Berlin, NASRI working group Hydrogeology (unpublished).

## 9 Enclosure experiments on UBA's experimental field

### 9.1 Introduction

The enclosures were constructed as semi-technical scale filter columns that allowed experiments on a smaller scale and therefore under conditions easier to change and to control than in the technical scale slow sand filters. The enclosure experiments with relatively short contact times were necessary especially for substances that are usually readily removed by sediment contact (e.g. cyanotoxins, viruses and bacteria). For these substances the observation wells at the transects with contact times of at minimum 2 weeks did not cover the time scale of interest. Figure 51 and Figure 52 give an overview of all investigations and experiments carried out on the enclosures during the NASRI project.

	January	February	March	April	May	June	July	August	September	October	November	December
<b>2002</b>												
<b>EI, EII, EIII</b>												
<b>2003</b>												
<b>EI</b>												
Filtration velocity												
Experiment No.												
Date												
Substances												
<b>EII</b>												
Filtration velocity												
Experiment No.												
Date												
Substances												
<b>EIII</b>												
Filtration velocity												
Experiment No.												
Date												
Substances												

**Figure 51:** Overview of the investigations and experiments carried out on the enclosures in 2002 and 2003. Legend: yellow fields: enclosures dry; light-blue: flooded with little or no clogging; darker blue: flooded with pronounced clogging; hatched fields: flooded, but no experiment.

**Figure 52:** Overview of the investigations and experiments carried out on the enclosures in 2004.

Legend: yellow fields: enclosures dry; light-blue: flooded with little or no clogging; darker blue: flooded with pronounced clogging; hatched fields: flooded, but no experiment.

Aim of experiments with cyanobacterial toxins (microcystins, MCYST): The aim of the first series of experiments was to investigate elimination processes and to quantify degradation rates of dissolved MCYST

- under “normal” conditions (aerobic, clogged and not clogged) and compare the results to those obtained in the SSF experiments (E2 to E5, see chapter 3.2.1),
  - under anaerobic conditions (E9, see chapter 3.3),
  - during continuous dosing over 3 weeks (E10, see chapter 3.4.1).

A final experiment with living cells of cyanobacteria (E12, see chapter 3.4.2) was conducted in order to obtain results most representative for the complex, natural system of extra-cellular and cell-bound MCYST during sediment passage.

## 9.2 Materials and Methods

### 9.2.1 Semi technical scale enclosures on the UBA's experimental field

#### 9.2.1.1 Experimental design

The enclosures were constructed as semi-technical scale columns and were placed in the center of one of the open infiltration ponds of the UBA's experimental field (Figure 53). They were installed with the upper edge about 0.1 m below the upper edge of the basin's rim, i.e. their bottom 1.3 m below sand surface, so that surface water can enter through the openings without additional pumping. The enclosures were filled from bottom to top with 0.3 m of gravel and 1 m of filter sand (the same as in the slow sand filter experiments) leaving about 0.4 m depth of the water reservoir at the top. Small sampling tubes were installed in different depths according to Table 14 and Figure 54.

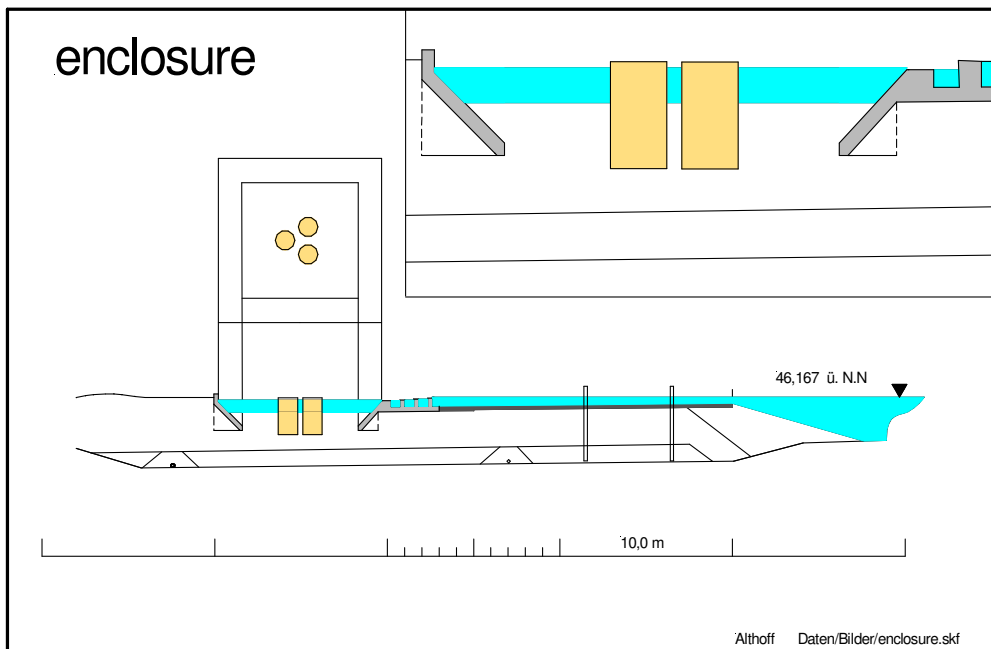


**Figure 53:** Position of the enclosures inside the infiltration ponds (cross section; dotted boxes show bird's-eye view and magnification), without tubing, pumps and sampling ports.

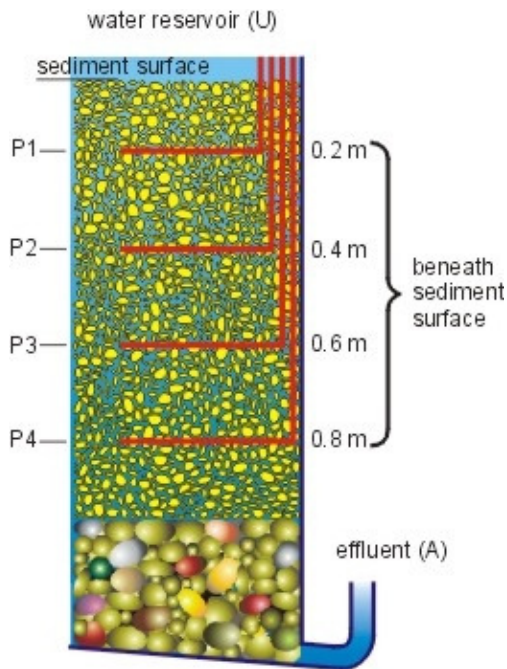


**Figure 54:** Cross section of enclosure III with sampling ports.

Table 14: Distribution of sampling tubes inside the enclosures.

Number of enclosure	Sampling tube in depth below sediment surface (m)			
	0.2	0.4	0.6	0.8
I	no sampling tubes, only outlet sampling			
II	no	yes	no	yes
III	yes	yes	yes	yes

### 9.2.1.2 Hydro- and geochemical conditions

#### 9.2.1.2.1 Geochemical properties of the virgin filter material

The filter sand used for the enclosures was the same as for the slow sand filter (for details see final NASRI Report working group algae, part IV). The filter sand is a medium to coarse sand with small amounts of fine sand. Silt and clay are not present. The gravel layer consists of fine gravel with large amounts of medium grained gravel.

The geochemistry resembles that of sand taken from the shore of Lake Wannsee fairly well, with exception of the total iron content (13 % less in the filter material) and the cation exchange capacity (CEC<sub>eff</sub>: 82 % less in the filter material). This is probably due to the coarser grain size of the filter material (Massmann et al. 2004).

### 9.2.1.2.2 Hydrochemistry under normal operating conditions

The surface water used for the experiments originates from the surrounding aquifer and is treated for iron and manganese in the water works of the experimental field before being fed into the storage pond. Its high electrical conductivity (about 968 µS/cm) is due to relatively high concentrations of salts ( $\text{HCO}_3^-$ : 132 mg/L,  $\text{SO}_4^{2-}$ : 254 mg/L,  $\text{Cl}^-$ : 99 mg/L,  $\text{Ca}^{2+}$ : 127 mg/L and  $\text{Na}^+$ : 46 mg/L, average of 8 samples taken during 2003 and 2004; more detailed data are given in appendix V-1). DOC ranges from 3.2 mg/L in summer (experiments E2 and E3) to 2.1 mg/L in late autumn (experiment E5). Calculations with PHREEQC show that compared to the atmosphere the surface water is slightly oversaturated with  $\text{CO}_2$  and  $\text{O}_2$ , probably due to biological activity of algae and water plants. This is also the reason for the slightly alkaline pH in the water reservoir (pH 8.0 in average).

During sand passage a reduction of pH (down to pH 7.7),  $\text{O}_2$  (by 50 %) and DOC (by 28 % in summer and by 14 % in late autumn) was observed. These reductions take place in the uppermost 20 cm and are more pronounced in summer than in winter.

Nitrate is usually not detectable in the water reservoir, during filter passage or in the effluent. In one case, however, during experiment E3, an increase in the nitrate concentrations during the filter passage from 0.1 mg/L in the water reservoir up to 1.1 mg/L in 60 cm depth was observed (Figure 55). After 80 cm of sand passage and in the effluent the concentrations dropped again to values around 0.5 mg/L.

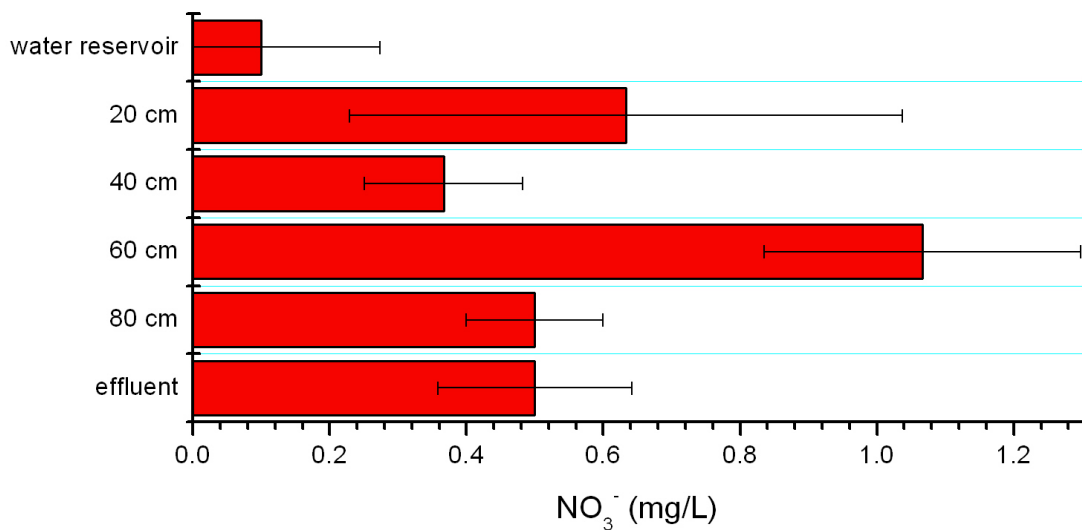


**Figure 55:** Average nitrate concentrations during experiment E3 (error bars indicating standard deviations of 3 samples).

## **9.2.2      *Experimental Methods***

### **9.2.2.1      Experiments with pulsed application (E1 to E7)**

The experiments E1 to E7 were carried out on enclosures II and III. In preparation of the experiments the flow rate was adjusted to the desired amount, corresponding to the filtration velocities given in Figure 51 and Figure 52. The tracer and the trace substances were applied by pouring them evenly across the water reservoir (in which a pump had been installed for better mixing) from a watering can containing the concentrated substances diluted with 10 L of surface water from the water reservoir. The tracer applied was sodium chloride (NaCl) so that the sampling intensity in the different sampling points could be adjusted by observing the electrical conductivity (EC). Care was taken not to increase the EC by more than 10 %.

Samples were taken from the water reservoir, from the sampling ports and from the effluent. The sampling intervals were adjusted to the expected change in concentration and the amount needed by the different working groups for the analyses. As the flow rate in the sampling ports amounted to only 1 mL/min (in order to minimize hydraulic disturbances inside the enclosure) and the volume needed for analyses in some cases added up to 1.5 L, samples from these locations could sometimes not be taken as frequently as desired. With exception of the samples for virus and bacteria detection, samples were usually collected in a mutual flask for all working groups and then divided into the different subsamples for subsequent analysis.

Physico-chemical parameters (EC, pH, redoxvalue, oxygen and temperature) and alkalinity were measured on three occasions at the different sampling locations: a) before the experiment, b) when the tracer peak was expected to break through and c) after the tracer had reached its background level again. The analytical methods for these measurements are described in chapter 2.3. Simultaneously samples were taken for analysis of main anions and cations ( $\text{Na}^+$ ,  $\text{Ca}^{2+}$ ,  $\text{Mg}^{2+}$ ,  $\text{K}^+$ ,  $\text{Cl}^-$ ,  $\text{SO}_4^{2-}$ ), nutrients ( $\text{NO}_3^-$ ,  $\text{PO}_4^{2-}$ ) as well as DOC and immediately filtered by membrane filter (RC 55, Schleicher & Schuell, 0.45  $\mu\text{m}$  pore size), conserved by addition of  $\text{HNO}_3$  (cation samples only) and stored cool at 4 °C or frozen (for determination of DOC) until analysis. The analysis of the main cations and anions as well as of the nutrients was carried out by the FU Berlin. The DOC was determined by the TU Berlin. For description of analytical methods refer to the respective reports.

Cyanobacterial Toxins (Microcystins): The MCYST applied was extracted from a mass culture of *Planktothrix agardhii* HUB 076 by centrifugation and freeze thawing in order to release the mainly cell-bound, highly water soluble microcystins. The freeze thawed extract was homogenized and then centrifuged to remove the cell debris, stored frozen and thawed over night prior to the experiment. The resulting MCYST concentrations in the water reservoir amounted to values between 6.1  $\mu\text{g/L}$  and 9.0  $\mu\text{g/L}$ . For details on analytical methods see final NASRI Report working group algae, part IIX.

### **9.2.2.2 Experiments under anaerobic conditions (E8, E9, E11)**

The experiments under anaerobic conditions were carried out in enclosure II (sampling ports in 40 cm and 80 cm depth). Initially the flow rate was adjusted to  $30 \text{ L/h} \pm 5\%$ , corresponding to 0.7 m/d filtration velocity. Due to clogging the flow rate decreased to  $26 \text{ L/h}$  (0.63 m/d filtration velocity) during the course of the experiments.

In order to eliminate oxygen from the infiltrating water, highly biodegradable DOC (acetic acid) was added continuously with a resulting concentration of 0.3 mmol/L additional DOC (resulting DOC concentration in water reservoir:  $9.6 \pm 0.5 \text{ mg/L}$ , i.e. approximately 3-fold higher than under aerobic conditions).

During experiment E8 DOC dosing commenced on 29th July 2004. Oxygen concentration and redox-values were measured every day until 23rd August, when they had reached stable anaerobic conditions ( $\text{O}_2 < \text{detection limit (0.1 mg/L)}$  and  $\text{EH} < 0 \text{ mV}$ ).

Then experiment E9 was conducted (30th Aug. to 3rd Sept. 2004) by adding trace substances and tracer using the same method as in experiments E2 to E5 (pulsed application, see chapter 2.2.1). Measurement of physico-chemical parameters and sampling were also carried out in a similar way, in order to obtain comparable results.

After a period of aerobic flow, a second attempt was made to establish anaerobic conditions in enclosure II (experiment E11) with dosing of DOC in November 2004. Probably due to lower temperatures oxygen was detectable in the sampling ports and in the effluent throughout the experiment which lasted 15 days, even though the DOC-dosing was increased to 0.5 mmol/L additional DOC. For this reason no second anaerobic experiment with trace substance application could be carried out.

### **9.2.2.3 Experiments with continuous application (E10, E12, E13)**

The experiments with continuous application were carried out on enclosure I (no sampling ports besides the effluent) and enclosure III (4 sampling ports plus effluent). Phages, dissolved microcystin and cyanobacterial cells were added to enclosure I during E10 and E12, whereas primary effluent was dosed to enclosure III during E13 (see also Figure 52). Care was taken to achieve constant flow rates within the full time of an experiment by adjusting the pump when flow rates decreased due to clogging. Hydraulic conductivity was observed by monitoring the suction pressure changes .

Tracer experiments with NaCl were conducted prior to each experiment in the same way as for the earlier experiments (see chapter 2.2.1).

Experiment E10 was carried out from 12th Oct. 2004 until 1st Nov. 2004. The stock solution was prepared each day from the frozen crude extract of the *Planktothrix agardhii* mass culture (MCYST concentration determined by HPLC: 62 mg/L). Prior to the experiment 15 aliquots of 96 mL each had been prepared so that only one had to be thawed per day. The stock solution was adjusted to the target concentration of 4 mg/L by adding 1.5 L of deionized water. It was then dosed continuously with  $1.08 \pm 0.05 \text{ mL/min}$  to the water reservoir of 350 L. In order to achieve a constant level of MCYST in the water reservoir as

quickly as possible, 300 mL of the undiluted MCYST extract were added at the same time as the continuous dosing commenced at the beginning of the experiment.

The stock solution was sampled after preparation and shortly before it was exchanged the next day and analyzed for MCYST content by ELISA. Daily samples were taken from the water reservoir and the effluent. Each sample was tested by ELISA for MCYST content and selected ones analyzed by HPLC. Shortly before dosing was terminated on the 27th October hourly samples were taken from the water reservoir and from the effluent for 24 h in order to assess short term changes in elimination.

Electrical conductivity and temperature were determined daily, the other parameters (pH, O<sub>2</sub>, EH, alkalinity, main anions and cations as well as DOC) prior to the beginning of the experiment and then on two occasions during the experiment.

#### **9.2.2.4 Experiment with continuous application of cell-bound MCYST (E12)**

Experiment E12 was carried out from 23rd Nov. until 9th Dec. 2004 and had to be terminated earlier than planned due to temperatures below 0 °C. Live cells of *Planktothrix agardhii* from the mass culture (total MCYST: 240 µg/L) were added to the water reservoir (350 L), first as a pulse of 15 L in order to achieve a concentration of about 10 µg/L total MCYST as quickly as possible and subsequently continuously at a rate of 20 mL/min from a 30 L tank containing material from the mass culture that was replenished daily for four days (until 26th Nov.). Technical problems lead to a flow interruption between 23rd Nov. and 24th Nov., so on 24th Nov. another pulse of 15 L mass culture was added. After 26th Nov. dosing was terminated, sampling however continued until 9th Dec.

Water samples were taken from the mass culture, from the water reservoir and from the effluent for determination of total and extracellular MCYST by ELISA, for cell-bound and extracellular MCYST by HPLC at regular intervals (twice daily at the beginning to once every two days in the end). Biovolume was determined additionally in the samples from the water reservoir. Physico-chemical parameters (pH, T, EC, oxygen, alkalinity and DOC) were determined in selected samples from water reservoir and effluent as described in chapter 2.3.

Before the beginning of the experiment, after 1, 3, 7 and 13 days sediment samples were taken from the uppermost 10 cm of the filter sand. The cores were obtained with a 2.5 cm diameter syringe from which the tip had been cut off or with a pipe (3.6 cm diameter). Two centimeter subsamples were taken, subsequently homogenized for biovolume determination and deep frozen for semi-quantitative analysis of total MCYST by ELISA.

#### **9.2.3 Analytical Methods**

The analytical methods used for the on-site determination of hydrochemical and -physical parameters are given in Table 15. Methods for sediment analysis and other hydrochemical

parameters can be taken from the final NASRI Report working group FU Berlin, and details on MCYST analysis can be taken from the final NASRI Report working group algae, part IIX.

**Table 15: Overview of the analytical methods used for on-site water analysis.**

Parameter	Method	Instrument	Measuring Range	Error
Electrical conductivity (EC), (temperature)	electrometric (temp.-corrected to 25°C)	Lf 325, Tetra-Con 325-sonde with integrated temperature sonde (WTW)	1 to 10.000 µS/cm (0 to 30 °C)	± 1 µS/cm (0.1 °C)
pH	Potentiometric (autom. temp.-compensation)	CG 837, N 6480-sonde with integrated temperature sonde (Schott)	1 to 13	± 0.1
Redox potential	Potentiometric (Ag/AgCl-standard)	CG 837, Pt 6880-sonde (Schott)	-200 - 1000 mV	± 10 mV
Oxygen	polarographic measurement	Oxi 325, CellOx 325-bzw. EO90-sonde (WTW)	1 % - 100 %	± 5 %

#### **9.2.4 Modelling**

For inverse modelling two different software tools are applied, VisualCXTFIT and MATLAB®, corresponding to the inversion of different parameters in two steps. Modelling is based on the general transport equation, a partial differential equation for the unknown fluid phase concentration c:

$$\theta R \frac{\partial c}{\partial t} = \nabla \mathbf{D} \nabla c - \mathbf{v} \nabla c - \theta R \lambda c \quad (1)$$

with the parameters: porosity  $\theta$ , retardation  $R$ , dispersion tensor  $D$ , Darcy-velocity  $v$  and degradation rate  $\lambda$ . For column or enclosure experiments it may be assumed that flow can be treated as one-dimensional (1D). Then the transport equation can be formulated in a simpler form:

$$R \frac{\partial c}{\partial t} = \frac{\partial}{\partial x} \alpha_L u \frac{\partial c}{\partial x} - u \frac{\partial c}{\partial x} - \lambda R c \quad (2)$$

with longitudinal dispersivity  $\alpha_L$  and interstitial 'real' flow velocity  $u$ . Altogether there are four parameters:  $\alpha_L$ ,  $u$ ,  $R$  and  $\lambda$ . Instead of  $u$  one may use the porosity  $\theta = v/u$  as parameter, because the Darcy-velocity  $v$  is given implicitly by the applied flow rate. In the literature one often finds the combination  $\mu = \lambda R$  used in estimation runs, for example in CXTFIT (1995).

The first two of the four parameters are species independent, the latter two are usually species dependent. The first two parameters can be best obtained from tracer experiments, because for tracers the 1D transport equation reduces to:

$$\frac{\partial c}{\partial t} = \frac{\partial}{\partial x} \alpha_L u \frac{\partial c}{\partial x} - u \frac{\partial c}{\partial x} \quad (3)$$

Within the project the inversion procedure was divided into two steps. In the first step species-independent parameters are determined from the tracer experiments, followed by the second step for the remaining parameters for each specie separately:

- Determination of velocity  $u$  and dispersivity  $\alpha_L$  from tracer experiments
- Determination of retardation  $R$  and degradation rate  $\lambda$  from experiments with non-tracers.

Step (1) was performed using VisualCXTFIT, which is a graphical user interface (GUI) for the CXTFIT code for parameter estimation. CXTFIT was developed at the U.S. Salinity Laboratories (Toride et al., 1995) and is based on analytical solutions of the 1D transport equation. Analytical solutions have the advantage that direct solutions of the differential equation have no problems with discretization errors, as they appear in numerical solutions. On the other hand analytical solutions exist only for specific conditions and can not be given for general boundary and initial conditions. However for the given experimental set-up in the enclosures as well as in the columns it was possible to use CXTFIT.

The VisualCXTFIT user interface for CXTFIT was developed within the NASRI project. An EXCEL-Add-in is produced, which allows the input and manipulation of measured data, as well as the specification of the inversion parameters and options. Moreover a graphical representation of the results is produced in the EXCEL sheet. A detailed description as well as application examples are given by Nützmann et al. (2005).

Step (2) was performed using a newly developed tool for parameter inversion, written as a m-file module in MATLAB® (2002). The module has been used for inversions of transport processes only, but could be used for other applications as well. The MATLAB® module works also for the inversion of temperature time series. For such an application the module is described in detail by Holzbecher (2005).

Within the MATLAB® module direct simulations of the transport equation are performed. The direct solution is obtained by using the ‘pdepe’-solver, which is part of core MATLAB®. The direct solver is called within an inversion procedure, which is based on the MATLAB® optimization module. There are various options, concerning the search algorithm and the numerical parameters can be specified.

In the module the user can specify the parameters, which are to be estimated. Within the automatic inversion procedure it is attempted to modify the selected parameters from their initial values, in order to obtain a better fit with the remaining time-series in the input-data set. The objective function is sum of the squares of the deviations between measured and modelled values, which is usually known as least squares optimization. Parameters not selected for the estimation procedure remain at their initial value.

Input into the MATLAB® inversion module requires time series, measured at least at two positions along the flow path. The first time series, given in the input data-set, is treated as a boundary condition; the other time series are used for the parameter estimation procedure. When several time-series are given there is the additional option to estimate parameters from various possible estimation intervals. For example, in case of three time series, the first can be treated as boundary condition and either the second, or the second and the third can be used for the estimation. Moreover, the second time series can be used as boundary condition, in order to use the third for the estimation. In that way it is possible to obtain an impression of the variability of the parameters with the spatial intervals.

For each estimation run MATLAB® finally produces a plot, visualizing the following:

- Measurements used as boundary conditions (one time series)
- Measurements used for parameter estimation
- Modelled concentration curve based on best-fit parameters.

In the estimation runs for the enclosures, slow sand filters and column experiments performed during the NASRI project, it turned out that the automatic inversion procedure did not deliver optimal results. The problem is well-known, as the algorithms find local minima of the objective function, which are not necessarily global minima. When the user suspects that the automatic solver has not found the global minimum yet, the algorithm is usually re-started again with a new starting set, which differs both from the obtained local minimum parameter set and from the previous starting values. Such ‘fine-tuning’ was required in almost all reported simulations.

Moreover the comparison of parameter values, obtained for different spatial intervals (as described above) mostly revealed substantial differences. It can be concluded that parameters are obviously not constant, but change with space. A more detailed description, concerning phage transport in the enclosures, is presented by Holzbecher et al. (2005).

## 9.3 *Results*

### 9.3.1 **Tracer experiments**

#### 9.3.1.1 **Differences between the enclosures**

In the course of every experiment conducted on the enclosures a tracer experiment was carried out in order to determine the exact hydraulic conditions. Table 16 gives an overview of the hydraulic parameters measured or obtained by modelling.

**Table 16: Hydraulic properties of the enclosures determined by tracer experiments (effluent data only).**

Experiment No.	Date of experiment	Filtration velocity [m/d]	Pore velocity [m/d]	Dispersion length ( $\alpha L$ ) [m]	Eff. Pore-volume (ne)	Hydraulic conductivity [m/s]
Enclosure I						
E6	17th Dec. 2003	0.86	2.40	0.020	0.360	0.95*10-5
E10	12th Oct. 2004	0.73	1.78	0.027	0.410	0.4*10-5
E12	19th Nov. 2004	0.48	1.32	0.013	0.363	0.1*10-5
Enclosure II						
E4	11th Nov. 2003	1.09	2.88	0.016	0.379	1.5*10-5
E5	25th Nov. 2003	1.22	3.07	0.023	0.398	1.7*10-5
E7	8th June 2004	1.20	2.88	0.032	0.420	4.4*10-5
E9	30th Aug. 2004	0.64	1.75	0.049	0.366	1.2*10-5
Enclosure III						
E2	5th Aug. 2003	1.25	3.36	0.011	0.37	1.8*10-5
E3	9th Sept. 2003	1.12	2.76	0.013	0.40	1.6*10-5

Enclosure I shows distinctively lower hydraulic conductivities in comparison to enclosure II and enclosure III. In enclosure I the values lie between  $0.1*10-5$  m/s and  $0.95*10-5$  m/s, whereas the conductivities observed in enclosure II and enclosure III were greater than  $1.2*10-5$  m/s, reaching a maximum of  $4.4*10-5$  m/s. This might be due to the fact that there are no sampling ports installed in enclosure I, so that preferential flow paths can not develop as easily as in enclosure II and enclosure III. Additionally, in 2004 the experiments carried out in enclosure I were characterized by continuous application of microcystin extract and live cyanobacterial cells, thus adding considerable amounts of organic load. This will surely have enhanced clogging.

All enclosures show decreasing hydraulic conductivities over time with exception of enclosure II where the uppermost centimeter was removed in preparation of experiments E5 and E7. Highest conductivities were observed in experiment E7, which was also the only experiment carried out during early summer while the other experiments took place between August and December.

In summary, the following parameters seem to influence hydraulic conductivities in the enclosures:

- constructional details (existence of sampling ports),
- history (application of any clogging enhancing substance or material beforehand),
- previous removal of a clogging layer.

### 9.3.1.2 Differences within the enclosures

Figure 56 and Figure 57 show the spatial variability of the effective pore volume calculated on the basis of the tracer breakthrough curves for different experiments carried out in 2003 and 2004.

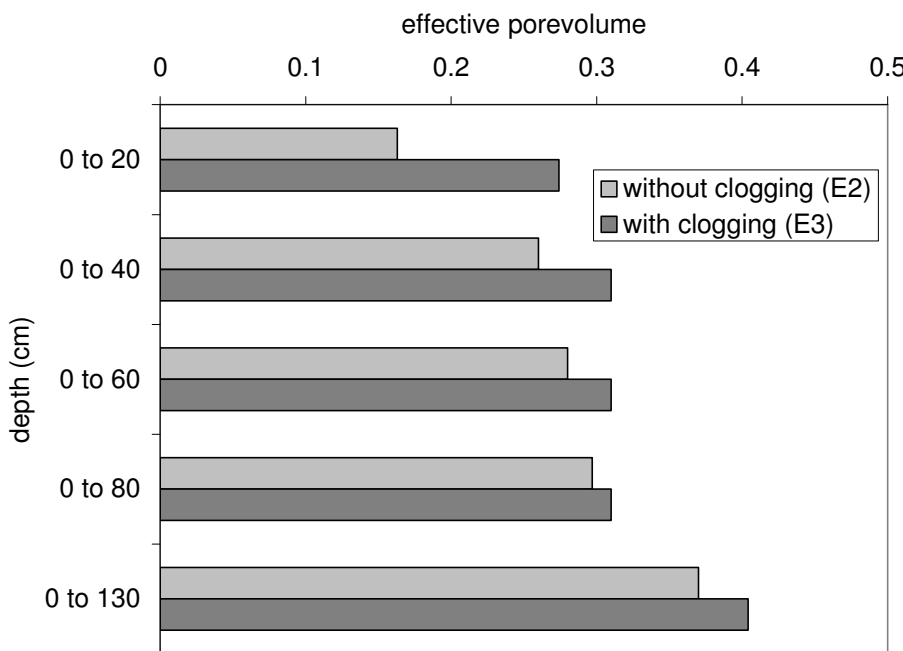


**Figure 56:** Effective pore volumes in enclosure III calculated from tracer breakthrough curves (“clogging” refers to the existence of a visible, superficial “schmutzdecke” on the filter).

The results show a distinctive increase in pore volume with depth. In the lower section between 80 cm and 120 cm this is due to the existence of a gravel drainage layer with higher porosity than the filter sand above. The surprisingly low values for effective porosity in the

upper section can, however, not be derived from initial differences in grain size. Here processes associated with clogging are likely to lead to diminished porosities. These processes are:

- physical clogging by sedimentation of small size organic and inorganic particles,
- biological and / or chemical clogging by growth of biofilm or precipitation of solids,
- formation of partially unsaturated conditions by degassing of the water passing through the filter due to high under-pressure.

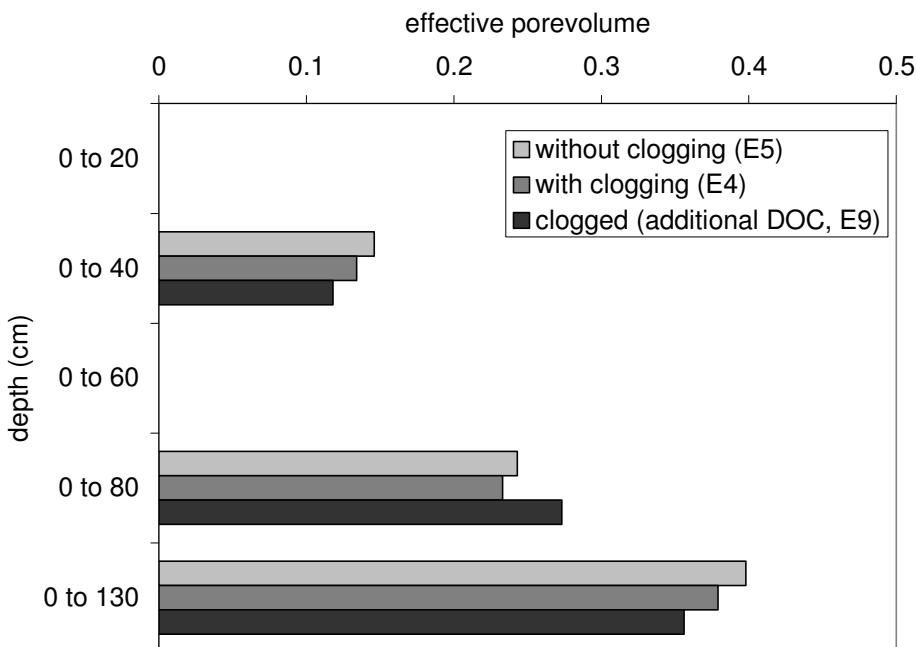


**Figure 57:** Effective pore volumes in enclosure II calculated from tracer breakthrough curves (“clogging” refers to the existence of a visible, superficial “schmutzdecke” on the filter).

Unsaturated conditions due to clogging were found to exist at least once in enclosure III after experiment E12 when gas bubbles appeared during clogging layer removal (Figure 58).



**Figure 58:** Gas bubble formation during removal of clogging layer on enclosure III in December 2004.

### **9.3.2      *Experiments with pulsed application of trace substances***

The aim of the series of experiments with pulsed application of dissolved MCYST, phages, bacteria, drugs and Gd-DTPA was to investigate elimination processes and quantify degradation rates under “normal” conditions (aerobic, clogged and not clogged) and compare the results to those obtained in the SSF experiments.

#### **9.3.2.1    Changes in hydrochemistry**

With exception of the electrical conductivity, chloride and sodium concentrations no significant changes (> 99 % level of significance) in hydrochemistry compared to the hydrochemistry under normal operating conditions (chapter 2.1.2.2) were observed during the experiments.

Significant differences in hydrochemical parameters between the experiments are limited to the temperatures (averages for experiments were: E2: 27°C, E3: 19°C, E4: 2.6°C and E5: 7.4°C) and some temperature related parameters (e.g. oxygen and alkalinity).

#### **9.3.2.2    Cyanobacterial Toxins (Microcystins)**

##### **9.3.2.2.1   Experimental Results**

Table 17 gives a summary of the initial parameters during the four aerobic enclosure experiments conducted with MCYST as pulsed application experiments. The MCYST concentrations were determined by HPLC and refer to the sum of all MCYST-variants. The

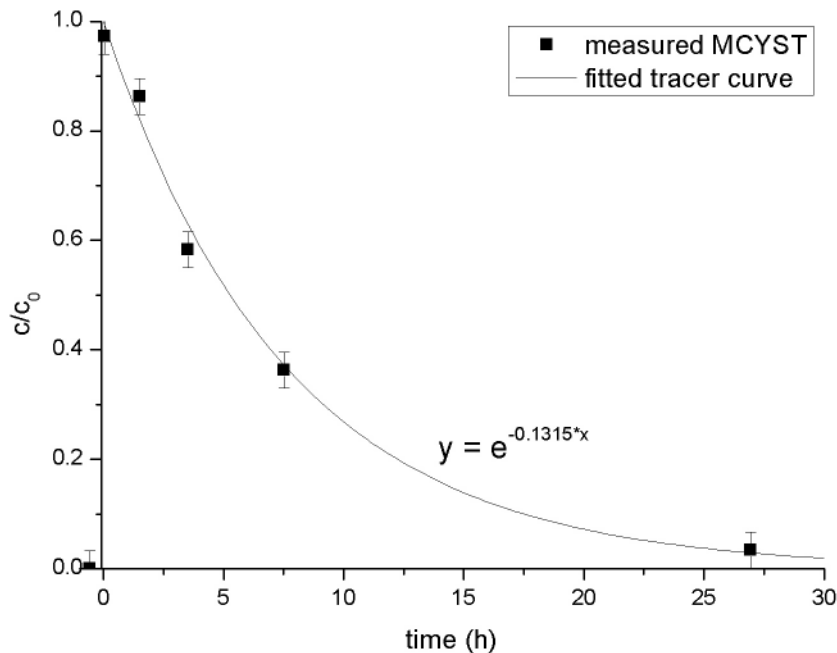
mean residence times were obtained by modelling the behavior of the tracer applied simultaneously. They represent the half life of the fitted exponential decay function.

**Table 17: Initial parameters of the enclosure experiments E2 to E5.**

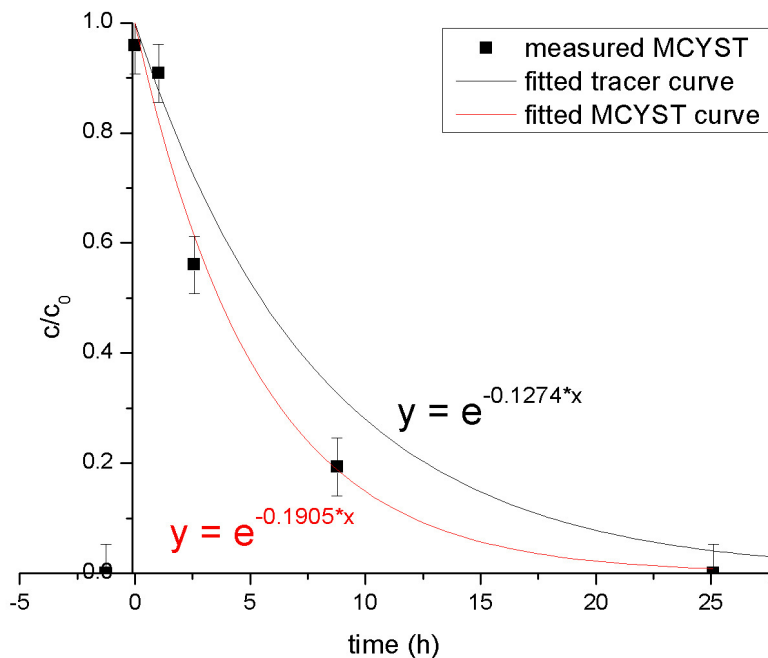
Experiment no.	Water temperature (min – max in °C)	Measured mean filtration velocity (m/d)	Clogging layer visible?	MCYST applied (mg) analyzed by HPLC	Initial concentration of MCYST analyzed by HPLC ( $\mu\text{g/L}$ ) in the reservoir	Mean residence time in water reservoir (h)
E2	23.6 - 31.6	1.23	No	2.8	6.1	5.4
E3	16.4 - 23.1	1.04	Yes	2.7	6.2	4.7
E4	0.6 - 4.7	1.03	Yes	3.9	9.0	6.3
E5	6.3 - 11.2	1.22	No	2.8	7.6	5.3

The data show that the mean filtration velocity was slightly lower during the two experiments with a visible clogging layer (1.0 m/d in contrast to 1.2 m/d without clogging layer). Additionally, as mentioned above, there are major differences in temperature with values around 25 °C during E2 and below 5 °C during E4. This may have had some impact already on the initial concentrations of MCYST which were highest (9  $\mu\text{g/L}$ ) in the experiment with the lowest temperatures (E4) and lowest (6.1  $\mu\text{g/L}$  and 6.2  $\mu\text{g/L}$ ) in those with temperatures above 16 °C. This indicates that some degradation might already have taken place during thawing of the frozen extract before application.

Figure 59 and Figure 60 show the relative MCYST concentrations in the water reservoir during the experiments E2 and E5. All experiments conducted at low to moderate temperatures (E3 through E5) show a decrease in MCYST concentration similar to that of the tracer, so that degradation in the water reservoir can be ruled out and the decrease can be attributed solely to dilution. During E2, however, the MCYST concentrations decreased by a third more rapidly (half life 3.6 h compared to 5.4 h). This may be due to enhanced degradation of MCYST at the extremely high temperatures between 24 and 32 °C during this experiment.



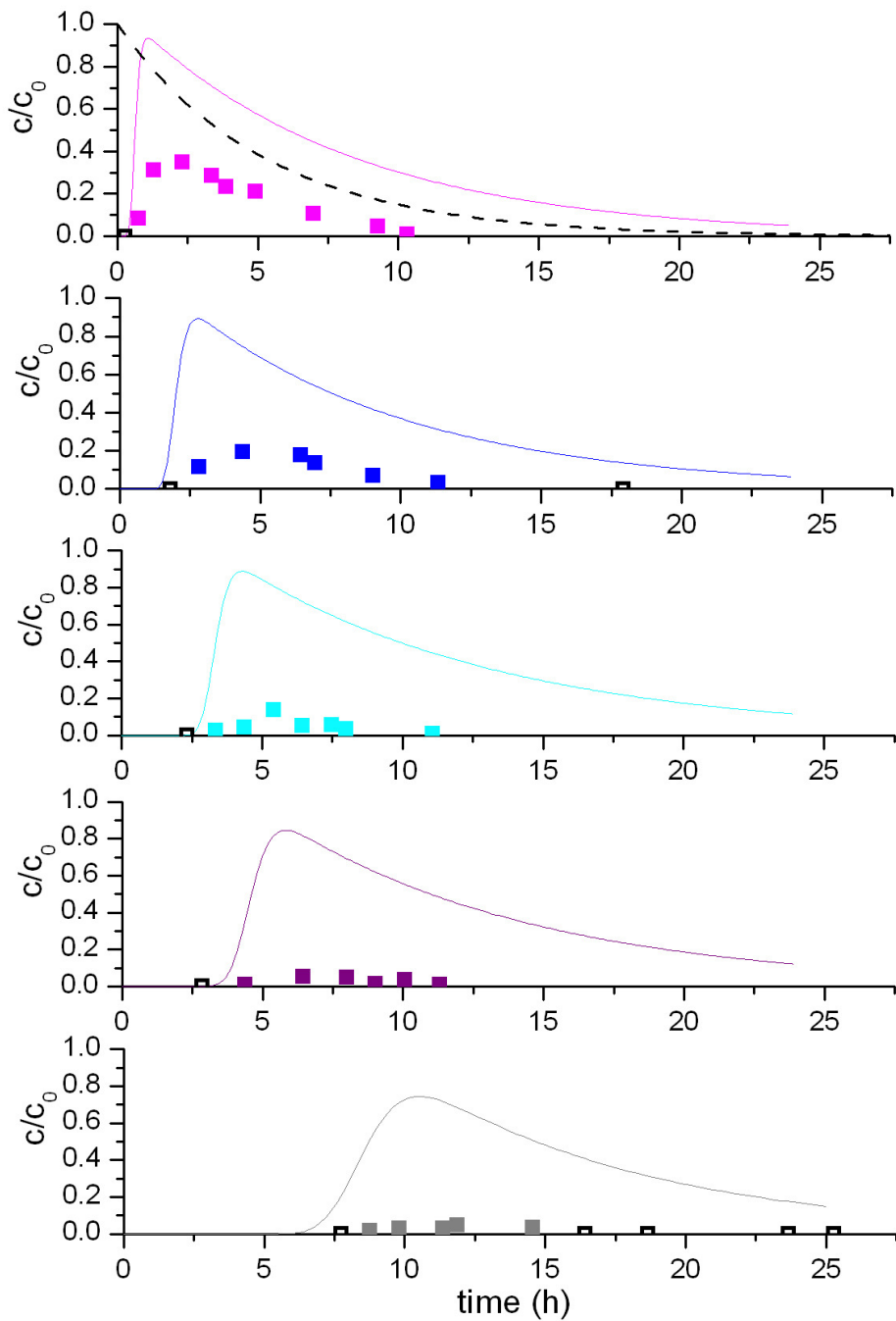
**Figure 59:** Measured MCYST concentration in the water reservoir and fitted tracer curve during experiment E 5 at moderate temperatures (< 23.5 °C).



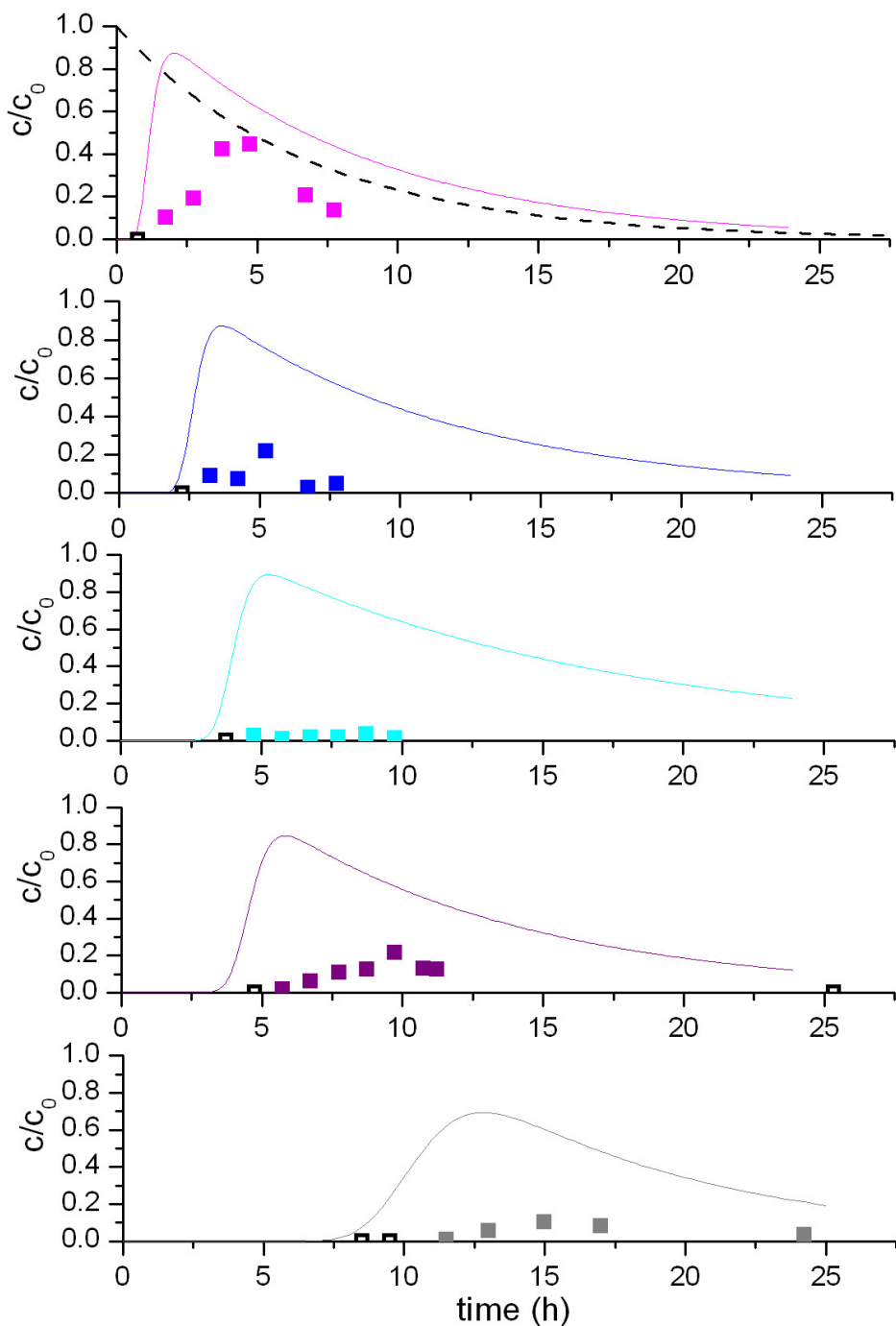
**Figure 60:** Measured MCYST concentration in the water reservoir, fitted decay function and fitted tracer curve during experiment E 2 at temperatures of 24 to 32 °C.

Figure 61 to Figure 64 show the concentrations of MCYST during the experiments with pulsed application (as sum of all MCYST variants determined by HPLC) as well as the tracer

breakthrough curves (obtained either by measuring (E4 and E5) or by fitting the tracer results with VCXTFIT; see chapter 2.4). In all four experiments MCYST shows a clear retardation and decrease in concentration compared to the tracer.



**Figure 61:** MCYST concentrations and modeled tracer breakthrough curves at sampling ports in 20 cm, 40 cm, 60 cm and 80 cm depth as well as in the effluent (from top to bottom) during E2 ( $c_0 = 6.1 \mu\text{g/L}$ ). Dotted curve: MCYST in water reservoir (modeled); Solid curves: tracer modeled at the respective port; solid squares; MCYST measured at the respective port; open squares: MCYST below detection limit, i.e.  $< 0.01 \mu\text{g/L}$ .



**Figure 62:** MCYST concentrations and modeled tracer breakthrough curves in sampling ports in 20 cm, 40 cm, 60 cm and 80 cm depth as well as in the effluent (from top to bottom) during E3 ( $c_0 = 6.15 \mu\text{g/L}$ ). Dotted curve: MCYST in water reservoir (modeled); Solid curves: tracer modeled at the respective port; solid squares: MCYST measured at the respective port; open squares: MCYST below detection limit, i.e.  $< 0.01 \mu\text{g/L}$ .

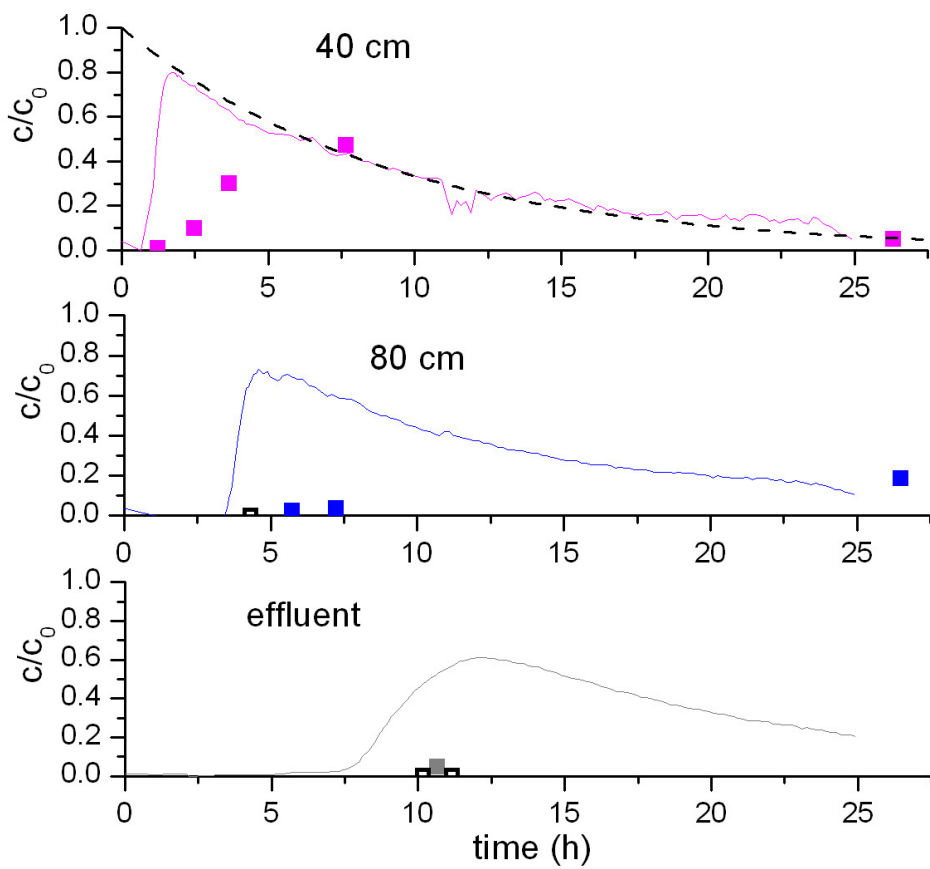


**Figure 63:** MCYST concentrations and measured tracer breakthrough curves in sampling ports in 40 cm and 80 cm depth as well as in the effluent during E4 ( $c_0 = 9.0 \mu\text{g/L}$ ). Dotted curve: MCYST in water reservoir (measured); Solid curves: tracer measured at the respective port; solid squares; MCYST measured at the respective port; open squares: MCYST below detection limit, i.e.  $< 0.01 \mu\text{g/L}$ .

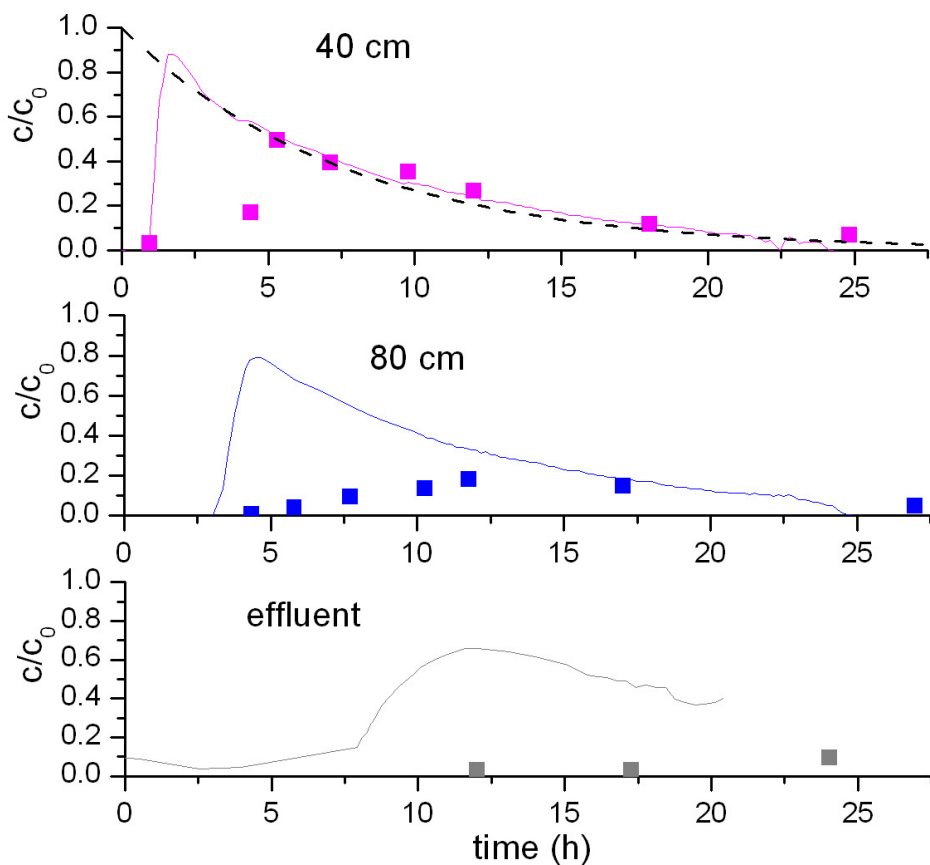


**Figure 64:** MCYST concentrations and measured tracer breakthrough curves in sampling ports in 40 cm and 80 cm depth as well as in the effluent during E5 ( $c_0 = 7.6 \mu\text{g/L}$ ). Dotted curve: MCYST in water reservoir (measured); Solid curves: tracer measured at the respective port; solid squares; MCYST measured at the respective port; open squares: MCYST below detection limit, i.e.  $< 0.01 \mu\text{g/L}$ .

Quantification of retardation and degradation rates was obtained by modelling the breakthrough curves, which was carried out by the working group “models” (IGB), see chapter 3.2.2.2.

Table 18 gives the shares of recovered MCYST (as the sum of all identified MCYST variants) for all four enclosure experiment with pulsed application. Both experiments carried out on enclosure III (four sampling ports), E2 and E3, show recovery rates between 2.5 % and 19 % and declining values with increasing depth. The existence of a visible clogging layer does not seem to be decisive – temperature probably plays a more important role. This can be derived from the fact that experiment E3, carried out with a visible clogging layer but at average

temperatures 10 °C lower than E2, shows higher recoveries, i.e. lower elimination rates. If the clogging layer had been decisive, the reverse result would have been expected.

Experiments E4 and E5, carried out on enclosure II (with 2 sampling ports), show clearly higher recoveries (i.e. lower elimination rates) with values ranging from 10 % to 82 %. Highest recoveries were obtained in experiment E5 which was conducted after the removal of the clogging layer and at higher temperatures than E4. Here the clogging layer seems to play a more important role.

**Table 18: Recovered amounts of MCYST in experiments E2 through E5.**

Experiment no.	Water temperature (min – max) [°C]	Clogging layer visible?	Share of recovered MCYST (by HPLC; %)				
E2	23.6 - 31.6	No	19	13	4.2	2.5	2.7
E3	16.4 - 23.1	Yes	17	15	(1)*	15	9.8
E4	0.6 - 4.7	Yes		66		21	(0.5)*
E5	6.3 - 11.2	No		82		44	10

\* uncertain value due to insufficient data

As all four experiments were conducted at similar filtration velocities and the same experimental setup the only explanation for the great differences in elimination rates between E2 / E3 and E4 / E5 are the varying water temperatures under which they were carried out. For further investigations laboratory experiments concerning this topic were conducted in cooperation with the TU Berlin in 2005 (see final NASRI Report working group algae, part VII).

### 9.3.2.2.2 Modelling Results

The following figures show best fit results for enclosure experiments E2 and E3 for different intervals of the flow path. Depicted are

- Measured concentrations at the top position of the respective spatial interval, here denoted as ‘inlet’; used as boundary condition for inverse modelling
- Measured concentrations at the bottom position of the respective spatial interval, here denoted as ‘outlet’ used for objective function in inverse modelling
- Modelled concentrations at the bottom position; simulated using best-fit parameter values.

Parameters given in the figures are: velocities  $v$  and longitudinal dispersivities  $\alpha_L$ , obtained from inverse modelling using VisualCXTFIT as well as retardation  $R$  and degradation rate  $\lambda$ , obtained from MATLAB® inverse modelling.

The results of the inversion modelling procedure are depicted Figure 65 to Figure 77. For some simulations an additional start was performed, in which one or two outliers, observed in the measurements, were not considered in the parameter estimation procedure (curves not shown). In all cases the restart improved the fit substantially and some parameter values changed significantly.

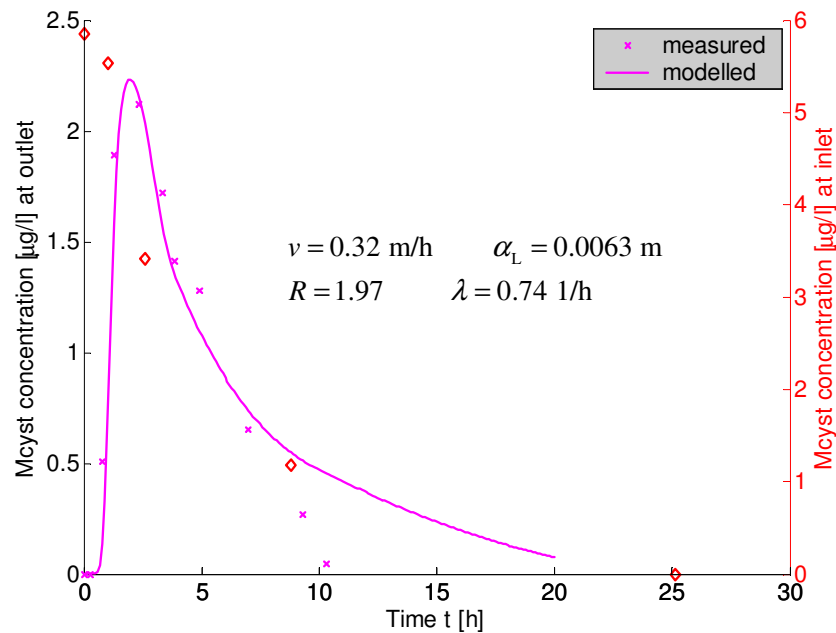


**Figure 65:** Inverse modelling result for experiment E2, inlet to 20 cm (solid curve, left scale); measured inlet values: diamonds, right scale; measured values in 20 cm depth: crosses, left scale.

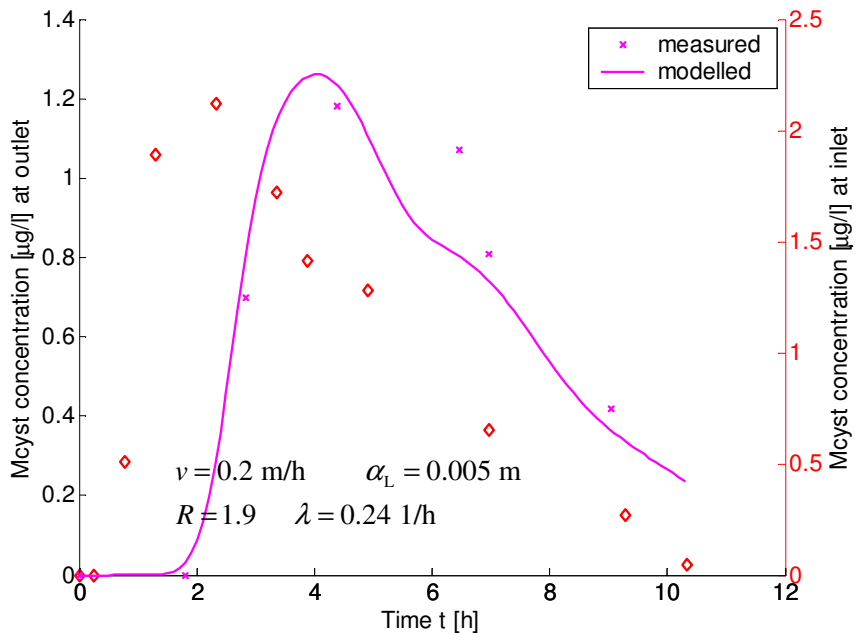


**Figure 66:** Inverse modelling result for experiment E2, 20 cm to 40 cm (solid curve, left scale); measured values in 20 cm depth: diamonds, right scale; measured values in 40 cm depth: crosses, left scale.

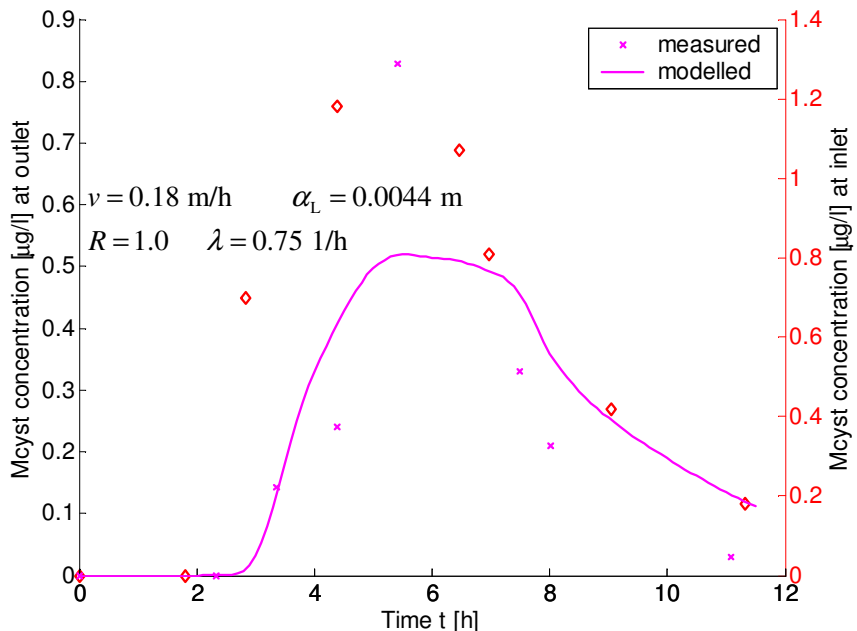


**Figure 67:** Inverse modelling result for experiment E2, 40 cm to 60 cm (solid curve, left scale); measured values in 40 cm depth: diamonds, right scale; measured values in 60 cm depth: crosses, left scale.

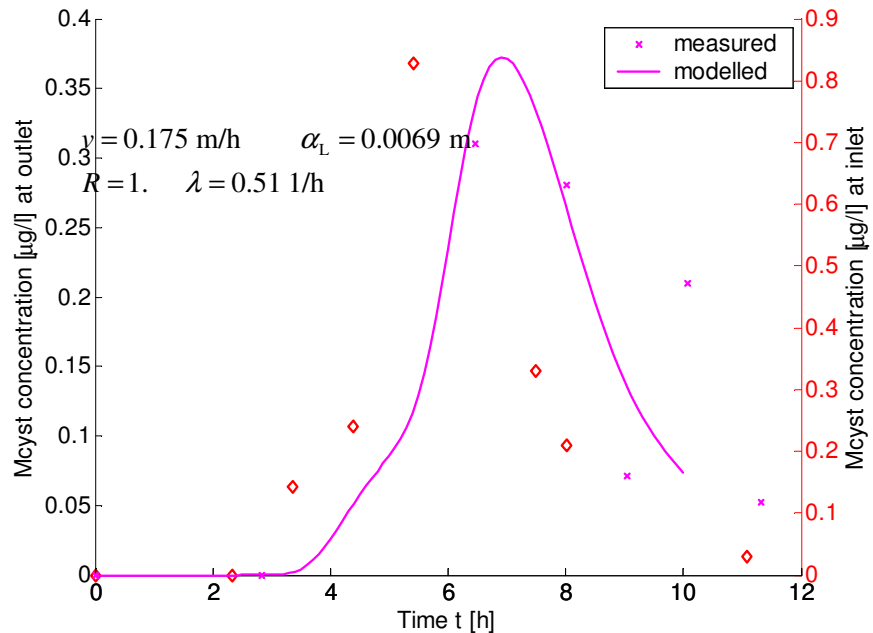


**Figure 68:** Inverse modelling result for experiment E2, 60 cm to 80 cm (solid curve, left scale); measured values in 60 cm depth: diamonds, right scale; measured values in 80 cm depth: crosses, left scale.

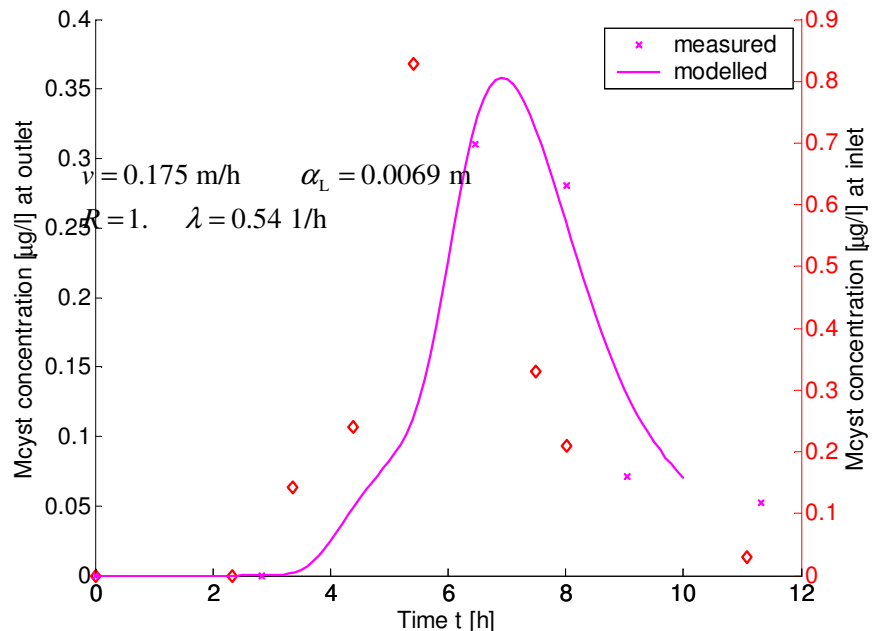


**Figure 69:** Inverse modelling result for experiment E2, 60 cm to 80 cm without outlier (solid curve, left scale); measured values in 60 cm depth: diamonds, right scale; measured values in 80 cm depth: crosses, left scale.

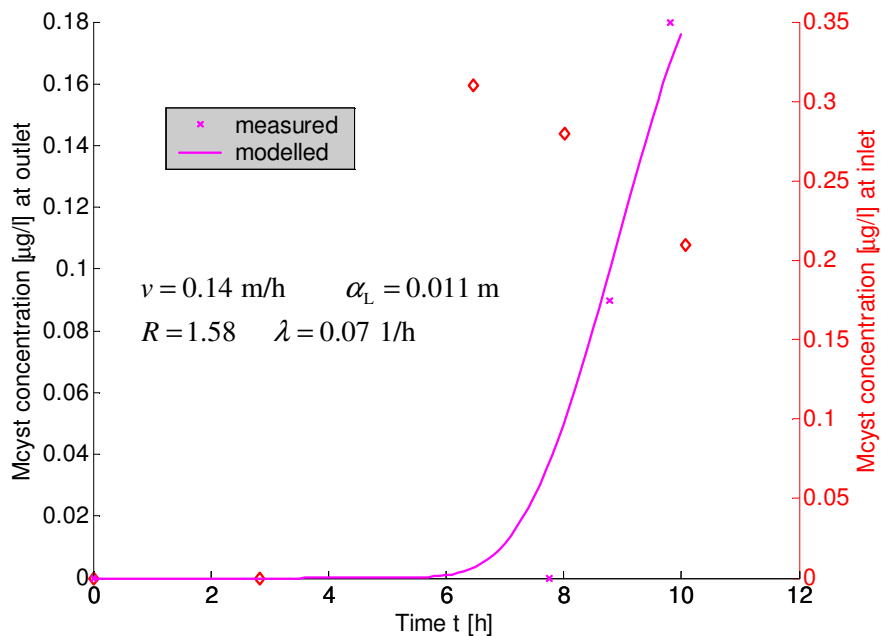


**Figure 70:** Inverse modelling result for experiment E2, 80 cm to effluent (solid curve, left scale); measured values in 80 cm depth: diamonds, right scale; measured values in effluent: crosses, left scale.

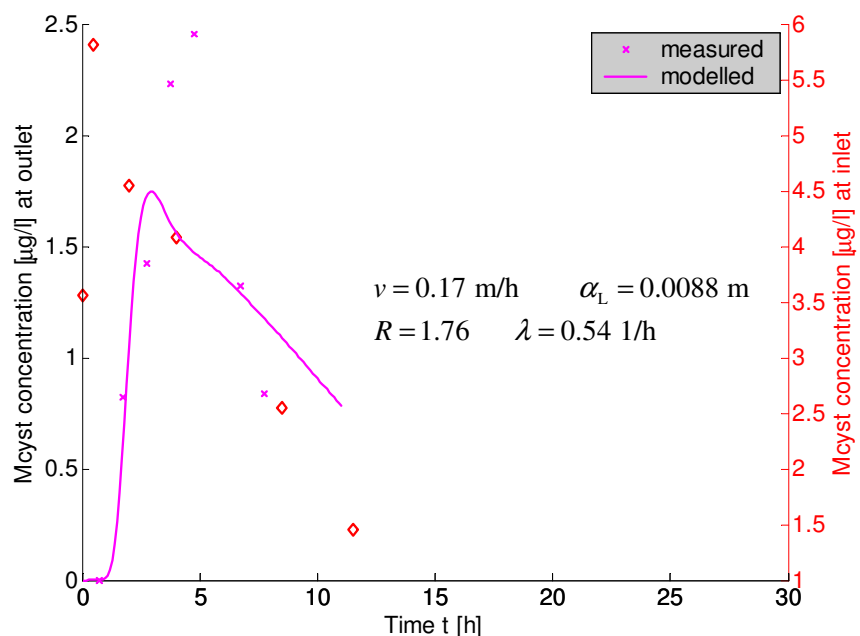


**Figure 71:** Inverse modelling result for experiment E3, inlet to 20 cm depth (solid curve, left scale); measured values in inlet: diamonds, right scale; measured values in 20 cm depth: crosses, left scale.

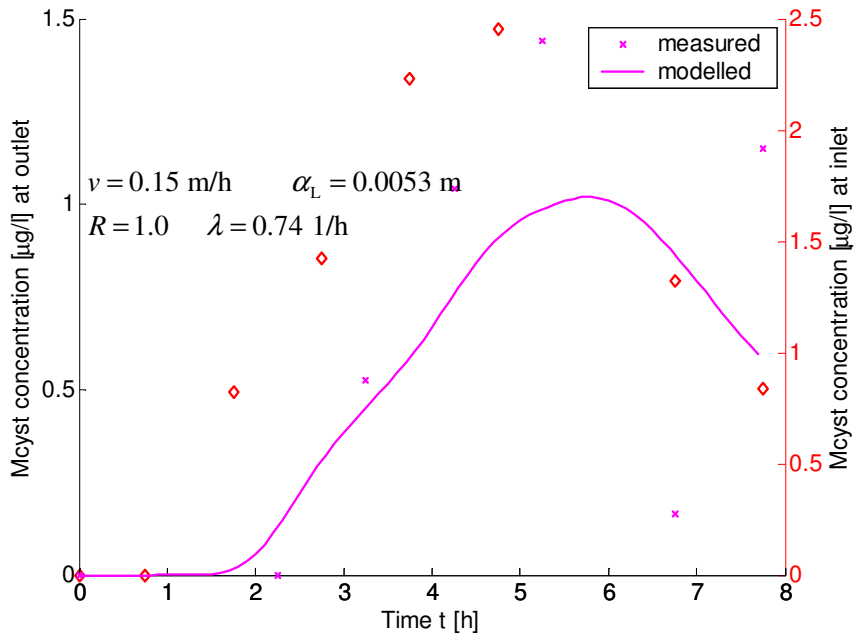


**Figure 72:** Inverse modelling result for experiment E3, 20 cm to 40 cm depth (solid curve, left scale); measured values in 20 cm depth: diamonds, right scale; measured values in 40 cm depth: crosses, left scale.

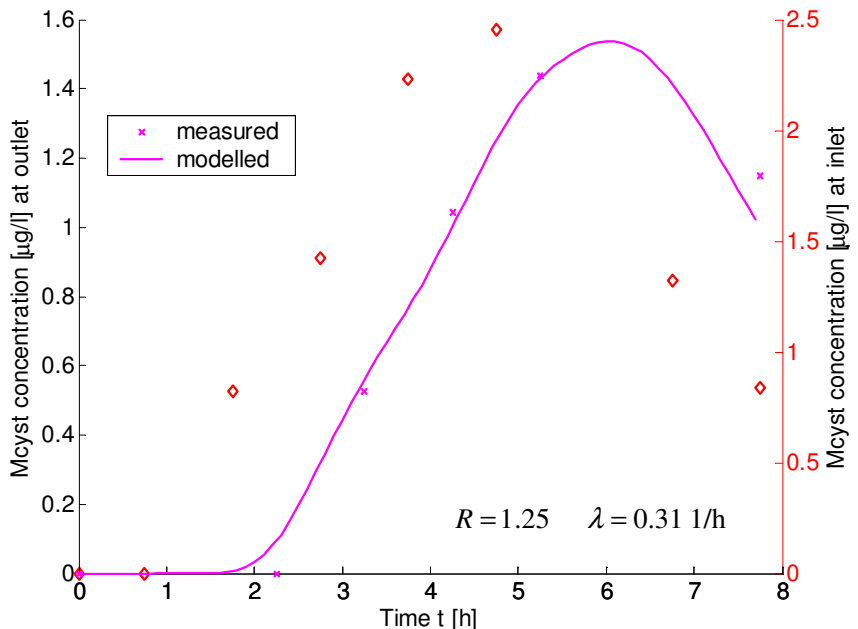


**Figure 73:** Inverse modelling result for experiment E3, 20 cm to 40 cm depth without outlier (solid curve, left scale); measured values in 20 cm depth: diamonds, right scale; measured values in 40 cm depth: crosses, left scale.

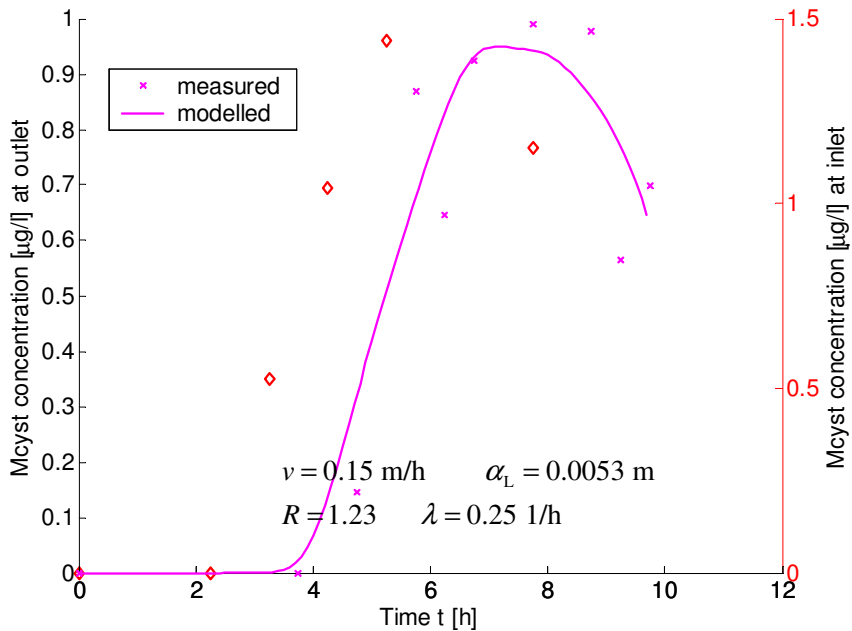


**Figure 74:** Inverse modelling result for experiment E3, 40 cm to 60 cm depth (solid curve, left scale); measured values in 40 cm depth: diamonds, right scale; measured values in 60 cm depth: crosses, left scale.

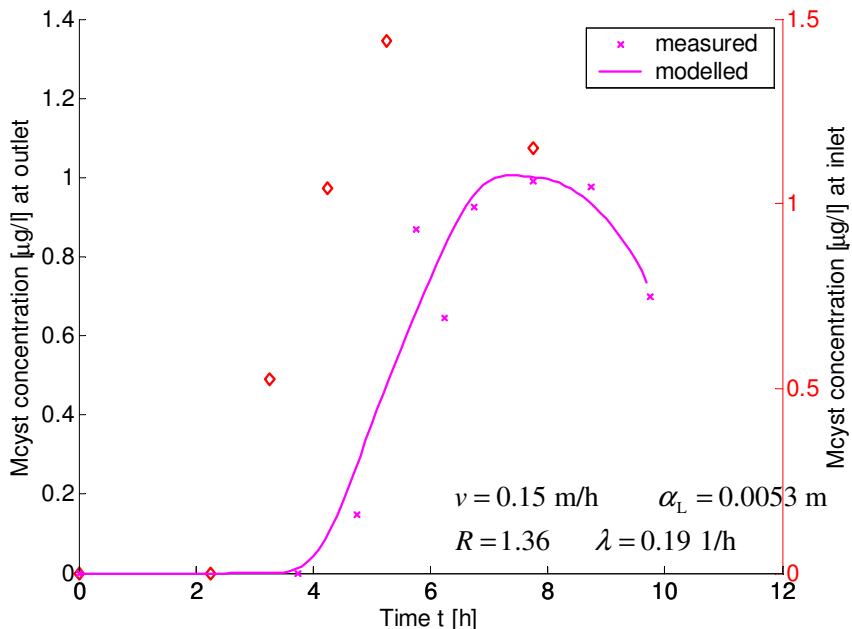


**Figure 75:** Inverse modelling result for experiment E3, 40 cm to 60 cm depth without outlier (solid curve, left scale); measured values in 40 cm depth: diamonds, right scale; measured values in 60 cm depth: crosses, left scale.

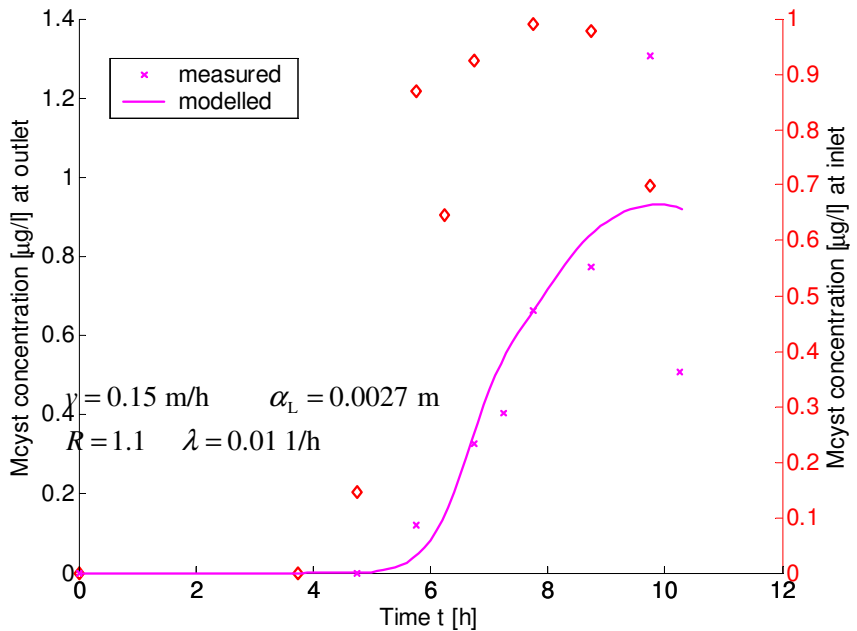


**Figure 76:** Inverse modelling result for experiment E3, 60 cm to 80 cm depth (solid curve, left scale); measured values in 60 cm depth: diamonds, right scale; measured values in 80 cm depth: crosses, left scale.

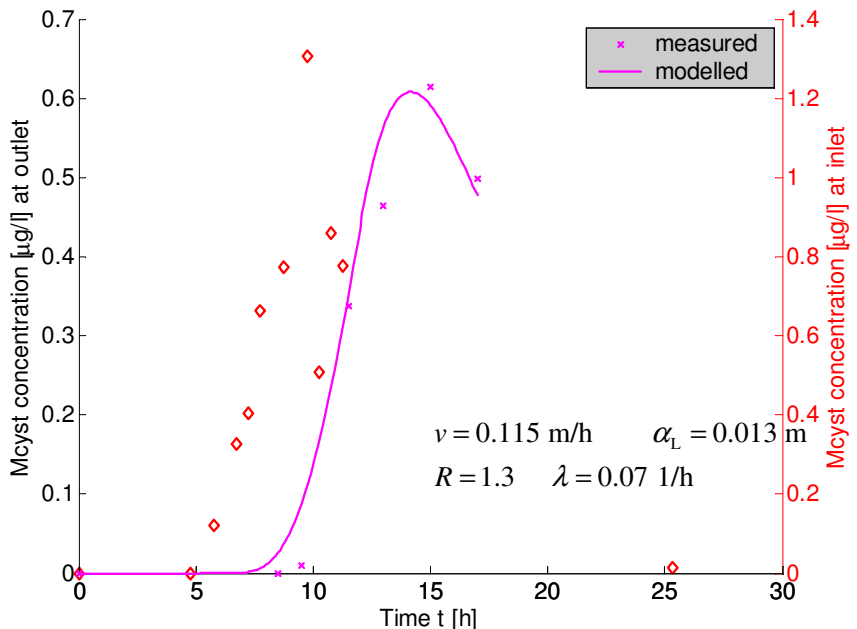


**Figure 77:** Inverse modelling result for experiment E3, 80 cm depth to effluent (solid curve, left scale); measured values in 80 cm depth: diamonds, right scale; measured values in effluent: crosses, left scale.

### **9.3.3        *Experiments under anaerobic conditions***

#### **9.3.3.1      Changes in hydrochemistry**

After 4 days of continuous dosing of additional DOC oxygen could not be detected in 40 cm depth and after 9 days, no more oxygen was found in the effluent (Figure 78). After 3 weeks the redoxpotential (EH) had dropped to values < 0 mV in both sampling points and in the effluent. Additionally iron and manganese reduction was observed (0.1 to 0.2 mg/L in all sampling ports), thus implying strictly anaerobic conditions after 40 cm of sand passage. Due to nitrate concentrations below detection limit in the inlet (< 0.1 mg/L) denitrification not was observed.

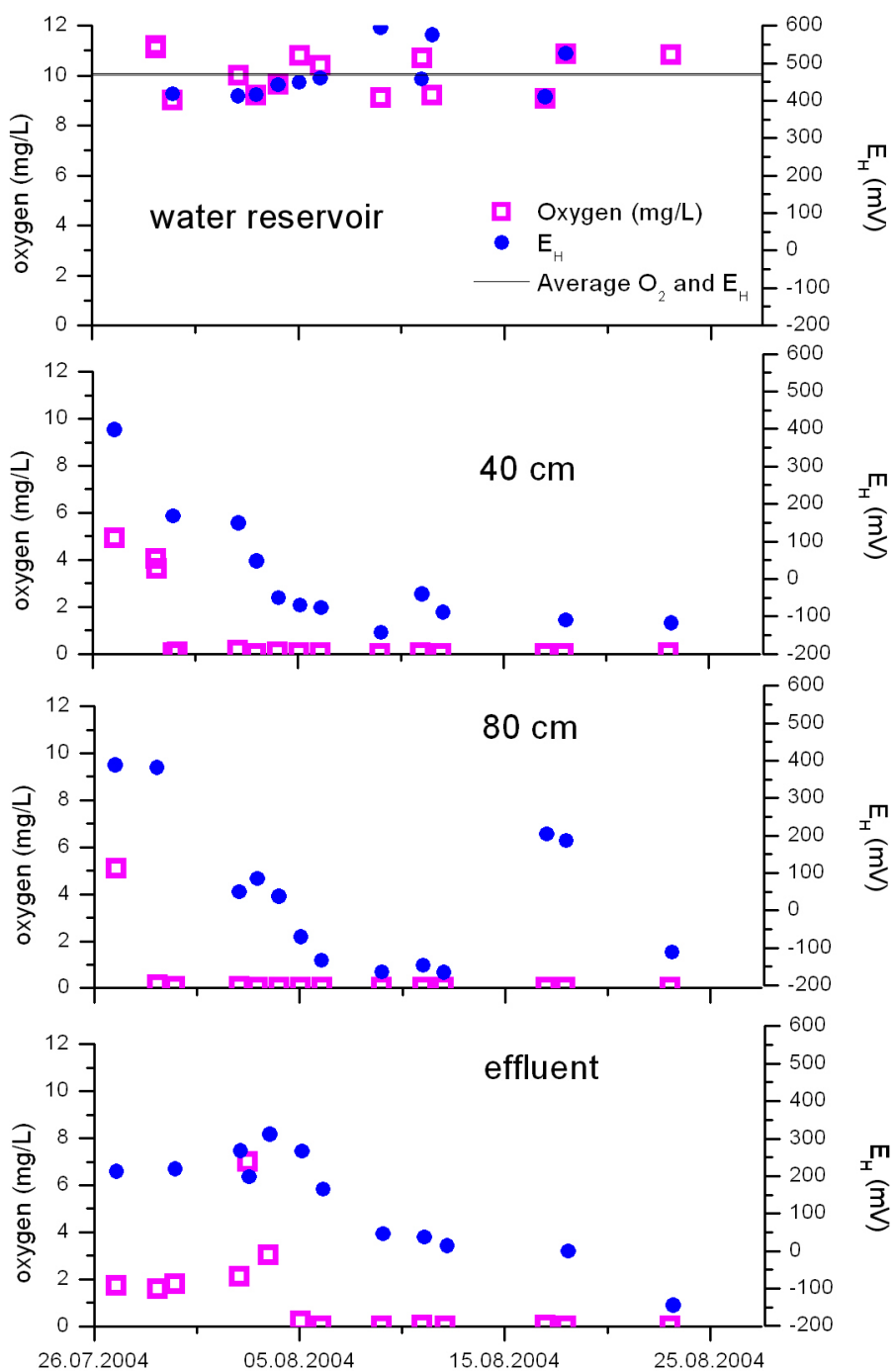


**Figure 78: Development of oxygen concentrations and redoxpotential during additional DOC dosing (experiment E8).**

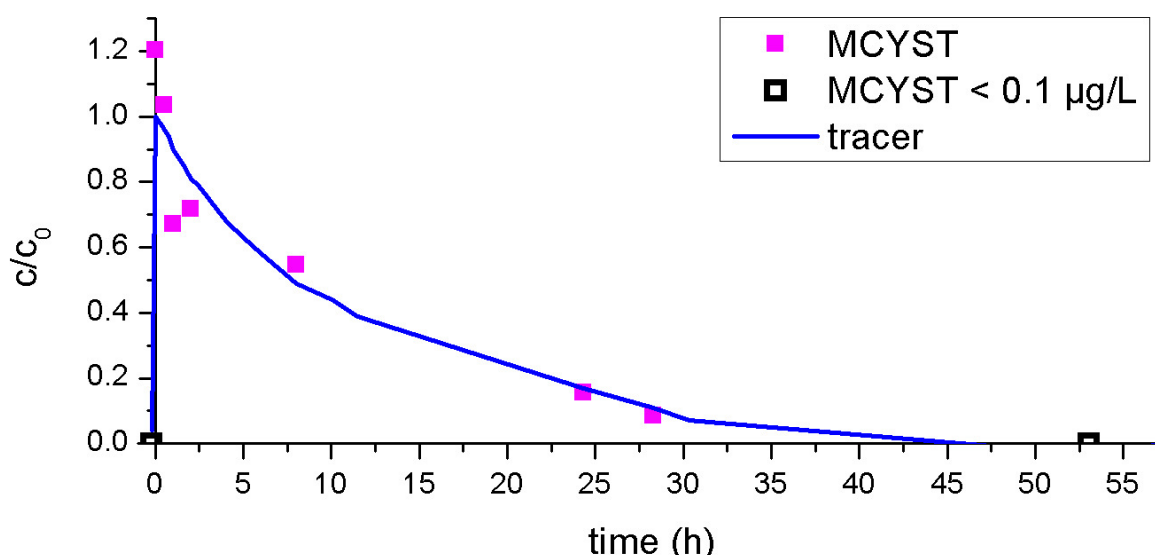
For the anaerobic experiment E9 slightly less MCYST was applied than in comparable aerobic experiments (see Table 19). Filtration velocity reached values of only 0.6 m/d, which was about half as high as during the aerobic experiments. Thus the residence time in the

water reservoir was distinctively greater. Nevertheless no relevant degradation was observed prior to infiltration (Figure 79).

**Table 19:** Initial parameters of the anaerobic enclosure experiment E9 in comparison to minimum and maximum values of similar aerobic experiments E2 to E5 (see Table 17).

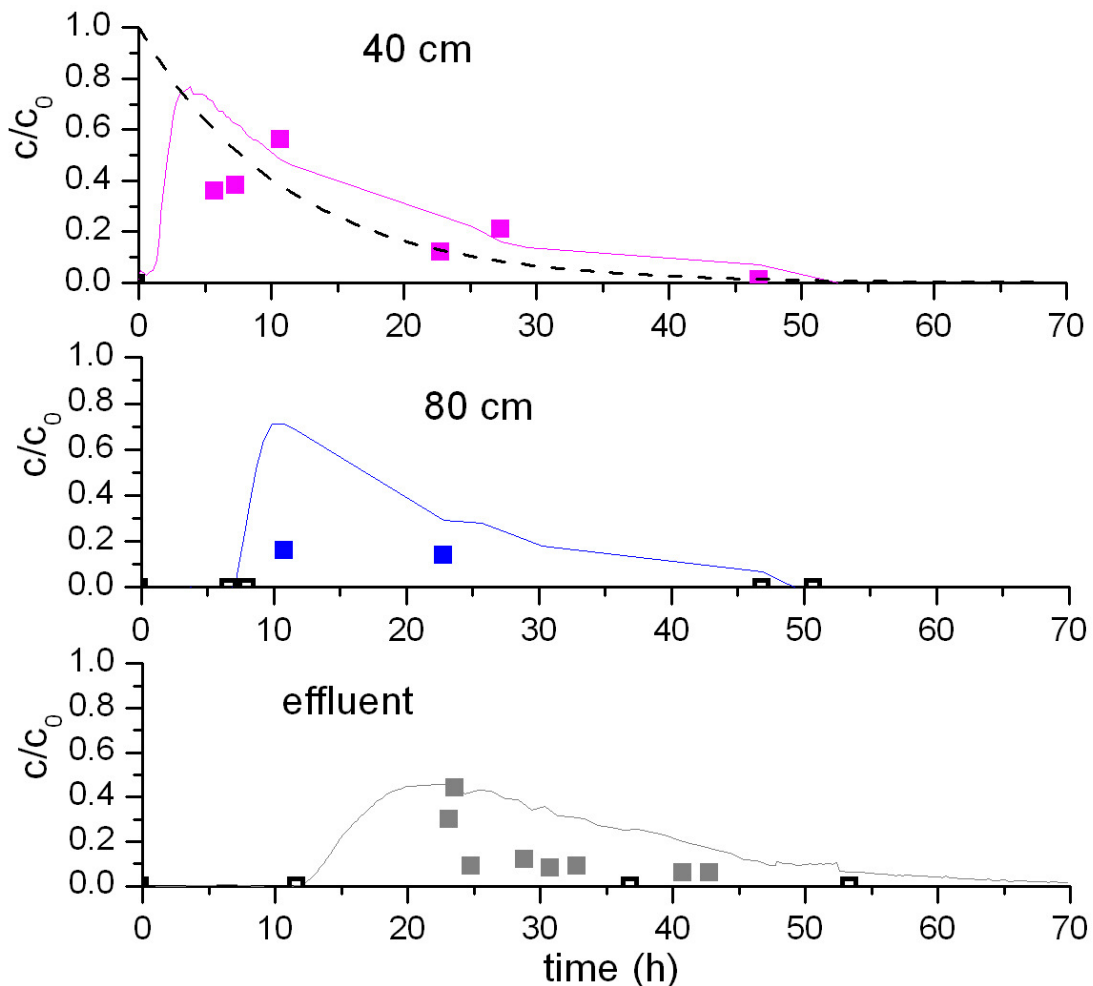
Experiment no.	Water temperature (min – max) [°C]	Measured mean filtration velocity [m/d]	Clogging layer visible?	MCYST applied by HPLC [mg]	Initial concentration of MCYST by HPLC ]µg/L in water reservoir	Mean residence time in water reservoir (h)
E9	23.0 – 27.0	0.62	Yes	2.34	6.03	7.6
E2 to E5	0.6 – 31.6	1.03 – 1.22	Partly	2.69 – 3.87	6.1 – 9.0	4.74 – 6.31

Figure 80 gives the relative MCYST concentrations measured in the sampling ports (40 cm and 80 cm depth) and the effluent as well as the relative tracer concentrations. In 40 cm depth the MCYST concentrations follow the tracer curve closely, showing only little retardation and degradation. Forty centimeters deeper only two samples showed MCYST values above the limit of determination ( $> 0.1 \mu\text{g}/\text{L}$ ). However, the results show that a higher sampling density would have better depicted the processes during the time span that proved to be of interest, also for the analyses done by ELISA (see appendix V-6). It is likely that maximum MCYST concentrations may have passed the sampling point during 12 to 20 h after MCYST application, when no samples were taken.



**Figure 79:** MCYST and tracer concentrations in the water reservoir during experiment E9. Due to the missing samples between 12 and 22 h maximum MCYST

concentrations were probably also missed in the effluent. Two unusually high MCYST values obtained by HPLC at 23 and 24 h could not be confirmed by ELISA, so they may bias the results towards higher recovery rates.



**Figure 80:** MCYST concentrations and tracer breakthrough curves in 40 cm and 80 cm depth as well as in the effluent (from top to bottom) during E9 ( $c_0 = 6.031 \mu\text{g/L}$ ). Dotted curve: MCYST in water reservoir (measured); Solid curves: tracer measured at the respective port; solid squares; MCYST measured at the respective port; open squares: MCYST below detection limit, i.e.  $< 0.01 \mu\text{g/L}$ .

Table 20 gives the shares of recovered MCYST (as the sum of all identified MCYST variants) for the anaerobic enclosure experiment in comparison with the aerobic experiments E2 to E5. Experiments E2 and E3 that were carried out at similar temperatures as experiment E9 show distinctively lower recoveries, i.e. higher elimination rates than the latter. Even experiments E4 and E5 that were conducted at clearly lower temperatures and showed higher amounts of MCYST in the effluent did not reach the recovery rates obtained during

the anaerobic experiment. Taking into account the uppermost 40 cm anaerobic conditions represent the worst case concerning MCYST elimination of all experiments carried out on the enclosures. The difference in elimination between the different aerobic experiments is, however, greater than between the anaerobic experiment and the worst case aerobic experiment (no clogging layer, low temperature, E5).

**Table 20: Recovered amounts of MCYST during experiments E9 (anaerobic) and E2 through E5 (aerobic).**

Experiment no.	Water temperature (min – max) [°C]	Clogging layer visible?	Share of recovered MCYST by HPLC [%]				
			20 cm	40 cm	60 cm	80 cm	effluent
Anaerobic							
E9	23 – 27	Yes		92		(33)*	42 / 15**
Aerobic							
E2	23.6 - 31.6	No	19	13	4.2	2.5	2.7
E3	16.4 - 23.1	Yes	17	15	(1)*	15	9.8
E4	0.6 - 4.7	Yes		66		21	(0.5)*
E5	6.3 - 11.2	No		82		44	10

\* uncertain value due to insufficient data.

\*\*2nd value without outliers.

### **9.3.4 Experiments with continuous application (E10, E12 and E13)**

#### **9.3.4.1 Changes in hydraulics and hydrochemistry during the experiment**

Flow rate, water table and suction pressure in front of the pump at enclosure I during experiment E10 are given in Figure 81. As the flow rate was maintained at a constant level, the suction pressure rose distinctively, probably due to clogging. The hydraulic conductivity declined from  $4.7 \cdot 10^{-6}$  m/s on 13th Oct. to  $1.95 \cdot 10^{-6}$  m/s on 3rd Nov.

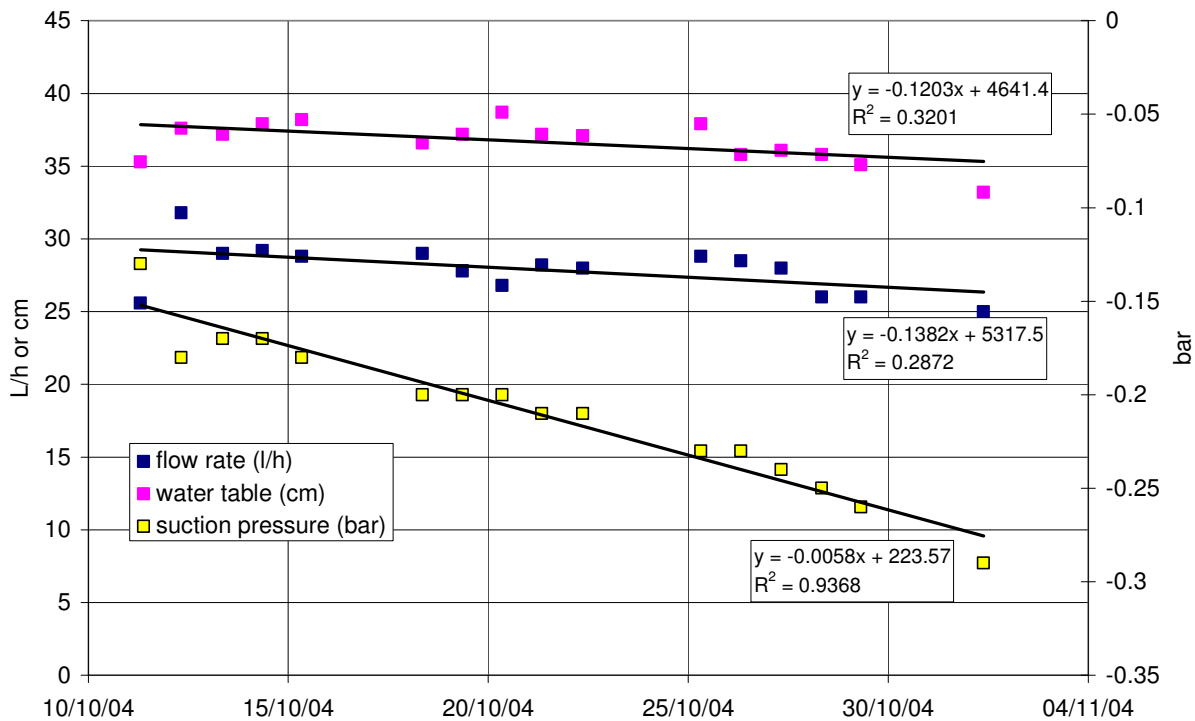


**Figure 81:** Hydraulic parameters during experiment E10 (12th Oct. 04 to 1st Nov. 04).

Hydrochemical parameters showed only very little variation during the experiment. The differences between water reservoir and effluent reflect the conditions that were observed under normal operating conditions (compare chapter 2.1.2.2).

**Table 21: Average values of hydrochemical parameters during experiment E10.**

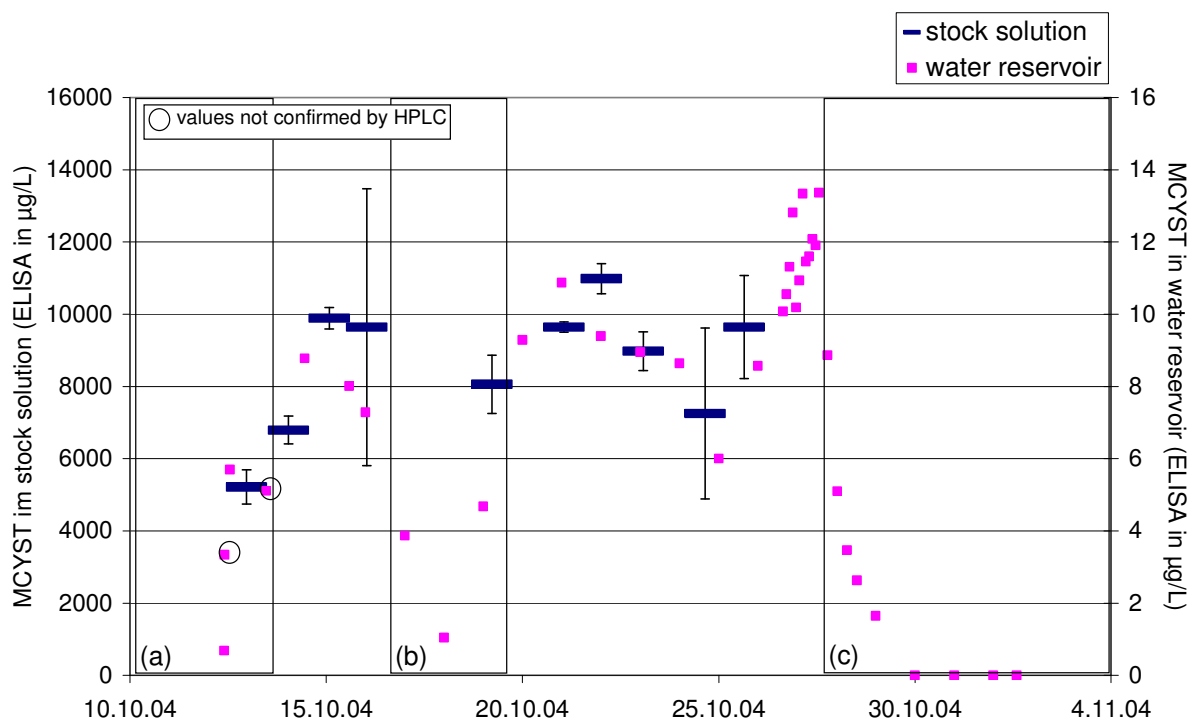
Parameters	Water reservoir Average $\pm$ stand. dev. (number of samples)	Effluent Average $\pm$ stand. dev. (number of samples)
EC ( $\mu\text{S}/\text{cm}$ ) without tracer experiment	$878 \pm 16$ (14)	$907 \pm 30$ (12)
Temperature ( $^{\circ}\text{C}$ )	$8.8 \pm 2$ (15)	$10.6 \pm 1.6$ (10)
pH	$8.5 \pm 0.2$ (6)	$7.8 \pm 0.1$ (6)
Oxygen (mg/L)	$12.1 \pm 0.2$ (2)	7.3 (1)
Oxygen (%)	$97 \pm 1.6$ (2)	64 (1)
Alkalinity (mg/L)	$50.8 \pm 2.7$ (5)	$60.6 \pm 4.5$ (5)
DOC (mg/L)	$4.4 \pm 1.9$ (7)	$2.4 \pm 0.5$ (7)

Figure 82 shows the concentrations of MCYST measured by ELISA in the stock solution (average of two samples taken before connection to the water reservoir and after disconnection one day later) and in the water reservoir of the enclosure. In order to be able

to adapt the experimental design to MCYST-concentrations, ELISA was chosen as rapid method to follow these, with occasional confirmation by HPLC-analyses (see final NASRI Report, part IIX). The error bars of the stock solution data points indicate minimum and maximum values of the two samples taken within these 2 days. High errors are due to analytical variations in two cases (16th and 25th Oct.) or, on one occasion (24th Oct.), some degradation may have taken place, as the stock solution was prepared and kept connected over two days, i.e. 1 day longer than otherwise.

The MCYST concentrations measured in the stock solution and in the water reservoir by ELISA show parallel fluctuations (Figure 82). This may be due to inhomogeneous distribution in the frozen and then thawed MCYST extract prior to the partitioning into aliquots. Very low concentrations in the water reservoir between 16th and 18th Oct. are due to a flow interruption from the stock solution to the water reservoir caused by technical problems.

The samples taken during the intensive sampling campaign on 26th to 27th Oct. show no trend with time. The 12 measurements distribute evenly around a value of 11.6 µg/L with a standard deviation of 1.1 µg/L (which in this case could be interpreted as the standard error for analyses and sampling).



**Figure 82:** MCYST concentrations in stock solution and water reservoir during experiment E10, measured by ELISA (error bars indicate minimum and maximum values)  
(a): starting phase with lower concentrations due to dilution and adsorption, b): low concentrations due to technical problems, c): end phase with declining concentrations).

Taking these uncertainties into account two phases with relatively constant experimental conditions can be defined (Figure 82):

- 14th to 16th Oct.,
- 20th to 27th Oct..

During this time the MCYST concentrations lie roughly between 8 µg/L and 11 µg/L with a tendency towards higher values with time.

Figure 83 shows the MCYST concentrations measured in the effluent together with the related, interpolated values for the water reservoir (considering a residence time of 16.25 h in the filter bed). The elimination was calculated as the ratio of effluent to related water reservoir concentration. Values below the limit of determination were replaced by half the limit of determination.

During the starting phase MCYST concentrations in the effluent rise to values of about 4 µg/L and elimination rates decline from values of 80 % on the first day after dosing started to 45 % on day two. The initially high elimination rate may be due to a retardation of the MCYST by adsorption. In average elimination rates during this initial phase are around 60 %, however influenced by unusually high elimination during the first day.

The first phase of constant experimental conditions (without shading in Figure 83) is characterized by more or less constant effluent concentrations between 1 and 2 µg/L. The elimination rates lie around 48 %, which is clearly below the rates observed during previous enclosure experiments.

After a short flow interruption (shaded area (b) in Figure 83) elimination rates rise to over 80 % and remain at this level even though input concentrations increase steeply after 26th Oct.. The difference between the two phases of constant experimental conditions (i.e. the two areas without shading in Figure 83) in arithmetic mean is significant (probability of error in t-test < 1%).

During the 24 h intensive sampling campaign the elimination rates varied between 79 % and 96 %, showing slightly higher recoveries during the night and early morning (2 am to 9 am average:  $16.6 \pm 5.8\%$ , n = 5) than during the day (11 am to 9 pm average:  $10.8 \pm 3.6\%$ , n = 7). The difference in arithmetic mean is, however, not significant (probability of error in t-test > 5 %).

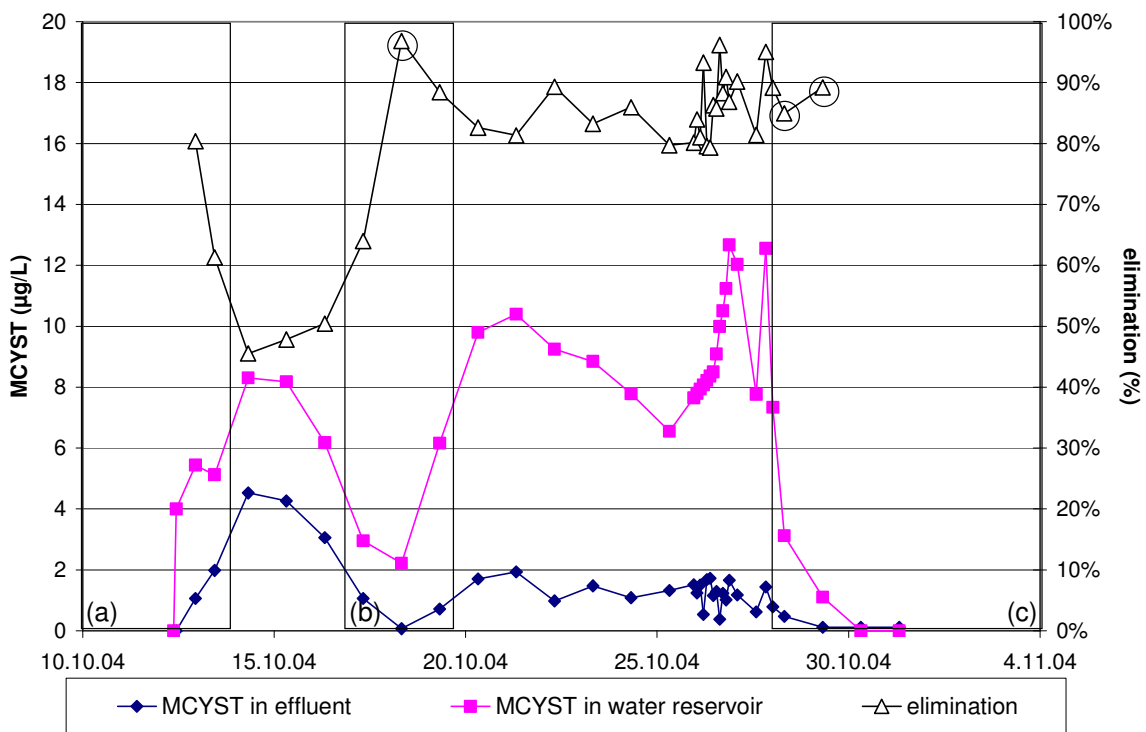


**Figure 83:** MCYST concentration in effluent and water reservoir as well as elimination rate during experiment E10 (shaded areas, see Figure 32, encircled values: effluent concentrations below limit of determination).

With the exception of 3 values, marked in light blue in Figure 84, the MCYST concentrations obtained by HPLC analysis confirm those measured by ELISA, although the HPLC values are generally lower (see final NASRI Report working group algae, part IIX).

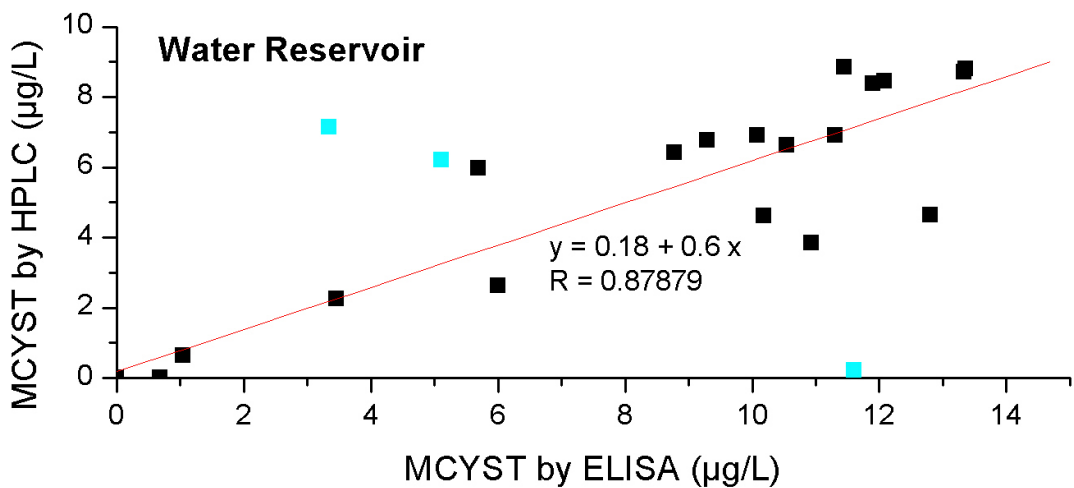


**Figure 84:** Correlation between MCYST concentrations measured by HPLC and by ELISA in the water reservoir during E10 (masked values in light blue).

In summary, the elimination rates obtained after eight days of continuous application under aerobic conditions show similar values as those calculated from the total recovered amounts of MCYST for pulsed application (90 % to 97.5 %, see Table 18).

### 9.3.4.2 Experiment with cyanobacterial cells (E12)

#### 9.3.4.2.1 Changes in hydrochemistry and hydraulics during the experiment

During the first days of the experiment dosing of cyanobacterial cells, the flow rate in enclosure I decreased rapidly from an initial value of 34 L/h to about 15 L/h after 3 days, where it remained constant until the end of the 16-day experiment. Hydraulic conductivity of the enclosure showed the same development with initially  $2.7 \times 10^{-6}$  m/s and later values around  $1.0 \times 10^{-6}$  m/s.

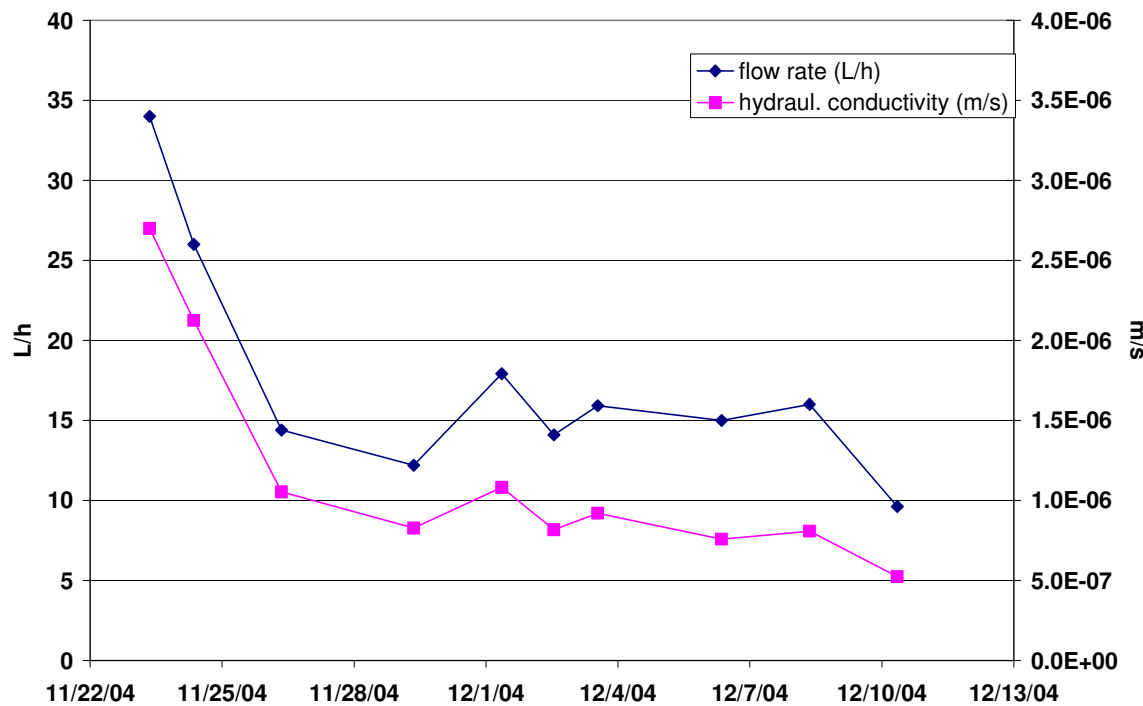


Figure 85: Development of flow rate and hydraulic conductivity during experiment E12.

Hydrochemical parameters showed only very little variation during the experiment. The differences between water reservoir and effluent reflect the conditions that were observed under normal operating conditions (compare chapter 2.1.2.2).

Table 22: Average values of hydrochemical parameters during experiment E12.

Parameters	Water reservoir Average ± stand. dev. (number of samples)	Effluent Average ± stand. dev. (number of samples)
EC ( $\mu\text{S}/\text{cm}$ ) without tracer experiment	$872 \pm 12$ (8)	$869 \pm 21$ (5)
Temperature ( $^{\circ}\text{C}$ )	$3.6 \pm 0.8$ (9)	$5 \pm 1.1$ (5)
pH	$8.3 \pm 0.1$ (5)	$7.8 \pm 0.03$ (3)
Oxygen (mg/L)	$13.8 \pm 0.3$ (3)	$10.2 \pm 0.3$ (2)
Oxygen (%)	$111 \pm 4.1$ (3)	$80.9 \pm 4.5$ (2)
Alkalinity (mg/L)	$95 \pm 3$ (3)	$98 \pm 5.7$ (5)
DOC (mg/L) (see Figure 86)	$3.4 \pm 1.8$ (8)	$2.5 \pm 0.8$ (4)

The only exception is the DOC (Figure 86), which rose from 2.2 mg/L in the water reservoir before the experiment to 7.3 mg/L on the last day of dosing (26th Nov.) and then declined slowly to 2.7 mg/L on 6th Dec.. In the effluent values around 2 mg/L were observed before the experiment, 3.8 mg/L on the last day of dosing (26th Nov.) and 2.5 mg/L on 6th Dec..

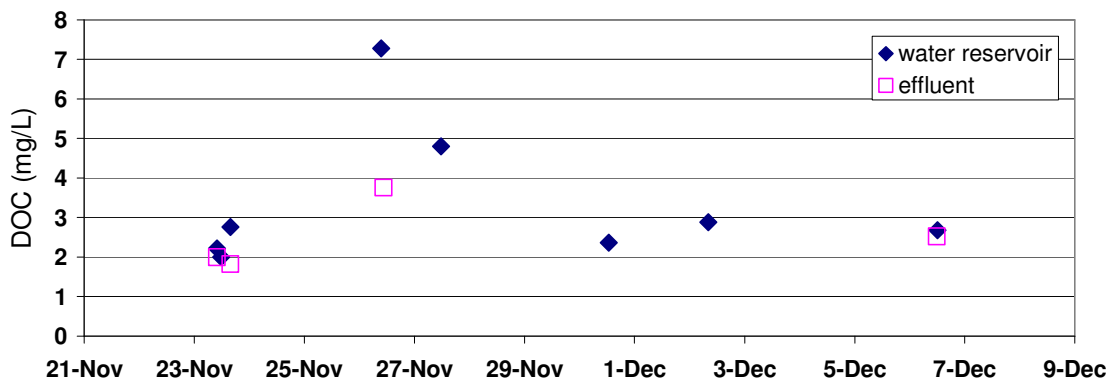
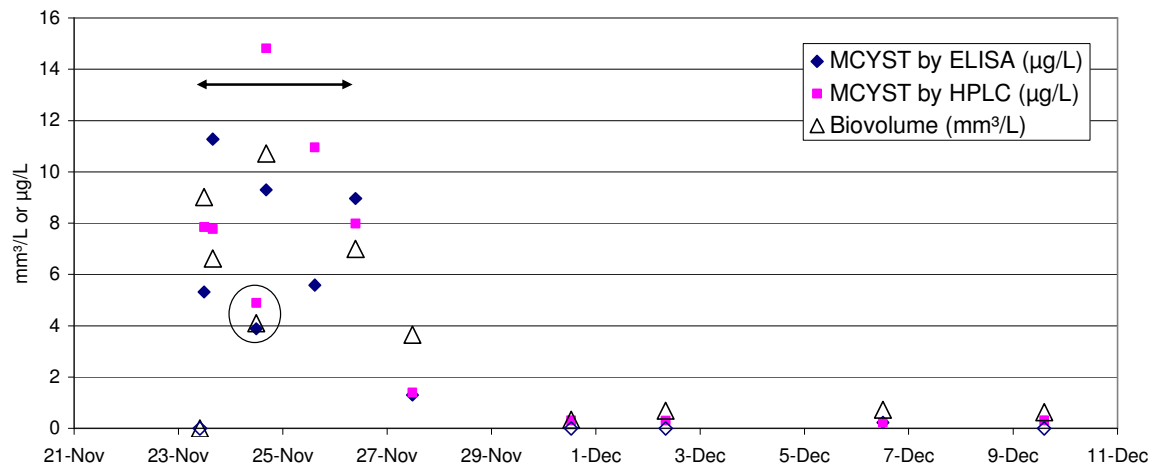


Figure 86: Concentrations of dissolved organic carbon (DOC) in water reservoir and effluent during experiment E12.

### 9.3.4.2.2 Microcystins (MCYST)

Average MCYST values in the water reservoir during dosing amounted to  $7.4 \pm 2.9 \mu\text{g}/\text{L}$  (MCYST by ELISA) or  $9.0 \pm 3.4 \mu\text{g}/\text{L}$  (MCYST by HPLC). Average biovolume of *Planktothrix agardhii* was determined as  $7.5 \pm 2.5 \text{ mm}^3/\text{L}$ . One day after dosing was terminated the biovolume had declined to  $3.7 \text{ mm}^3/\text{L}$  and the MCYST concentrations amounted to  $1.3 \mu\text{g}/\text{L}$  and  $1.4 \mu\text{L}$  by ELISA and HPLC, respectively (Figure 87).

From 31st Nov. on the biovolume remained quite constant at 0.6 mm<sup>3</sup>/L and MCYST determined by HPLC amounted to 0.3 µg/L. After dosing had been terminated the ELISA showed detectable MCYST only in one case with 0.2 µg/L on 6th Dec..



**Figure 87:** MCYST (by HPLC and ELISA) and Planktothrix biovolume in the water reservoir during experiment E12 (circle: values influenced by flow interruption, arrow: time span of dosing; open diamonds indicate values below detection limit).

In the effluent MCYST was not determined at any time, neither by ELISA, nor by HPLC.

The sediment cores showed an accumulation of MCYST in the uppermost 2 cm of the filter sand (Figure 88) at the end of the dosing phase (Nov. 26th). After dosing ceased, however, MCYST concentrations decreased rapidly so that no more MCYST was detected in the uppermost 2 cm after 10 days.

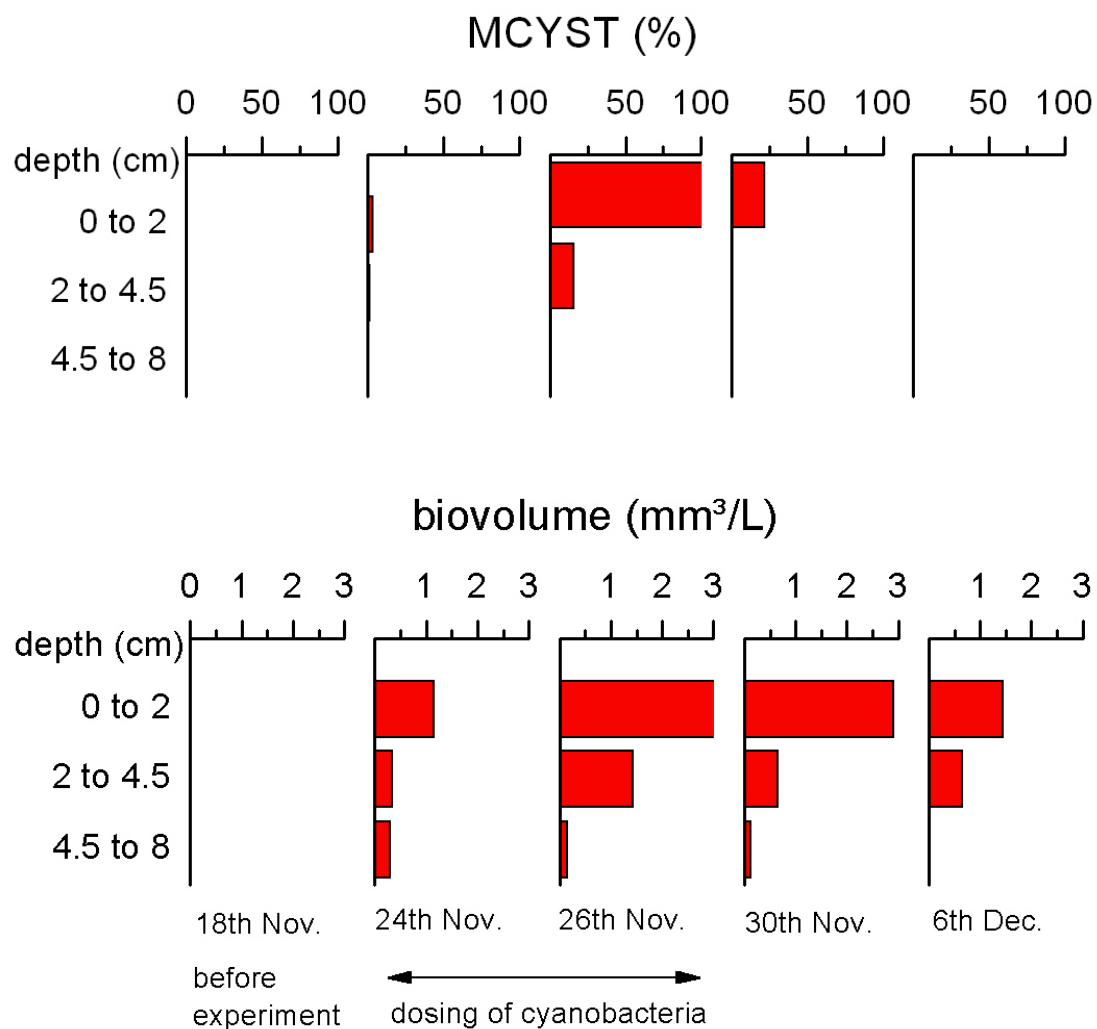


**Figure 88:** Total MCYST (in percent of maximum concentration - 1023 µg/L - at the end of the dosing phase) in the pore water of sediment cores during experiment E12.

Biovolume in the upper sediment layers, however, did not show any substantial decrease after dosing had been terminated (Figure 88). This leads to the assumption that although accumulated cells persist on the sediment surface and within the top few cm, no accumulation of MCYST takes place. This might be due to a) rapid degradation and / or b) release and rapid transport of dissolved MCYST, though at levels in the effluent that range below the detection limit.

## 9.4 Interpretation and Discussion

### 9.4.1 Clogging of the enclosures

The tracer experiments carried out simultaneously with the different enclosure experiments yielded varying effective pore volumes (calculated from measured filtration velocity and modeled pore velocity) and dispersion coefficients (obtained by modelling) in the course of the two years in which the experiments were carried out (Table 10). Effective pore volumes ranged from 36 % to 41 % for the total enclosure. In the uppermost 20 cm to 40 cm of the filter, however, effective pore volumes reached a minimum value of 12 % (experiment in enclosure II under anaerobic conditions, see Figure 57). Between 40 cm and 80 cm effective pore volumes usually ranged from 23 % to 31 %. Below 80 cm values ranged from 36 % to 40 %, probably influenced by the gravel drainage layer beneath 100 cm.

Values below 20 % were observed in different experiments in the uppermost part of the enclosures and seem to relate directly to clogging, with one exception: one tracer experiment in enclosure III yielded similar effective pore volumes directly after the uppermost centimeters had been removed (see Figure 56, experiment E2). This is probably explicable by partially unsaturated conditions, as this was the first experiment to be carried out after the water table had been lowered in order to remove the clogging layer, so that incomplete saturation during the rising of the water level is likely.

In all other cases, low effective pore volumes developed with increasing run time after removal of the clogging layer and reached minimum values during experiment E9. During this experiment additional DOC was dosed in order to reach anoxic and anaerobic conditions by oxygen consumption due to high biological activity, and this further enhanced clogging.

The processes that lead to diminished pore volumes or clogging can be (Schwarz 2004):

- physical clogging (caused by fine particles or gas bubbles),
- chemical clogging (e.g. by precipitation of carbonate or iron and manganese),
- biological clogging (by growth of biofilms, or by trapped gas bubbles produced by biological activity).

Evidence for all three processes can be found during the experiments:

- gas bubble formation was observed during removal of the uppermost centimeter in enclosure III (Figure 58) as well as visible accumulation of organic detritus indicating physical clogging by gas and fine organic particles,
- accumulation of inorganic carbon (i.e. chemical clogging) was detected during analysis of the SSF clogging layer (as chemistry of water and sediment resemble that of the SSF, a similar reaction for the enclosures seems reasonable),
- although no relevant increase in total cell count by DAPI was observed in the SSF clogging layer (see final NASRI Report working group algae, part IV) the gas bubbles

observed during disturbance of the clogging layer are probably produced by biological activity (indirect biological clogging),

On the basis of the different measurements and observations all experiments carried out were characterized concerning the clogging situation as given in Table 23. This shows that, although the uppermost layer was destroyed prior to experiments E2 and E5 no totally unclogged conditions were generated. Clogging might therefore be not only due to "outer" clogging (e.g. due to a "schmutzdecke"-formation), but also due to "inner" clogging, i.e. reduction of effective porosity inside the filter (Grombach et al., 2000).

**Table 23: Hydraulic data of all enclosure experiments with resulting assessment of the clogging situation.**

Experiment No.	Date of experiment	Filtration velocity [m/d]	Pore velocity [m/d]	Dispersion length ( $\alpha L$ ) [m]	Eff. Pore-volume (ne)	Hydraulic conductivity [m/s]	Clogging situation
Enclosure I							
E6	17th Dec. 2003	0.86	2.40	0.020	0.360	0.95*10-5	Not clogged
E10	12th Oct. 2004	0.73	1.78	0.027	0.410	0.4*10-5	Clogged
E12	19th Nov. 2004	0.48	1.32	0.013	0.363	0.1*10-5	Clogged
Enclosure II							
E4	11th Nov. 2003	1.09	2.88	0.016	0.379	1.5*10-5	Clogged
E5	25th Nov. 2003	1.22	3.07	0.023	0.398	1.7*10-5	Partially clogged
E7	8th June 2004	1.20	2.88	0.032	0.420	4.4*10-5	Not clogged
E9	30th Aug. 2004	0.64	1.75	0.049	0.366	1.2*10-5	Clogged
Enclosure III							
E2	5th Aug. 2003	1.25	3.36	0.011	0.37	1.8*10-5	Partially clogged
E3	9th Sept. 2003	1.12	2.76	0.013	0.40	1.6*10-5	Clogged

For the interpretation of the enclosure experiments this means that no totally unclogged situations were simulated (with exception of experiments E6 and E7).

#### **9.4.2 Cyanobacterial Toxins (*Microcystins*)**

The first series of enclosure experiments carried out with cyanobacterial toxins (pulsed application, aerobic conditions) had the aim to identify and quantify processes related to short term microcystin transport through sediment with and without visible clogging and to compare these results to those obtained on technical scale slow sand filters (SSF).

Previous laboratory and field scale experiments had shown that biodegradation is the most important elimination process for microcystin removal in sandy material (Grützmacher et al., 2004, Miller, 2000). Degradation was confirmed as the most important process in the enclosure experiments as only little retardation was observed in relation to the tracer applied simultaneously. Modelling yielded R-values between 1.0 and 1.97 (Table 24). The existence of more or less visible clogging did not seem to have a relevant effect on retardation, as R-values with clogging (E3) ranged from 1.25 to 1.76 and were only slightly less with only partial clogging (E2: from 1.0 to 1.95). The retardation coefficients lie in the same range as those described previously for sandy material (Miller, 2000:  $R = 1.07$ ; Grützmacher et al., 2002:  $R = 1.23$ ).

**Table 24: Summary of retardation coefficients and degradation rates obtained by modelling.**

Depth segment of enclosure	Retardation		Degradation [h-1]	
	Experiment E2 (no clogging visible)	Experiment E3 (visible clogging)	Experiment E2 (no clogging visible)	Experiment E3 (visible clogging)
water reservoir to 20 cm	1.97	1.76	0.74	0.54
20 cm to 40 cm	1.90	1.25	0.24	0.31
40 cm to 60 cm	1.00	1.36	0.75	0.19
60 cm to 80 cm	1.00	1.14	0.54	0.01
80 cm to effluent	1.58	1.30	0.07	0.07

For elimination of MCYST over the depth profile of the enclosures, (Table 24) the following statements summarize key results:

- For all experiments highest retardations and degradation rates are observed in the upper 20 cm.

- Retardation coefficients and degradation rates show a tendency to decline along the flow paths.
- Most peculiar is the flow path between 20 and 40 cm, with either a reduced degradation (E2), or reduced retardation (E3); a possible explanation is variable water saturation, which could occur in that horizon, as the applied negative pressure reaches a maximum near to the top of the filter bed.
- Also the last depth segment (80 cm to effluent) shows some peculiarities, which may be explicable by column-end-effects as the final part of the flow path is located in a gravel layer and the measurements were made in the outlet tube.

The portions of MCYST recovered in the effluent ranged from 2.7 % to 10 % (elimination rates 90 % to 97.3 %) and the development of MCYST amounts in the different sampling ports showed a distinct difference between experiments E2/E3 on the one hand and E4/E5 on the other hand (Figure 89) even though the uppermost layer ("schmutzdecke") had been removed prior to experiments E2 and E5. The following differences can be determined between these two sets of experiments:

- different enclosures with different pretreatment:
  - E2/E3 were conducted in enclosure III (4 sampling ports, continuous operation since July 2003, four weeks prior to first experiment),
  - E4/E5 in enclosure II (2 sampling ports, continuous operation since November 2003, four days prior to first experiment),
- different temperature ranges:
  - E2/E3 were carried out in August and September with temperatures between 16.4 °C and 31.6 °C,
  - E4/E5 were carried out in November with temperatures between 0.6 °C and 11.2 °C.

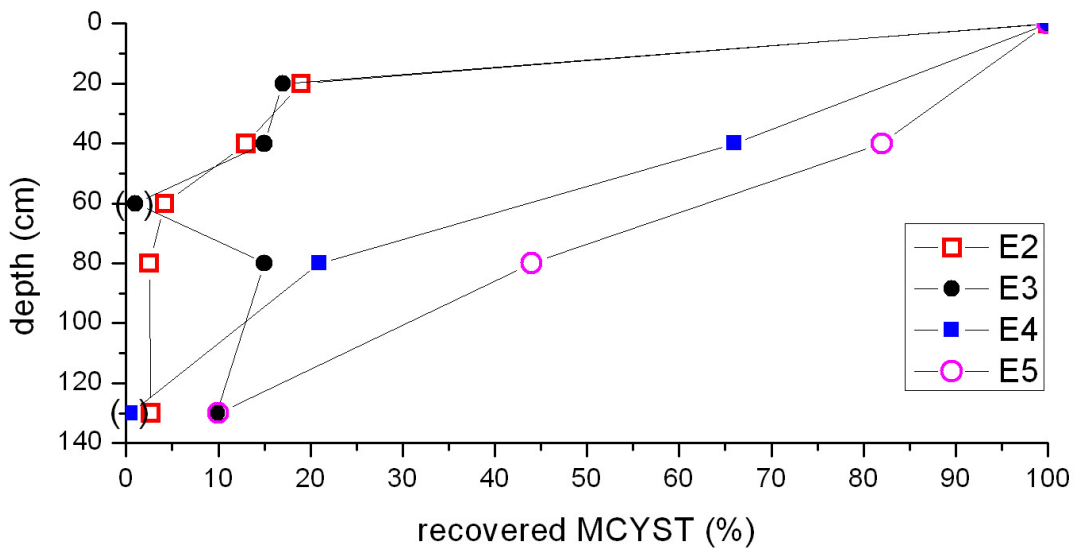


**Figure 89:** Recovered portions of MCYST during aerobic enclosure experiments E2 through E5.

These results support the hypothesis that the existence of a visible, superficial clogging layer or "schmutzdecke", is not of decisive importance concerning biodegradation of MCYST. Temperature as well as pre-treatment of the filter as a whole (conditioning or maturation) play a much more important role. This is supported by Ellis (1975) who states that the "schmutzdecke" or organic filter adds substantially to the effectiveness of the straining process. Biological activity, however, is observed up to a depth of 40 cm or more.

Further experiments concerning temperature effects on MCYST degradation carried out in the laboratory (see final NASRI Report working group algae, part VII) confirm this finding.

Figure 90 shows that the recovered amounts of MCYST in the anaerobic experiment, that was conducted in September 2004 after continuous operation for 4 months, are only slightly higher than in aerobic experiments carried out in the same enclosure, E4 and E5 (however without preconditioning and under lower temperatures). Experiments E2 and E3 that were conducted at similar temperatures and on a well preconditioned filter yielded distinctively lower recoveries (compare Figure 89). This leads to the assumption that there is MCYST degradation under anaerobic conditions and the degradation rates are comparable to those obtained under unfavorable, aerobic conditions (no preconditioning, low temperatures). This is in agreement with laboratory experiments carried out by Holst et al. (2003) that had shown that MCYST degradation was possible under anoxic conditions and could be accelerated by addition of nitrate and glucose. As true for aerobic conditions, there are, however, reported cases in which MCYST degradation is not detectable (Holst et al., 2003, Miller, 2000). The reasons for this will be discussed further on.

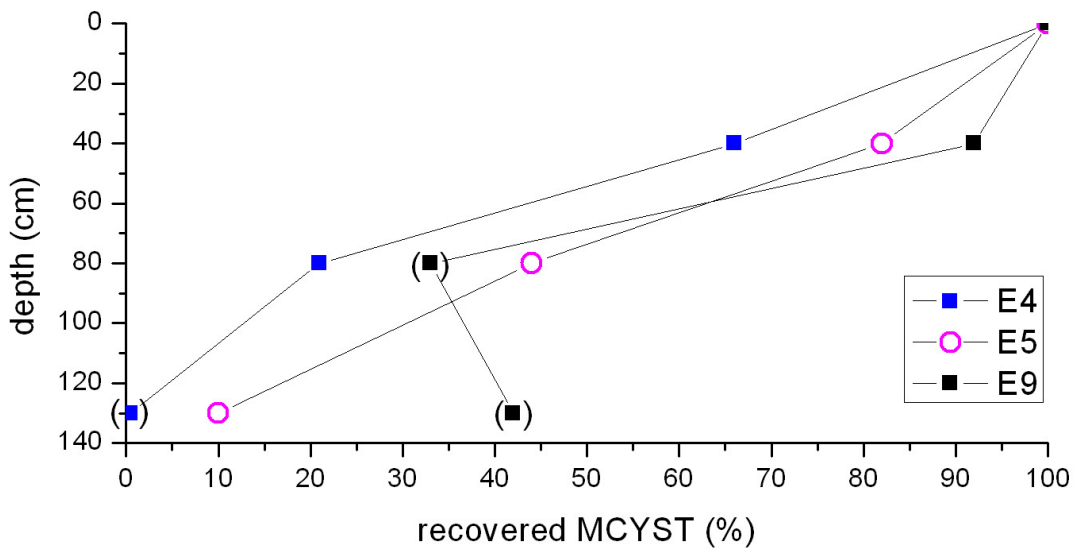


**Figure 90:** Recovered portions of MCYST during anaerobic (E9) and aerobic enclosure experiments (E4 and E5).

Continuous application of MCYST yielded a reduction of recovered portions (100 % minus eliminated portion) in the effluent ranging from 52 % during the first phase of constant experimental conditions (2 to 4 days), to 14 % during the second phase (day 8 to 15).

Compared to the experiments with pulsed application the recovered amounts during the first phase seem unusually high. Enclosure I, in which the experiment was carried out, had been in operation for 7 months before the beginning of the experiment. Therefore incomplete preconditioning, as for experiments E4 and E5, can be ruled out as a cause. Temperatures were also in the same range as during the experiments with pulsed application. Higher recoveries / lower elimination might explained by different elimination processes dominating only during short term, pulsed application and are less relevant for continuous application (e.g. irreversible sorption). In contrast, higher elimination rates / lower recoveries in the further course of the continuous dosing experiment (phase 2 and phase 3) would be compensated by the further adaptation of microbiology, leading to elimination rates around 90 % at the end of the experiment. These rates are in agreement with many previous publications with clearly higher contact times (e.g. Gützmacher et al., 2002, Lahti et al., 1997, Lahti et al., 1998).

In experiment E12 with continuous dosing of cyanobacteria a realistic scenario with cell-bound MCYST (7.4 µg/L by ELISA and 9 µg/L by HPLC) was simulated. In spite of low temperatures (clearly < 10 °C) no MCYST could be detected in the effluent. The total amount of cell-bound MCYST during the dosing phase was 15.2 mg (ELISA) or 18 mg (HPLC), the total biovolume applied was 17 cm<sup>3</sup>. Four days after dosing has ceased, the biovolume in the uppermost 2 cm of sediment had not shown a relevant reduction. The concentrations of total MCYST in the porewater had, however, decreased to 22 % of the maximum concentration at the end of the dosing phase (this being the worst case, as degradation during the dosing

phase itself was not taken into account). 10 days after dosing was terminated no more MCYST was detectable in the porewater, biovolume, however, still amounted to 48 % of the maximum value.

These results show that even at low temperatures MCYST, though primarily cell-bound, is degraded by far more readily than the cells of the cyanobacteria themselves, indicating a) that MCYST may be released from the intact cells (thus being available for rapid extracellular degradation) and / or b) degradation may also take place within the cyanobacterial cells (there have been no reported indications for this so far, though senescent cells under poor growth conditions have not been studied).

Although no worst-case scenario was simulated (maximum biovolumes of cyanobacteria may reach values 10-fold higher than the ones generated in the water reservoir), it can be concluded that although accumulation of cyanobacterial cells on the sediment surface may take place, MCYST accumulation is unlikely to occur in the same manner, probably due to rates of degradation being more rapid than rates of MCYST release from the cells, even in a population under detrimental growth conditions, i.e. dark and cold.

There have been, however, indications that in some cases MCYST degradation rates are not sufficient for complete elimination of toxin being released from cyanobacterial cells during sand filtration (e.g. Grützmacher et al., 2002). This is probably due to conditions unfavorable for toxin biodegradation (low temperatures) while in other cases cyanobacterial cells were transported through coarsely grained material (e.g. Bricelj & Sedmak, 2001) thus protecting the mainly cell-bound MCYST from biodegradation. Furthermore our experiment did not totally simulate the situation of a senescent population at the very end of the growing season, as the cells used were derived from very good growth conditions in our large-scale culture.

Other investigations on interactions between cell-bound and extracellular MCYST are limited to observations in lake water without sediment contact. While experiments conducted by Kirivanta et al. (1991) yielded low degradability of MCYST-LR released by lysed cells in contact with river water (initially the batch cultures were run axenic), many other experiments (e.g. Jones et al., 1994, Christoffersen et al., 2002) showed very rapid degradation of initially already extracellular MCYST.

In summary, the enclosure experiments confirmed the importance of biodegradation for MCYST elimination in sandy material and yielded generally high degradation rates (0.01 h<sup>-1</sup> to 0.75 h<sup>-1</sup>) under optimal conditions. Optimal conditions can be defined as the following:

- Previous conditioning of the filter for more than 4 days, better for several weeks,
- aerobic conditions,
- moderate temperatures (> 10 °C).

Lower degradation rates can be due to the following circumstances:

- Previous flushing of the filter for less than 4 days,
- low temperatures (< 10 °C),
- anoxic conditions.

Continuous application of dissolved MCYST can lead to an increase in elimination rates, although under optimal conditions this is not necessary for nearly complete elimination within less than 1 day. Under suboptimal conditions this may be a method to achieve better elimination.

MCYST is unlikely to accumulate on the surface of a filter or sediment in the same way as cyanobacterial cells do, due to rapid degradation, probably more rapid than release.

## 9.5 References

- Bricelj, M. & Sedmak, B. (2001): Transport of biologically active substances through gravel strata. - in: Seiler & Wohnlich (eds.): New Approaches Characterizing Groundwater Flow, p. 25 - 29, Swets & Zeitlinger Lisse.
- Christoffersen K., Lyck S. & Winding A. (2002): Microbial activity and bacterial community structure during degradation of microcystins., *Aq. Microb. Ecology*, 27: 125 – 136.
- Ellis K.V. (1985): Slow sand filtration., CRC Critical Reviews in Environmental Control, 15 (4): 315 – 354.
- Grombach, P., Haberer, K., Merkl, G., & Trueb, E.U. (2000): Handbuch der Wasserversorgungstechnik. Oldenbourg Verlag, München. 3. Auflage.
- Grützmacher, G., Wessel., G., Chorus, I. & Bartel, H. (2004): Strategien zur Vermeidung des Vorkommens ausgewählter Algen- und Cyanobakterienmetabolite im Rohwasser, Teilprojekt: Wirksamkeit der Infiltration / Bodenpassage für die Retention von Algen- und Cyanobakterienmetaboliten. – Abschlussbericht des BMBF-Forschungsvorhabens, Förderkennzeichen: 02 WT9852/7.
- Grützmacher, G., G. Böttcher, I. Chorus & H. Bartel (2002): Removal of microcystins by slow sand filtration. *Environm. Tox.* , 17: 386 – 394, John Wiley & Sons.Holst et al. 2003.
- Holst, T., Jørgensen, N.O.G., Jørgensen, C. & Johansen, A. (2003): Degradation of microcystin in sediments at oxic and anoxic, denitrifying conditions. - *Wat. Res.* 37: 4748 - 4760.
- Holzbecher E., Inversion of temperature time series from near-surface porous sediments, *Journal of Geophysics and Engineering*, Vol. 2, 343-348, 2005.
- Holzbecher E., Dizer H., Grützmacher G., Lopez-Pila J., Nützmann G., The influence of degradation and sorption within biogeochemical cycles, submitted to: *Environmental Engineering Science*, 2005.
- Jones G.J., Bourne D.G., Blakeley L. & Doelle H. (1994): Degradation of cyanobacterial hepatotoxin microcystin by aquatic bacteria., *Natural Toxins*, 2: 228-235
- Lahti K., Rapala J., Färdig M., Niemelä M., Sivonen K. (1997): Persistence of cyanobacterial hepatotoxin, microcystin-LR, in particulate material and dissolved in lake water, *Wat. Res.*, 31 (5): 1005 – 1012.

- Lahti K., Vaitomaa J., Kivimäki A.L., Sivonen K. (1998): Fate of cyanobacterial hepatotoxins in artificial recharge of groundwater and in bank filtration, Artificial Recharge of Groundwater, Peters et al. (eds.) Balkema, Rotterdam.
- Massmann, G., Taute, T. , Bartels, A. & Ohm, B. (2004): Characteristics of sediments used for batch-, enclosure- and column-studies. Internal Report, FU Berlin.
- MATLAB® Version 6.5, Release 13 (2002). The MathWorks, Inc., 3 Apple Hill Drive, Natick, MA 01760-2098, USA.
- Miller M.J. (2000): Investigation of the removal of cyanobacterial hepatotoxins from water by river bank filtration . PhD Thesis, Flinders University.
- Nützmann G., Holzbecher E., Strahl G., Wiese B., Licht E., Knappe A., Visual CXTFIT – a user-friendly simulation tool for modelling one-dimensional transport, sorption and degradation processes during bank filtration, Proceedings ISMAR 2005.
- Schwarz, M. (2004): Mikrobielle Kolmation von abwasserdurchsickerten Bodenkörpern: Nucleinsäuren zum Nachweis von Biomasse und Bioaktivität. - Schriftenreihe des ISWW Karlsruhe: Band 116.
- Toride N., Leij F.J., van Genuchten M. Th., The CXTFIT code for estimating transport parameters from laboratory or field tracer experiments, U.S. Salinity Lab., Agric. Res. Service, US Dep. of Agric., Research Report No. 137, Riverside (CA), 1995.